Distribution Agreement

In presenting this thesis or dissertation as a partial fulfillment of the requirements for an advanced degree from Emory University, I hereby grant to Emory University and its agents the non-exclusive license to archive, make accessible, and display my thesis or dissertation in whole or in part in all forms of media, now or hereafter known, including display on the world wide web. I understand that I may select some access restrictions as part of the online submission of this thesis or dissertation. I retain all ownership rights to the copyright of the thesis or dissertation. I also retain the right to use in future works (such as articles or books) all or part of this thesis or dissertation.

Signature:

_____ _____

Shardule Pankajkumar Shah Date

Heat Shock Factor 1 Regulation of Multiple Myeloma Pathogenesis

By

Shardule Pankajkumar Shah
Doctor of Philosophy

Graduate Division of Biological and Biomedical Science
Immunology and Molecular Pathogenesis

_____
Lawrence H. Boise, Ph.D.
Advisor

_____
Neal Iwakoshi, Ph.D.
Committee Member

_____
Joshy Jacob, Ph.D.
Committee Member

_____
Periasamy Selvaraj, Ph.D.
Committee Member

_____
Keith Wilkinson, Ph.D.
Committee Member

Accepted:

_____
Lisa A. Tedesco, Ph.D.
Dean of the James T. Laney School of Graduate Studies

_____
Date

Heat Shock Factor 1 Regulation of Multiple Myeloma Pathogenesis

By
Shardule Pankajkumar Shah

B.S., Case Western Reserve University, 2007
M.S., University of Pennsylvania, 2009

Advisor: Lawrence H. Boise, Ph.D.

An abstract of
A dissertation submitted to the Faculty of the
James T. Laney School of Graduate Studies of Emory University
in partial fulfillment of the requirements for the degree of
Doctor of Philosophy
in the Graduate Division of Biological and Biomedical Science
Immunology and Molecular Pathogenesis
2016

Abstract

Heat Shock Factor 1 Regulation of Multiple Myeloma Pathogenesis

By

Shardule Pankajkumar Shah

Multiple myeloma is a plasma cell malignancy with estimated 30,330 new cases and the cause of 12,650 deaths in 2016 in the United States. Proteasome inhibitors have dramatically improved patient outcome but there is no functional cure. The proteasome inhibitors bortezomib and carfilzomib work in part because they exploit the plasma cell backbone of a myeloma cell. Myeloma cells upregulate the heat shock response in order to protect themselves from bortezomib-induced apoptosis.

In chapter two, we show that knockdown of the master regulator of the heat shock response, Heat Shock Factor 1 (HSF1), sensitizes myeloma cells to bortezomib-induced apoptosis. HSF1 knockdown results in a greater additive effect on apoptosis than simultaneous knockdown of multiple HSF1-mediated heat shock proteins. We show HSF1 phosphorylation upon bortezomib treatment and that HSF1 serine 326 phosphorylation is an activating post-translational modification and also detail novel HSF1 post-translational modifications. Chapter four details that cell lines stably overexpressing wildtype HSF1 or a serine-to-alanine or serine-to-glutamate mutation at amino acid position 326, all result in downregulation of the bortezomib-induced heat shock response and increased bortezomib-induced apoptosis.

Identification of kinases responsible for HSF1 phosphorylation may inform an HSF1 indirect inhibition strategy. In chapter five, we show that the kinase is cytosolic and classify candidate kinases responsible for serine 326 phosphorylation. Also, we

show a novel mechanism of action for the multi-kinase inhibitor TG02: inhibition of serine 326 phosphorylation and the proteasome inhibitor-induced heat shock response. We also demonstrate that a TG02 and bortezomib or carfilzomib combination leads to an additive effect on apoptosis in myeloma cells. Our data indicate that the kinase responsible for serine 326 phosphorylation is a cytosolic TG02 target which has likely not yet been elucidated.

Our studies show how myeloma cells hijack the HSF1-mediated heat shock response in order to avoid proteasome inhibitor-induced apoptosis. We also demonstrate that inhibition of serine 326 phosphorylation is a novel TG02 mechanism. Ultimately, our work could improve the efficacy of myeloma therapeutic strategies, and can also be broadened to additional malignancies for which proteasome inhibition is a frontline therapy, such as mantle cell lymphoma. Additionally, HSF1 inhibition strategies could inform therapeutic strategies for malignancies which activate HSF1 for apoptosis evasion, such as breast cancer, prostate cancer, and chronic lymphocytic leukemia.

Dissertation queries are welcomed and can be e-mailed to:

Shardule P. Shah, shardule@gmail.com or Lawrence H. Boise, lboise@emory.edu

Heat Shock Factor 1 Regulation of Multiple Myeloma Pathogenesis

By
Shardule Pankajkumar Shah

B.S., Case Western Reserve University, 2007
M.S., University of Pennsylvania, 2009

Advisor: Lawrence H. Boise, Ph.D.

A dissertation submitted to the Faculty of the
James T. Laney School of Graduate Studies of Emory University
in partial fulfillment of the requirements for the degree of
Doctor of Philosophy
in the Graduate Division of Biological and Biomedical Science
Immunology and Molecular Pathogenesis
2016

Acknowledgments

The journey to get here required a herculean effort. Not by me, but by those around me. Dissertation completion required unwavering support from more individuals than I can remember. To anyone who did something as simple as ask, 'How is your day going?' to those who picked me up during times when the path ahead wasn't very clear, thank you. This accomplishment belongs to you as much as it belongs to me.

The path to my Ph.D. started with the encouragement of my family. My mother and father, Manorama & Pankaj, and my siblings, Achira & Adam, and Shrenik have always been by my side. I am lucky to have been born into a loving family whose sole goal for the past ten years was (seemingly) to make sure I finished my Ph.D. And I am blessed with my wife Ami's family as well. Her parents, Nalini & Mahendra, and Neena & Harakhchand, and siblings, Dhenu & Mitesh, Nimit & Sneha, and Avni & Shrenik, have been an unending source of support. Writer Alex Haley wrote, "In every conceivable manner, the family is a link to our past, and the bridge to our future."

I would like to acknowledge the people I have spent more time with in the past six years than anyone else: my lab members. I tell everyone that you are my work family. I leave out the "occasionally dysfunctional but always loving" prefix, but most people wouldn't understand anyway. You all had a huge hand in helping me to get this done, and I could not have picked a better group of people to work beside on a daily basis. Thank you to Shannon, Vikas, Brian, Jason, Dave, Cathy, Katie, Tyler, Tony, and Pamela.

I could not have made it to today without the unending love and support from my wife. Ami, I cannot thank you enough for all that you have sacrificed for me. You have asked nothing of me during this odyssey, constantly reminding me that as long as I get my work done, you will take care of everything else. You have fulfilled that and so much more. You are my rock, and I am excited to take the next step in our lives. And if my children ever end up reading this, I will do everything to help you achieve your goals and dreams, just like your mother and all those mentioned here have helped me to achieve mine.

A huge thank you to my dissertation committee: Drs. Iwakoshi, Jacob, Selvaraj, and Wilkinson. It has been an honor to have you serve on my committee. You have always pushed me to ask the right questions, perform the best science, and communicate it clearly. Your guidance has helped mold me into the scientist I have become today.

Finally, I would like to say thank you to my mentor, Dr. Boise. Larry, in April 2011, you took a chance on me and I have worked every day to show that I have never forgotten that. You understood when and how to motivate me, made me feel that my work was the greatest thing since sliced bread, and mentored me not only as a student, but also as a young professional and a person. As I move forward, I will be taking all of the scientific and life lessons you've imparted upon me. Thank you for everything; I am forever indebted to you.

TABLE OF CONTENTS

I. INTRODUCTION 1

A. Abstract 2

B. Introduction 2

C. Proteasome Inhibition 3

D. The Heat Shock Response and Heat Shock Proteins 7

E. Heat Shock Factor 1 9

F. Regulation of HSF1 by Post-translational Modifications 11

G. HSF1 Inhibition in Cancer Treatment 16

H. Conclusions 22

I. Acknowledgments 22

J. Tables and Figures 23

K. Statement of Problem 29

II. HSF1-MEDIATED REGULATION OF BORTEZOMIB-INDUCED HEAT SHOCK RESPONSE IN MULTIPLE MYELOMA 32

A. Abstract 33

B. Introduction 34

C. Results 36

D. Discussion 42

E. Materials and Methods 46

F. Acknowledgments 51

G. Tables and Figures 52

H. Supplementary Material 61

III. HSF1 OVEREXPRESSION AND PROTEASOME INHIBITOR STUDIES IN MULTIPLE MYELOMA 66

A. Introduction 66

B. Hypothesis 66

C. Materials and Methods 66

D. Results 67

E. Discussion 69

F. Figures 71

IV. TG02 REGULATION OF PROTEASOME INHIBITOR-INDUCED HSF1 ACTIVATION IN MULTIPLE MYELOMA 75

A. Materials and Methods 80

B. Figures 83

C. Supplemental Table 86

V. DISCUSSION 87

A. Implications from Bortezomib-Induction of Heat Shock Factor 1 Serine 326 Phosphorylation Studies 87

1. Characterization of the MPH 87

2. The Role of the MPH and HSF1 Activation in Combination Therapy 88

3. Non-HSR HSF1 Functionality in MM 90

4. Non-pS326 HSF1 PI-induced Phosphorylation in MM 91

5. Acetylation Regulation of HSF1 Activation 92

6. pS326 as a MM Biomarker 93

7. Summary 94

B. Implications from TG02 and Proteasome Inhibitor Studies 96

1. The PI-pS326 Kinase is Cytosolic 96

2. TG02 Sensitizes MM Cell Lines and Patient Samples to Proteasome Inhibition and Inhibits PI-pS326 97

3. Have We Moved Closer to Identifying the PI-pS326 Kinase? 98

4. Early Detection of TG02-Mediated PI-pS326 Inhibition in MM.1s Cells 100

5. Summary 100

6. Figures 101

VI. REFERENCES 107

TABLE OF FIGURES AND TABLES

CHAPTER 1

Table 1: Human Myeloma Cell Lines 23

Table 2: HSF1 Kinases, Their Targets, and Functional Consequences 24

Table 3: HSF1 Inhibitors 25

Figure 1A: HSF1 Post-Translational Modifications 26

Figure 1B: HSF1 Activation Lifecycle 27

Figure 2: Inhibitors of the HSF1-dependent Heat Shock Response 28

CHAPTER 2

Table 1: Patient Sample Clinical Diagnostics 52

Figure 1: Bortezomib Induces HSP Expression in Multiple Myeloma Cells, and HSF1 Silencing Sensitizes Multiple Myeloma Cells to Bortezomib Treatment 53

Figure 2: In Combination with Bortezomib Treatment, HSF1 Silencing is More Effective than HSP Silencing at HSR Downregulation 55

Figure 3: HSF1 is Phosphorylated upon Bortezomib Treatment in Multiple Myeloma Cells 57

Figure 4: Phosphoproteomics Reveals that HSF1 Serine 326 is a Bortezomib-Inducible Phosphorylation Site and Serine 303 is a Constitutive Phosphorylation Site 58

Figure 5: Phospho-specific Antibodies Confirm that HSF1 Serine 326 is a Bortezomib-Inducible Phosphorylation Site and Serine 303 is a Constitutive Phosphorylation Site 59

Supplementary Table 1 64

Supplementary Figure 1: HSP or HSF1 Silencing Leads to Robust Knockdown 48h After Transfection 65

CHAPTER 3

Figure 1: Schematic of HSF1 Overexpressors 71

Figure 2: HSF1 Overexpression Sensitizes Myeloma Cells to Bortezomib Treatment 72

Figure 3: HSF1 Overexpression Inhibits the Bortezomib-inducible HSR 73

Figure 4: HSF1 Overexpression Falsely Activates the HSR and Inhibits the Bortezomib-inducible HSR 74

CHAPTER 4

Figure 1A: HSF1 Serine 326 is Phosphorylated in the Cytoplasm 83

Figure 1B: Human Kinome Phosphoprotein Microarray Identifies BZ-induced Targets 83

Figure 2A: TG02 Inhibits Proteasome-Inhibitor Induced HSF1 Serine 326 Phosphorylation and Proteasome Inhibitor-Induced HSR in Myeloma Cells 84

Figure 2B: TG02 and Proteasome Inhibitor Combination Leads to an Additive Effect on Apoptosis in MM.1s Cells 84

Figure 2C: TG02 Inhibits Bortezomib-induced HSF1 Serine 326 Phosphorylation and Bortezomib-induced HSR in H929 Cells and HSF1 Serine 326 Phosphorylation in U266 Cells 84

Figure 2D: TG02 and Bortezomib Combination Leads to an Additive Effect on Apoptosis in H929 Cells but not U266 Cells 84

Figure 2E: TG02 Inhibits Carfilzomib-Induced HSF1 Serine 326 Phosphorylation and Bortezomib-Induced HSR in Patient Samples 84

Figure 2F: CDK9 is not Responsible for Bortezomib-Induced Serine 326 Phosphorylation and Its Silencing does not Sensitize Cells to Bortezomib-Induced Apoptosis 84

Supplemental Table 86

CHAPTER 5

Figure 1: Proteasome Inhibition Skews HSF1-Dependent HSP Upregulation Toward Large (≥40 kDa) HSPs 101

Figure 2: HSF1 Inhibition Can Lead to Dual Inhibition of Glucose Metabolism 102

Figure 3: HSF1 Phospho-serine 326 Staining is Observed in a Patient Sample Both Pre- and Post-Oprozomib Treatment 103

Figure 4: A Proposed Schematic for HSF1 Biomarker Studies to Predict Proteasome Inhibitor Response 104

Figure 5: HSF1 Serine 326 Phosphorylation Occurs in the Cytosol Followed by HSF1 Nuclear Translocation 105

Figure 6: The Threshold for PI-induced HSF1 Serine 326 Phosphorylation is Lower than that of HSP Upregulation 106

Abbreviation List

Abbrevation	Explanation
A	Acetylation
BZ	Bortezomib
CZ	Carfilzomib
E	Glutamate
HDAC	Histone deacetylase
HSE	Heat shock element
HSF	Heat Shock Factor
HSP	Heat Shock Protein
HSR	Heat shock response
IMiD	Immunomodulatory drug
K	Lysine
MM	Multiple myeloma
MPH	MM.1s proteasome inhibitor-induced heat shock response
P	Phosphorylation
PI	Proteasome inhibitor, Proteasome inhibition
pS	Phosphoserine
PTM	Post-translational modification
RD	Regulatory domain
S	Serine
S326A	Serine 326 to alanine mutation
S326E	Serine 326 to glutamate mutation
shRNA	Short hairpin RNA
si(-)	Non-targeting control small interfering RNA
siRNA	Small interfering RNA
T	Threonine
wt	Wildtype

I. INTRODUCTION

(*Modified from originally published form in Molecular Cancer Research, August 2015*)

When Cancer Fights Back: Multiple Myeloma, Proteasome Inhibition, and the Heat Shock Response

Shardule P. Shah[1], Sagar Lonial[1], and Lawrence H. Boise[1,2]

Departments of Hematology and Medical Oncology[1] and Cell Biology[2], Winship Cancer Institute of Emory University and the Emory University School of Medicine, Atlanta, GA

Running title: Multiple Myeloma, Proteasome Inhibition, and the Heat Shock Response

Keywords: Multiple myeloma, HSF1, proteasome inhibition

Financial support: Support provided by P30 CA138292 and The TJ Martell Foundation. LHB is a Georgia Cancer Coalition Distinguished Cancer Scientist.

Correspondence:
Lawrence H. Boise
Department of Hematology and Medical Oncology
Winship Cancer Institute of Emory University
Emory University School of Medicine
1365 Clifton Road NE
Room C4012
Atlanta, GA 30322
404-778-4724
lboise@emory.edu

Disclosures:
Lonial: Consultancy - Millennium: The Takeda Oncology Company, Celgene, Novartis, Bristol-Myers Squibb, Onyx Pharmaceuticals, Janssen Pharmaceutical Companies: The Pharmaceutical Companies of Johnson & Johnson

Boise: Consultancy - Onyx, Novartis

Word count: 5,356

Figures and tables: Two figures (one with two parts) and two tables

Abstract

Multiple myeloma (MM) is a plasma cell malignancy with an estimated 26,850 new cases and 11,240 deaths in 2015 in the United States. Two main classes of agents are the mainstays of therapy - proteasome inhibitors (PIs) and immunomodulatory drugs (IMiDs). Other new targets are emerging rapidly, including monoclonal antibodies and histone deacetylase (HDAC) inhibitors. These therapeutic options have greatly improved overall survival but currently only 15-20% of patients experience long-term progression-free survival or are cured. Therefore, improvement in treatment options is needed. One potential means of improving clinical options is to target resistance mechanisms for current agents. For example, eliminating the cytoprotective heat shock response that protects myeloma cells from proteasome inhibition may enhance PI-based therapies. The transcription factor Heat Shock Factor 1 (HSF1) is the master regulator of the heat shock response. HSF1 is vital in the proteotoxic stress response and its activation is controlled by post-translational modifications (PTMs). This review details the mechanisms of HSF1 regulation and discusses leveraging that regulation to enhance PI activity.

Introduction

From 1971-1996, the overall survival rate for MM patients remained largely unchanged[1]. Despite the use of alkylators, corticosteroids (dexamethasone and prednisone), and autologous bone marrow transplantation, little improvement was noted. Then, in 1999, thalidomide (in combination with dexamethasone) became the first new agent with major activity against MM in 37 years[2]. Thalidomide (Thalomid® - 2006 FDA approval) belongs to a class of structurally similar drugs known as immunomodulatory drugs (IMiDs), along with lenalidomide (Revlimid® - 2006) and

pomalidomide (Pomalyst® - 2013). IMiDs have helped to improve patient outcomes in recent years along with another major class of MM agents: proteasome inhibitors[3]. The two FDA-approved PIs are bortezomib (Velcade® - 2003) and carfilzomib (Kyprolis® - 2012).

Proteasome Inhibition

The main effector in the ubiquitin-proteasome system (UPS) is the proteasome, a cytoplasmic protein complex responsible for protein degradation[4]. The 26S proteasome is about 2000 kilodaltons (kDa) in molecular mass and consists of one 20S protein subunit and two 19S regulatory cap subunits. Proteasomal degradation removes denatured, misfolded, damaged, or improperly translated proteins from cells. The UPS plays an essential homeostatic role in regulating intracellular protein concentration, as well as being a regulator involved in many cellular processes including DNA repair, sodium channel function, regulation of immune and inflammatory responses, signal transduction and cell cycle progression[5].

Proteasome-mediated degradation is particularly vital for plasma cell quality control because of its role as a professional secretory cell that produces copious amounts of immunoglobulin in a constitutive manner. Therefore, proteasome inhibition can dramatically alter protein homeostasis leading to stress responses and if not resolved, apoptosis[6].

Bortezomib is a highly selective and reversible PI that has a boron atom which binds the β5 subunit (PSMB5)/chymotrypsin-like activity of the 26S proteasome[7]. The proteasome has an ATP-dependent proteolytic activity, therefore, bortezomib's targeting

of β5 results in decrease or loss of proteasome function. Bortezomib was first reported as an anti-inflammatory agent for treating polyarthritis in 1998. Palombella et al., used bortezomib as a means for inhibiting NF-κB activation by preventing proteasome-mediated degradation of IκBα, an NF-κB negative regulator[8]. For cancer, bortezomib was first tested in vitro in by Adams et al., in a 60 tumor cell line NCI screen, and was most potent in the prostate cancer cell line, PC-3[9]. Cytotoxicity was speculated to be due to stabilization and dysregulation of cyclins, CDK inhibitors, tumor suppressor proteins, IκB, and other proteins associated with cell cycle progression. Hideshima et al., published the first report on bortezomib in MM cell lines and freshly isolated patient samples[10]. In addition to the NF-κB mechanism described above, bortezomib was shown to alter cellular interactions and cytokine secretion in the bone marrow milieu to inhibit tumor cell growth, induce apoptosis, and overcome drug resistance. Mitsiades et al., used high-dose bortezomib in the human MM cell line, MM.1S, to probe gene expression changes[11]. (A listing of selected human myeloma cell lines is provided in Table 1.) These changes included a downregulation of growth/survival signaling pathways, upregulation of molecules implicated in pro-apoptotic cascades, and upregulation of ubiquitin/proteasome pathway members and heat shock proteins (HSPs). HSP27, 40, and 70 upregulation was seen as early as two hours post-treatment. Bortezomib was FDA-approved in 2003 for patient use in large part due to the results of a Phase II study of its use in relapsed/refractory MM[12].

Up to this point, while gene expression profiling had been used to characterize the molecular sequelae of bortezomib treatment, mechanisms mediating anti-MM activity had not yet been defined. Questions remained unanswered including, 'Through what

pathway(s) does PI induce apoptosis?' and 'Is there a cellular event specific to plasma cells that can predict its effectiveness?' Hideshima et al., began to scratch the surface of the bortezomib-cell biology connection by linking bortezomib, p53 phosphorylation, JNK activation, caspase-3 and 8 activation, inhibition of DNA damage repair, and cell death[13].

This study led to further investigation into the cell biology changes caused by bortezomib. However, what had not been looked at up to that point was specifically the *plasma cell* nature of a myeloma cell. Because of their role as immunoglobulin producers, plasma cells are heavily reliant on the unfolded protein response (UPR) for protein quality control[14]. Lee et al., suggested that UPR inhibition, through IRE1α (a UPR transducer) suppression and splicing impairment of its downstream target, XBP1, plays a role in MM PI-induced death[15]. Our group showed that PIs can lead to an accumulation of misfolded proteins and an induction of terminal components of the UPR including PERK, eIF-2α, ATF4, and its downstream target, CHOP[16]. This was one of the first reports detailing how bortezomib was exploiting plasma cell biology, specifically immunoglobulin accumulation and terminal UPR activation, to induce apoptosis. Meister et al., concluded that bortezomib-induced apoptosis is associated with the buildup of defective ribosomal products (DRiPs) and other unfolded proteins in the ER[17]. Also, Bianchi et al., determined that the balance between proteasome workload and degradative capacity represents a critical determinant of apoptotic sensitivity of MM cell lines to PI[18]. Furthermore, Ling et al., showed that low XBP1 levels predict poor response to bortezomib, both in vitro and in MM patients, and ATF6 (a UPR transducer) expression correlates with bortezomib sensitivity[19]. Leung-Hagesteijn et al., proposed that the existence of PI-insensitive $Xbp1s^{-}$ tumor progenitors within primary MM tumors may

produce class-effect PI resistance independent of drug identity[20]. Mechanistically, MM Xbp1s suppression induces bortezomib resistance via decommitment to plasma cell maturation and immunoglobulin production, diminishing ER stress-associated cytotoxicity.

In addition to direct inhibition of the proteasome, PI-induced ER stress can also occur from aggresome formation and autophagy[21-23]. Both are thought to be survival mechanisms used by cancer cells, and a recent study suggests that targeting the integrated networks of aggresome formation, proteasome, and autophagy may potentiate ER stress-mediated cell death pathways[21]. However, one potential counter to PI effectiveness is the development of acquired mutations.

The direct target of bortezomib, PSMB5, is the most well-characterized mutation site[24]. The PSMB5 mutation A49T has been shown to play in role in bortezomib resistance[25,26]. This mutation reduces bortezomib-induced apoptosis through the prevention of ubiquitinated protein accumulation and fatal ER stress in MM. Despite this concern, no clinical evidence of an acquired proteasome subunit mutation has been published[25].

With the success of bortezomib in the clinic, second generation PIs have been developed that have different activities, bioavailability (oral) and toxicity profiles. These agents have been the subject of intense preclinical and clinical studies. The first of these new inhibitors, Carfilzomib, has now been FDA-approved for the treatment of relapsed/refractory MM. Carfilzomib is an intravenous irreversible PI which binds to β5 with greater selectivity than bortezomib[27]. NPI-0052 (marizomib), ONX 0912 (oprozomib), and MLN9708/2238 (ixazomib) are all involved in clinical trials[7,27].

Marizomib is being tested intravenously and oprozomib and ixazomib are being tested orally in MM. Marizomib is a β-lactone-γ-lactam inhibitor which irreversibly binds β2 and β5 with high affinity and β1 with low affinity, and was granted "orphan drug" status by the FDA for MM treatment. Phase I combination studies are being conducted using marizomib, pomalidomide, and dexamethasone in subjects with relapsed/refractory MM[28]. Oprozomib is an epoxyketone which irreversibly binds β5 with high affinity and was also recently granted "orphan drug" status by the FDA for MM and Waldenström macroglobulinemia treatment. Ixazomib is a boric acid analog which reversibly binds β5 with high affinity and at higher concentrations is able to inhibit β1 and β2. Two recently published companion reports from Phase I oral ixazomib studies in relapsed/refractory MM patients showed that 15-18% of patients achieved partial response or better with 76% reaching a state of stable disease or better in one of the studies[29,30].

Continued improvement in current treatments and clinical trials including those for second-generation PIs have led some researchers to state that prolonged disease-free survival and a cure for a majority of patients are on the horizon[31]. Improved disease-free survival can only occur if we can identify and target cellular resistance mechanisms. Resistance mechanisms, including HSP upregulation as part of the heat shock response (HSR), can limit PI effectiveness. Therefore, inhibiting the HSR is a therapeutic opportunity for improving PI efficacy.

The Heat Shock Response and Heat Shock Proteins

As mentioned above, HSP family members were reported amongst genes that were highly upregulated by bortezomib[11]. The HSR is part of a cell's internal repair machinery and maintains homeostasis under stressful conditions including infection,

inflammation, exercise, exposure to toxins or pharmacological agents, starvation, or hypoxia[32]. This response is carried out by HSPs, many of which act as chaperones assisting in protein folding and establishment of proper conformation while also preventing undesired protein aggregation. HSPs are categorized into five families: (1) HSP70 superfamily (2) DNAJ (HSP40) family (3) HSPB (small heat shock protein) family (4) HSP90/HSPC family (5) Chaperonins and related genes[33]. While the cytoprotective HSR is desired in healthy cells, it could also protect cancer cells from bortezomib's pro-apoptotic effects and is a potential resistance mechanism as demonstrated in bladder cancer cells[34]. Zhang, et al., have published a detailed review of the connection between bortezomib and HSPs in MM[32].

The cytoprotective nature of HSPs has stimulated preclinical testing and clinical trials of HSP90 and HSP70 inhibitors in MM and other cancers. HSP90 inhibitors have been tested either alone or in combination with bortezomib and/or dexamethasone in MM[35,36]. However, the results of these studies to date have been disappointing and have yet to lead to an FDA-approved HSP90 inhibitor. Usmani et al., have comprehensively reviewed the promise and difficulty of HSP90 inhibition as a therapeutic strategy in MM[37]. Numerous other reports have been published regarding HSP90 inhibitors[32,38,39]. HSP70 inhibitors have shown promise in preclinical settings, including MM, both alone and in combination with bortezomib and/or HSP90 inhibitors, but have not progressed to clinical trials[40-43]. Detailed overviews of the role of HSP70 in cancer and the challenges of various HSP70 inhibition strategies have previously been published[44,45]. For several reasons, both HSP70 and HSP90 inhibitors face a similar challenge: single-target HSP inhibitors may not work in cancer. First, some HSP inhibitors cannot induce apoptosis by

themselves at biologically relevant levels[42,46]. For those inhibitors that do, studies have shown that they induce other chaperones including HSPs as a compensatory mechanism. For example, HSP90 inhibitors induce HSP70 and HSP27, and lead to an increase in HSP90 client proteins[43,47-53]. In addition, Acquaviva, et al., showed that the treatment of H1975 non-small cell lung cancer or A375 melanoma cells with the HSP90 inhibitor ganetespib leads to an additional compensatory mechanism, nuclear accumulation of the HSR master regulator, Heat Shock Factor 1 (HSF1)[53]. These and other results indicate that individual HSP inhibition only targets a part of the HSR. The combination of compensatory HSP induction and nuclear HSF1 accumulation could lead to increased drug resistance and negate any pro-apoptotic effect of single-target HSP inhibitors. Therefore, to inhibit the entirety of the HSR one would need to inhibit HSF1.

Heat Shock Factor 1

HSF1 is one of four proteins (HSF1-4) involved in stress response and development[54]. It is the factor primarily responsible for HSP gene upregulation when myeloma cells are treated with bortezomib[55]. HSF1 also drives a heat shock-independent tumorigenesis program supporting oncogenic processes such as cell-cycle regulation, signaling, metabolism, adhesion, translation, and reprogramming of neighboring stromal cells to permit a malignant phenotype[56,57]. HSF2 has a minor role during the stress response[58]. HSF1-HSF2 heterocomplexes form under conditions of cell stress including proteasome inhibition, and HSF2 can modulate inducible HSF1-mediated gene expression[58,59]. Avian and murine, but not human, HSF3 has been characterized and may have a HSF crosstalk-independent role in activating nonclassical heat-shock genes[58,60].

HSF4 is involved in the development of different sensory organs in cooperation with HSF1, but has no known role in the HSR[58].

HSF1 is a 57 kDA, cytoplasmic, and inactive protein under non-stress conditions. It forms an inert heterotetramer with HSP40, 70, and 90. HSP90 has been identified as HSF1's major repressor. However, there is evidence that HSF1-HSP70 interactions are also repressive[61,62]. When activated by stress such as proteasome inhibition, the tetramer dissociates. HSP90 is a cytoplasmic chaperone that binds misfolded proteins while HSP70 and HSP40 can either act as cytoplasmic chaperones or remain associated with HSF1[63,64]. Upon dissociation, HSF1 trimerizes and translocates into the nucleus. However, there are conflicting views regarding which of these steps occurs first[65,66]. After trimerization and translocation, HSF1 binds to the heat shock element (human HSE consensus sequence: nTTCnnGAAnnTTCn) in the promoter region of target HSPs. There are multiple HSE within each HSP promoter allowing for binding of multiple HSF1 trimers[67]. In addition, there are interactions between HSF1-HSE and newly recruited activating molecules such as general transcription factors, e.g., ATF1, Mediator complex, elongation factors, the chromatin remodeling complex SWI/SNF, histone modifying proteins, e.g., EP300/CBP, and RNA polymerase II (Pol II)[54,68]. HSF1 transactivation includes continued binding to HSP70 and/or 40 complexes until shortly after HSF1 binds to HSE[63]. HSP70 and/or 40 associate with HSF1 even when it is bound to DNA, and may continue to repress HSF1 until a secondary stimulus promotes its dissociation.

HSE binding can increase HSP gene transcription by over 100-fold[69]. Transcription attenuation is mediated by a negative feedback loop. The newly translated

HSPs themselves, most notably 70 and 40 and potentially 90, bind to the HSF1 transactivation domain (amino acids 440-529, near the HSF1 C-terminus)[63,70]. Then, HSF1 detaches from the promoter region and leaves the nucleus, mediated in part by members of the 14-3-3 regulatory protein family. Preliminary evidence suggests that the HSF1 trimer is converted back to cytoplasmic monomers, but degradation also remains a possibility. Monomeric HSF1 complexes with HSP40, 70, and 90 to re-form the inactive tetramer.

Regulation of HSF1 by Post-translational Modifications

Since HSF1 is present in an inactive form, activation is mediated through PTMs (Figure 1). These include phosphorylation, sumoylation, and acetylation, in addition to 14-3-3 binding. Table 2 lists kinases and associated phosphorylation sites that have been shown or speculated to be involved with HSF1 dissociation (from the inert cytoplasmic heterotetramer), trimerization, nuclear translocation, HSE binding, transactivation, and HSR attenuation[71].

Sourbier, et al., have shown that PKCθ activates HSF1 by S333 phosphorylation in the stress responsive regulatory domain, potentially leading to dissociation of the repressive cytoplasmic HSF1-HSP90 interaction[72]. HSF1-S333A, a mutant HSF1 lacking S333 phosphorylation, associated with endogenous HSP90 to a greater extent than did HSF1-S333E, a mutant HSF1 with constitutively active S333 phosphorylation (phosphomimetic). Also, S333E was twice as efficient at activating HSF1 than S333A.

To date, no published phosphorylation events have been specifically linked to positive regulation of HSF1 trimerization. Kim et al., showed that nuclear translocation is

regulated by PLK1-mediated phospho(p)Serine(S)419, but has no role in HSE binding or transactivation[73]. Also, Murshid, et al., demonstrated that shRNA against PKAcα blocked S320 phosphorylation, preventing HSF1 nuclear translocation in addition to disrupting other activation events discussed below[74].

HSE binding and transactivation are distinct activation steps but are regulated by several common phosphorylation events. pS320 is critical for *hsp70.1* promoter HSE binding, transactivation, and reversal of HSF1 nuclear export[74]. CKII-mediated pT142 phosphorylation is also vital in HSE binding and transactivation[75]. Soncin et al., showed that a T142A mutant inhibits HSE-binding ready nuclear HSF1 and ultimately, *HSP70B* gene transcription. In addition, Holmberg et al., observed that the molar ratio between CaMKII-mediated pS230 and repressive PTM sites determines the magnitude of transactivation[76]. However, pS230 is not needed for either stress-induced HSE binding activity or the formation of nuclear stress bodies (the main site of accumulated HSF1, RNA Pol II, and other RNA-binding proteins in stressed cells).

Two related studies demonstrated that an early phosphorylation event, pS195, is critical for breakage of intramolecular interactions between leucine zipper domains (LZ) 2 and 3, an unmasking step required downstream for HSF1 transactivation[77,78]. In addition, the role of pS326 in transactivation has been widely published on. Guettouche et al., observed in HeLa cervical carcinoma cells that a S326A mutant stimulated HSP70 expression several times worse than wild type HSF1 while having no effect on heat stress-induced DNA binding and nuclear translocation[79]. Li et al., noted that in MDA231 breast cancer cells, direct interaction of mutant p53 with activated pS326 facilitates HSF1

recruitment to HSE and stimulates transactivation under conditions of proteasome inhibition[80].

Chou et al., showed that mTOR is responsible for pS326[81]. Studies have also linked the MAPK/ERK pathway to pS326. However, the role of specific pathway members has not yet been resolved. For example, two studies have shown that MEK directly phosphorylates S326[82,83]. However, Kim et al., concluded that pS326 is catalyzed by ERK1/2[84].

Sumoylation also positively regulates HSF1 activity. Hong et al., observed K298-dependent HSF1 co-localization with SUMO-1 in nuclear stress bodies[85]. K298 mutation resulted in a significant decrease in stress-induced transactivation in vivo. pS303 has been shown to stimulate K298 sumoylation by causing a conformation change that relieves the inhibitory effect of HSF1's lone C-terminal leucine zipper (LZ4)[86].

Interestingly, Raychaudhuri et al., showed that K298 is acetylated during the stress response in addition to K208. Catalyzed by the acetyltransferase EP300, K298 and K208 stabilize and prevent degradation of the HSE-bound HSF1 trimer[87]. EP300 maintains HSF1 stability in a phosphorylation-independent manner[87]. Ten potentially phosphorylated serines were replaced with alanines, yet HSF1 remained acetylation competent. Notably, HSF1 acetylation kinetics do not match those of transactivation[88]. Stabilizing acetylation is delayed upon onset of HSF1 transactivation and persists when HSF1 activity and DNA binding have attenuated.

PTMs also mediate negative regulation. HSF1 is maintained in an inactive heterotetramer by constitutive phosphorylation at S121, S303, S307, and potentially

S363. Liu et al., showed that the linker region enclosing pS121 might be a negative regulator of the monomer to trimer transition[89]. Wang et al., identified MAPKAP-K2 (MKII) as the pS121-specific kinase and noted that pS121 promotes cytoplasmic HSP90 binding to HSF1 to help maintain its inactive state[90]. Another negative regulatory event is ERK1/2-mediated S307 phosphorylation, which has been shown to be a priming event for GSK3β-mediated phosphorylation of S303[91]. pS303 prevents HSF1 trimerization upon stress-induced activation. Thus, the priming requirement by pS307 provides a potential link between the MAPK cascade and HSF1.

However, a contrasting study by Batista-Nascimento et al., showed that when human HSF1 was expressed in yeast, Slt2 (MAPK7) phosphorylated S303 independently of both GSK3β and the pS307 priming event[92]. The authors concluded that differences in HSF1 structure between in vitro and in vivo systems may help to explain why different kinases can mediate S303 phosphorylation under different conditions. Downstream of these phosphorylation events, Wang et al., showed that both GSK3β-mediated pS303 and ERK1-mediated pS307 are prerequisites for HSF1-14-3-3ε binding[93]. HSF1-14-3-3ε binding results in cytoplasmic HSF1 sequestration, specifically of the active, DNA-binding trimers. In addition, Chu et al., demonstrated that pS363 is an early negative regulatory event that ultimately decreases *HSP70*B promoter activity though exactly where this phosphorylation event occurs is unclear[94]. Contrasting studies suggest S363 is phosphorylated by PKCα/ζ (in vivo and in vitro), JNK (in vitro), or ERK (in vitro)[91,94,95].

Post-nuclear translocation negative regulation decreases HSF1 activity through a variety of mechanisms, ultimately leading to HSF1 release from the promoter region of its target gene(s) and export back to the cytoplasm. For example, pS121 can also inhibit

HSE binding[90]. In contrast to the positive regulation K298 sumoylation described above, Brunet Simioni et al., have published on a SUMO-2/3 modification at K298 that has been shown to block transactivation capacity[96]. pS303 is also a pre-requisite for this modification. Large HSP27 oligomers were shown to act as an E3 factor and serve as a scaffold to strengthen the repressive interaction between the SUMO-E2-conjugating enzyme, Ubc9, and HSF1. Furthermore, Raychaudhuri et al., published on two destabilizing acetylation sites, K80 and K118[87]. K80 and K118 acetylation occurs within the HSF1 DNA binding domain (amino acids 16-123) and these events lead to inhibition of chromatin binding by HSF1. This is a crucial step in the regulated release of HSF1 trimers from DNA, ultimately leading to HSR attenuation. K118 is positively regulated by EP300 like its stabilizing counterparts K208 and K298. (K80 was shown to be EP300-independent.) K118 is negatively regulated by the deacetylase, SIRT1. SIRT1 is regulated by AROS (a deacetylase promoter) and DBC1 (a deacetylase inhibitor). Raynes et al., demonstrated that AROS and DBC1 have an impact on HSF1 acetylation status, HSF1 recruitment to the *hsp70* promoter, and *hsp70* transcription[97].

In addition to the roles described above, pS303 and pS307 have also been linked to accelerated HSF1 nuclear export through 14-3-3ε[93]. 14-3-3ε binding influences HSF1 interaction with the nuclear export protein CRM1 and leads to enhanced nuclear export. 14-3-3β binding has also been linked to HSF1 nuclear export[98]. Ultimately, a better understanding of positive and negative regulation through HSF1 PTMs may lead to treatments that alter HSF1 activation and help increase the efficacy of PI-based MM therapy.

HSF1 Inhibition in Cancer Treatment

Targeting HSF1 could be a more effective therapeutic strategy than pursuing individual HSP inhibition. However, developing transcription factor inhibitors is difficult for many reasons. One, transcription factors bind negatively charged DNA and therefore their exposed regions are largely positive. This requires that any inhibitor must be negatively charged, but charged molecules cannot freely diffuse across the cell membrane. Also, the DNA-protein interface is large and developing effective small molecule inhibitors is difficult. To cover the entirety of their binding pockets, a large molecule may have to be developed. Bioavailability may become a concern and promiscuous binding to other targets could cause side effects. Finally, screens for transcription factor inhibitors are less straightforward than those for kinase inhibitors, which are reliant on easier to detect processes such as ATP hydrolysis or phosphate transfer to a substrate. Despite these complexities, multiple HSF1 inhibitor screens have been performed and their various methods are described below.

Whitesell and Lindquist detailed drug-like inhibitors of the HSF1-regulated HSR and concluded that all HSP induction inhibitors suffer from low potency and/or poor specificity[99]. At the time of that publication, those inhibitors included quercetin and its prodrug QC12, NZ28 and its structural analog emunin, KNK437, stresgenin B, and triptolide. Table 2 is an updated HSF1 inhibitor listing and Figure 2 is an illustration of published inhibitor mechanisms. NZ28/emunin and triptolide will be discussed in detail below along with recently published inhibitors, cantharidin, 2,4-bis(4-hydroxybenzyl)phenol, KRIBB11, and Rohinitib (RHT).

NZ28/emunin was discovered as the result of a high-throughput screen for small molecules that inhibit HSP induction[100]. The first step was performing a cell-based screen for inhibitors of HSP-mediated refolding of heat-denatured luciferase followed by a counterscreen for toxicity. The second step was direct testing for HSP induction inhibition by immunoblotting against HSP70. Out of 20,000 compounds from several diversity libraries, emunin was found to sensitize PC-3 human prostate cancer cells and MM.1S to proteasome and HSP90 inhibitors without significant toxicity. However, its precise mechanism HSP translation inhibition mechanism is unknown, and may involve events downstream of HSF1, leading to significant concerns over specificity[99].

Triptolide is a diterpenoid epoxide derived from *Tripterygium wilfordii*, a plant long used in Chinese medicine[101]. Heimberger et al., used triptolide to take advantage of a myeloma cell's sensitivity to proteasome inhibition and subsequent reliance on the cytoprotective HSR[102]. In MM.1S and INA-6 (another human MM cell line), triptolide in combination with bortezomib synergistically induced apoptosis. While this is a promising result, concerns about the specificity of this agent exist. Triptolide interferes with NF-κB, NFAT, AP-1, and p53 activity, and inhibits global gene transcription by inducing RNA Pol II degradation and inhibiting the ATPase activity of the DNA helicase ERCC3[103]. In addition, the in vivo tumor model in mice measuring tumor burden did not extend past 11 days, which raises the question about the durability of triptolide's in vivo effects[102]. While triptolide holds promise as a MM therapeutic, its specific mechanisms must be better understood.

Yoon et al., identified KRIBB11 from a synthetic chemical library screen[104]. A heat shock-dependent luciferase reporter plasmid was used to identify HSF1 inhibitors

and KRIBB11 was chosen for further testing from a ~6,230 compound chemical bank. KRIBB11 abolished heat shock-dependent HSP70 induction through HSF1 inhibition in colon carcinoma HCT-116 cells and also inhibited the growth of HCT-116 cells in a nude mouse xenograft regression model. KRIBB11 inhibited PI or HSP90 inhibitor-mediated HSP induction, indicating its potential use in combination therapy. Interestingly, while KRIBB11 does not inhibit heat shock-induced recruitment of HSF1 to the *hsp70* promoter, it does inhibit P-TEFb (positive transcription elongation factor, a heterodimer of CDK9 and cyclin T) recruitment. This study was able to show by affinity chromatography and competition assays that KRIBB11 specifically inhibits HSF1. In the competition assay, HSF2, HSP90, and CDK9, common HSF1 binding partners, were not detected, thus further strengthening the argument that KRIBB11 is HSF1-specific. In a separate study, Wiita et al., combined KRIBB11 with low-dose bortezomib in MM.1S and saw an additive apoptotic effect[105]. KRIBB11 shows HSF1 specificity and will be worth monitoring as it progresses through further preclinical studies.

Kim et al., identified the blister beetle-derived compound cantharidin as an HSF1 inhibitor from a similar screen to the one used for KRIBB11[106]. Cantharidin was shown to have inhibitory effects on HSP70 and BAG3 expression in HCT-116 cells. Here, cantharidin blocked HSF1-dependent P-TEFb recruitment to the *HSP70* promoter. Cantharidin demonstrated anticancer effects and an additive effect with bortezomib, but its HSF1-specificity is questionable. Cantharidin is known as a PP2A inhibitor[107]. Additionally, it has also been shown to be an activator of serine proteases in epidermal cells[108].

Another natural compound, 2,4-bis(4-hydroxybenzyl)phenol [referred to as (1) in the original publication and here as well], derived from the orchid *Gastrodia elata*, was identified from a screen using a luciferase reporter under the control of a HSE to find inhibitors of HSF1 activity in NCI-H460 human lung cancer cells[109]. Similar to the previously mentioned studies, data from Yoon et al., indicate that (1) can lead to HSP suppression and an increase in apoptosis. The mechanism proposed is that (1) induces degradation of HSF1 through S326 dephosphorylation. However, HSF1 knockdown with siHSF1 + (1) resulted in increased degradation compared to (1) alone, yet cell death with siHSF1 + (1) is less than that of (1) by itself. Therefore, while this study points to a specific mechanism by which its compound works, more work is needed to confirm that observation.

Santagata et al., used a 300,000+ compound chemical screen to look for HSF1 inhibitors and found that the rocaglate, rocaglamide A, was the most potent and selective hit[110]. Rocaglamide A inhibits translation initiation factor eIF4A, thus providing a link between HSF1 and protein translation flux. Rocaglate specificity for HSE reporter activity inhibition was demonstrated by stably transducing NIH3T3-HGL mouse embryonic fibroblasts with two constructs; one encoding a green fluorescent protein (GFP) driven by HSEs and the other encoding a red fluorescent protein (RFP) driven by a doxycycline-regulated control promoter. Rocaglates suppressed GFP but not RFP activity whereas triptolide, quercetin, and KNK437 (among other previously reported HSF1 inhibitors), suppressed both GFP and RFP. An analog, Rohinitib (RHT, for Rocaglate Heat Shock) was found to be more potent than rocaglamide A while retaining similar selectivity and was used for in vivo mouse studies. An M0-91 mouse acute

myeloid leukemia (AML) xenograft model showed that RHT treatment resulted in significantly decreased tumor volume in addition to a dramatic reduction in HSPA8 mRNA. However, rocaglamide derivatives are known to inhibit NF-κB and therefore, RHT HSF1-specificity needs to looked at in further detail[111]. Regardless, investigation of the relationship between the ribosome, translation flux, and HSF1 will provide novel insight into targeting the biology of a cancer cell.

As noted earlier, the main difficulty of finding small molecule transcription factor inhibitors stems from the size and complexity of the DNA-protein interface. In this regard, RNA aptamer technology may prove useful. RNA aptamers are small oligonucleotides that specifically bind to targets such as small proteins[112]. RNA molecules share some common structural features with DNA, and RNA aptamers have been shown to target the DNA-binding domains of molecules such as NF-κB. Though aptamer technology is in its infancy as a therapeutic strategy, it can currently be used for drug target validation. For example, Salamanca, et al., modified iaRNA^{HSF1}, a Drosophila RNA aptamer, to block HSE binding in HeLa cells and promote apoptosis[113].

In addition to direct HSF1 inhibition, targeting its activation by modulating PTMs is also a potential therapeutic strategy. HSF1 PTMs happen in all stages of activation and attenuation as previously described. The majority of published studies on HSF1 PTMs focus on phosphorylation events and their respective kinases. For example, the aforementioned study describing how HSP90 inhibition leads to nuclear HSF1 accumulation also showed that that accumulation was reduced by mTOR inhibition[53]. Therefore, targeting kinases that activate HSF1 could be a simpler way of modulating targeting this pathway than developing HSF1 inhibitors.

Taken together, the findings described here show that HSF1 is involved in several cancers including MM. HSF1 has drawn interest as a biomarker though there are no known translocation groups or mutations associated with its activity[57,114,115]. A broad variety of tumors including carcinomas of the breast, cervix, colon, lung, pancreas and prostate as well as mesenchymal tumors such as meningioma, show increased HSF1 gene copy number, protein expression, or activation compared to their normal counterparts[56,116]. Dai et al., have shown a therapeutic window between cancer and normal cells by demonstrating that HSF1 depletion minimally impacts normal cell viability, whereas cancer cells are strongly affected by HSF1 depletion[117,118]. HSF1 inhibitors will likely play a role in treating a diverse range of malignancies including MM because of HSF1's multifaceted role in promoting tumorigenesis[56,57]. We anticipate that one target MM population will be those who are bortezomib-resistant. An HSF1 inhibitor could help unblock one potential bortezomib resistance mechanism and increase MM apoptosis.

Though there is a demonstrated need for an HSF1 inhibitor, the future of HSF1 drug development will depend in part on the ability for therapeutic agents to be able to effectively and specifically target HSF1. Direct HSF1 inhibition has proven to be an elusive task but the studies presented demonstrate progress. In addition to direct inhibition, new drugs could target HSF1 activation through PTM inhibition; for example, kinase or HDAC inhibition, or anti-SUMO therapies. Regardless of the mechanism, drugs should show the ability to work in tandem with current therapies such as proteasome inhibition because the majority of current induction therapy is based on combination and not single agent treatments.

Conclusions

There is no universal cure for MM but recently developed therapies such as IMiDs and PIs have dramatically increased patient survival. Bortezomib is effective in MM therapy for a variety of reasons including targeting its plasma cell biology. However, MM cells counteract bortezomib treatment by activating the heat shock response. This cytoprotective mechanism is regulated by the master transcription factor, HSF1. Developing a specific and effective HSF1 inhibitor has proven to be a challenge. While that aim is being pursued, a more practical approach is targeting HSF1 regulation. This strategy could have a dramatic impact on patient survival especially when combined with current PI-based therapies, even beyond MM. A genome-wide siRNA screen identified proteasome addiction as a vulnerability of basal-like triple-negative breast cancer (TNBC) cells[119]. MM, TNBC, and bladder cancer are three examples of malignancies whose patients could benefit from a therapeutic strategy of proteasome and HSF1 inhibition.

Acknowledgments

We thank Faith E. Davies for her thoughtful feedback.

Table 1: Human Myeloma Cell Lines

Cell line	Patient age (yrs)	Gender (Male [M], Female [F])	Ethnicity	Isotype	Immunogloublin Translocation	Additional karyotypic characteristics	Notes	Production/secretion
8226	61	M		λ light chain	t(14;16) + t(8;22)	Unstable karyotype in triploid range of 68-70 chromosomes. Two large marker chromosomes with terminal centromeres. t(16;22)(q23;q11) and t(1;14)(p13;q32)	c-maf expression	TGF-β
H929	62	F	Caucasian	IgA κ light chain (Recent tests for IgA, κ have not detected the production of IgA; the cells are producing κ light chain.)	t(4;14)(p16;q32)	Near tetraploid. Most copies of chromosome 8 have the 8q+ abnormality.	The cells have a rearrangement of the c-myc proto oncogene and express c-myc RNA. There is also an activated ras allele and MAF and MMSET overexpression.	
KMS18	60	M		IgA λ light chain	t(4;14)(p16.3;q32.3)		Loss of sequences centromeric to c-MYC. MMSET overexpression.	Ammonia
MM.1s	42	F	Black	IgA λ light chain	t(14;16)(q32;q23) + t(8;14)		Robust MYC expression and c-maf expression	
U266	53	M		IgE λ light chain	t(11;14)		Robust L- and N-MYC expression	TNF-β, IL-6

Table 2: HSF1 Kinases, Their Targets, and Functional Consequences

Kinase	Amino acid target	Functional consequences
AMPKα	S121	Represses HSE binding and promotes HSF1 binding to HSP90
CAMKII	S230	Promotes transactivation
Casein Kinase II	T142	Promotes HSE binding and transactivation
CDK1		Meiosis regulation
ERK1/2	S307,S326,S363	Represses HSE binding and transactivation and is required for 14-3-3ε binding (S307); promotes transactivation (S326) or may inhibit MEK phosphorylation (S326); may repress HSE binding and transactivation (S363)
GSK3α	S303	Represses trimerization and is required for 14-3-3ε binding
JNK	TAD,S307,S320, S363	Promotes transactivation and prolongs nuclear localization of HSF1 (TAD); represses HSE binding and transactivation (S307); promotes nuclear localization, HSE binding, transactivation, and may reverse nuclear export (S320); may repress HSE binding and transactivation (S363)
MAPKAP-K2	S121	Represses HSE binding and promotes HSF1 binding to HSP90
MEK	S326	Promotes transactivation
mTOR	S326	Promotes transactivation
P38MAPK		Promotes HSE binding and transactivation
PI3K	S326	Promotes transactivation
PKAcα	S320	Promotes nuclear localization, HSE binding, transactivation, and may reverse nuclear export
PKCα, θ, ζ	S333,S363	Promotes HSF1 dissociation from HSP90 (S333 [PKCθ only]); may repress HSE binding and transactivation (S363)
PLK1	S216,S419	Mitosis regulation (S216); promotes nuclear translocation (S419)
Rim15		Yeast only; promotes HSE binding when PKA activity is lowered by glucose deprivation
RSK2		Represses HSE binding
Slt2/MAPK7		Represses trimerization
Snf1		Yeast only; promotes HSE transactivation under conditions of glucose deprivation
Yak1		Yeast only; promotes HSE binding when PKA activity is lowered by glucose deprivation

Table 3: HSF1 Inhibitors

Compound	Class
2,4-bis(4-hydroxybenzyl)phenol	Benzyl derivative
Cantharidin	Terpenoid
Emunin	Emetine derivative
KNK437	Benzylidene lactam
KRIBB11	Diaminopyrimidine
NZ28	Emetine derivative
QC12	Quercetin prodrug
Quercetin	Flavonoid
Rohinitib	Flavagline derivative
Stresgenin B	Streptomyces fermentation product
Triptolide	Diterpene triexpoxide

Figure 1A

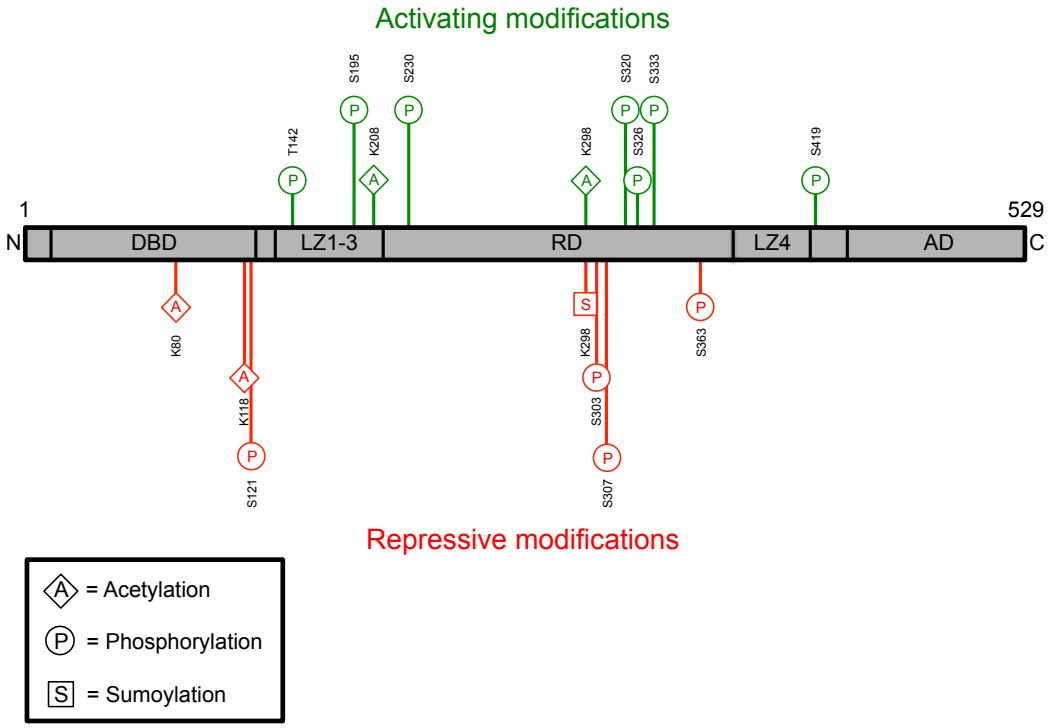

Figure 1A: HSF1 Post-Translational Modifications Heat Shock Factor 1 (HSF1) activating (green) and repressive (red) post-translational modifications (PTMs) are shown above. The bottom left box displays a PTM abbreviation key. Amino acids - K, lysine; S, serine; T, threonine. AD, activation domain; C, c-terminus; DBD, DNA-binding domain; LZ, leucine zipper domain; N, n-terminus; RD, regulatory domain.

Figure 1B

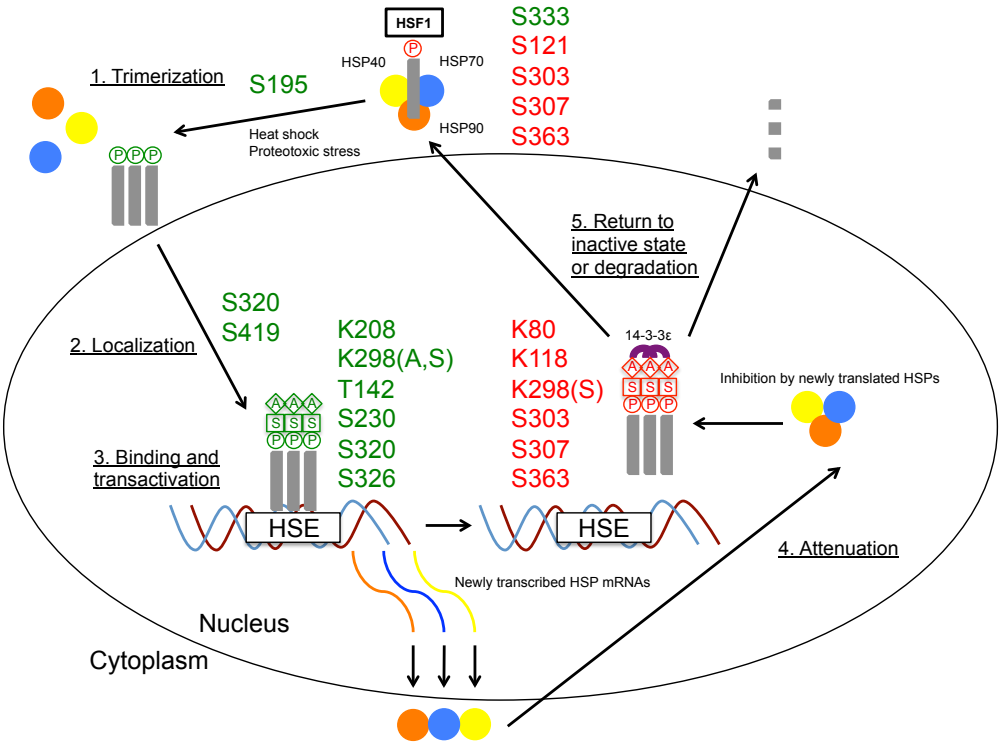

Figure 1B: HSF1 Activation Lifecycle The Heat Shock Factor 1 (HSF1) activation and attenuation cycle, with associated post-translational modifications (PTMs) is shown above. HSF1 forms a constitutively inactive heterotetramer with Heat Shock Protein (HSP) 40, 70, and 90. Serine (S) 121, S303, S307, and S363 phosphorylation aid in heterotetramer maintenance. (1) Upon heat shock or proteotoxic stress, the heterotetramer dissociates and S333 phosphorylation has been linked to dissociation of the repressive HSF1-HSP90 interaction. HSF1 trimerizes and translocates to the nucleus, though which occurs first has not yet been resolved. Here we show trimerization occurring first. S195 phosphorylation occurs concurrently with trimerization but this event effects transactivation downstream and not trimerization. (2) Nuclear localization is positively regulated by S320 and S419 phosphorylation. (3) After trimerization and translocation, HSF1 trimers bind to the Heat Shock Element (HSE) on HSP promoter regions. Binding is followed by transactivation. Binding is positively regulated by T142 and S320 phosphorylation and transactivation is regulated by T142, S230, S320, and S326 phosphorylation, and Lysine (K) 298 sumoylation. In addition, stabilizing acetylation events have been shown at K208 and K298. Notably, stabilizing acetylation is delayed upon transactivation and may proceed even after attenuation has begun. (4) Attenuation is initiated by newly translated HSPs, which bind to HSF1 to block HSE binding and transactivation as part of a regulatory feedback loop. K298 sumoylation and S363 phosphorylation are associated with transactivation repression. Furthermore, K80 and K118 acetylation destabilizes HSE binding. In addition, S303 and S307 phosphorylation are involved in 14-3-3ε binding to HSF1, which helps facilitate its nuclear export. (5) Upon export, HSF1 either returns to its cytoplasmic inactive state or is degraded. A, acetylation; P, phosphorylation; S, sumoylation.

Figure 2

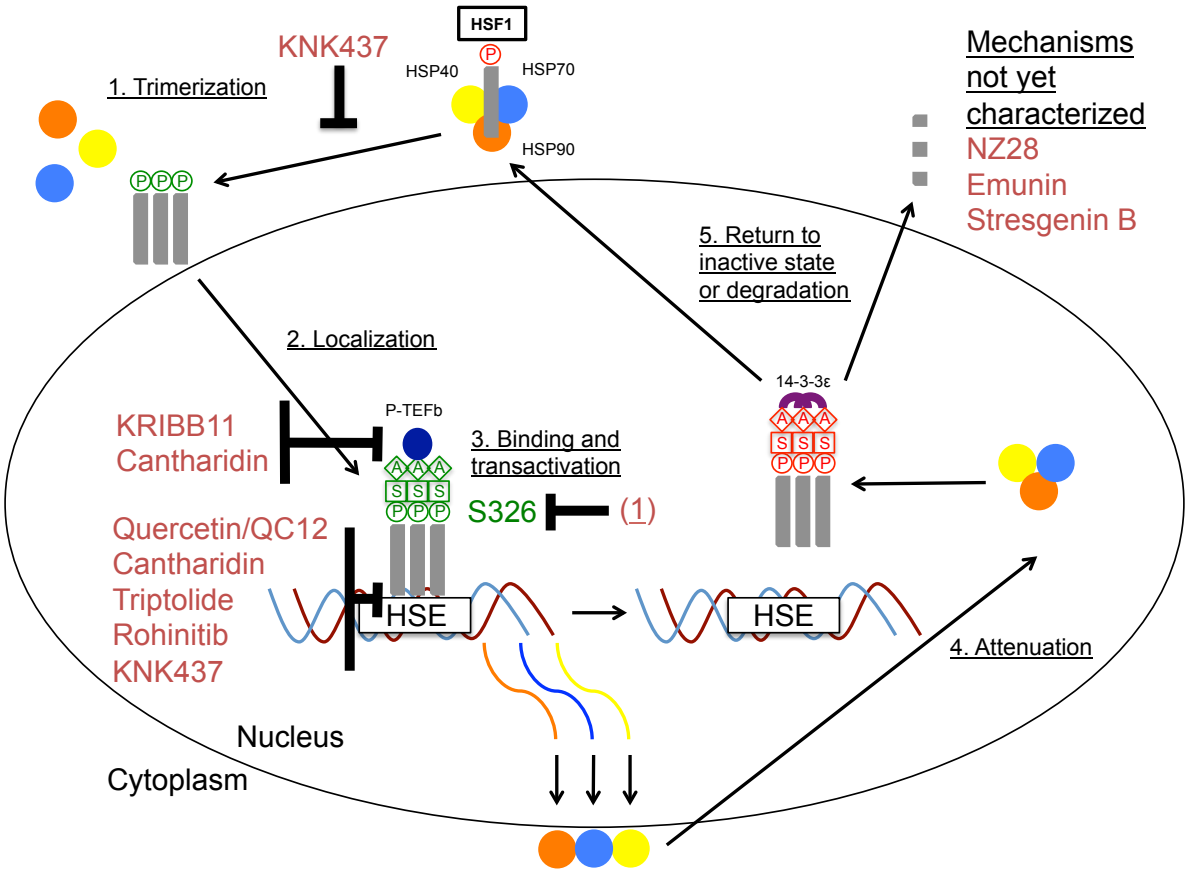

Figure 2: Inhibitors of the HSF1-dependent Heat Shock Response Inhibitors of the Heat Shock Factor 1 (HSF1)-dependent heat shock response are shown above. The mechanism for KRIBB11, Cantharidin, Quercetin/QC12 [a Quercetin prodrug], Triptolide, Rohinitib, and 2,4-Bis(4-hydroxybenzyl)phenol (referred to as (1) above) has been published, while the mechanism for KNK437 has been speculated about. However, the mechanism for NZ28, Emunin, and Stresgenin B remains uncharacterized. (1) KNK437 may repress HSF1 trimerization though no studies have confirmed this hypothesis. (2) To date, no inhibitors have been shown to effect nuclear localization. (3) KRIBB11 and Cantharidin inhibit Positive Transcription Elongation Factor b (P-TEFb) recruitment to HSP promoters. Quercetin/QC12, Cantharidin, and Rohinitib inhibit HSE binding while KNK437 may also inhibit HSE binding. Triptolide inhibits transactivation, and though not shown here, has also been found to decrease HSF1 protein levels in multiple myeloma cell lines.) (1) induces Serine 326 dephosphorylation, leading to a decrease in HSF1 stability and as a result, increased degradation. (4,5) The inhibitor mechanisms presented in (3) accelerate attenuation while no inhibitor to date has been linked to nuclear export. A, acetylation; P, phosphorylation; S, sumoylation.

Statement of Problem

There is no silver bullet for MM, however, the introduction of PIs to MM therapy has dramatically improved patient survival. The PI, bortezomib, was FDA-approved in 2003 for refractory MM and has since become a mainstay of MM therapy. For patients diagnosed between the ages of 65-75, 6-year overall survival increased from 31% for 2001-2005 diagnoses to 56% for 2006-2010 diagnoses in large part due to the introduction of bortezomib.[120] Improving PI-based treatment efficacy and development of new therapies will further increase survival rates and quality of life.

Previous work from our group has shown that PIs work in part because a myeloma cell retains many features of its normal plasma cell counterpart, including reliance on the proteasome for quality control.[3,16] However, all patients encounter PI resistance during treatment. Resistance mechanisms include upregulation of proteasome subunits, alterations of gene and protein expression in stress response, cell survival and antiapoptotic pathways, and multidrug resistance.[121] Activation of the cytoprotective HSR is amongst these. The HSR protects non-malignant cells from stress associated with environmental toxins, radiation, and extreme temperatures by upregulating HSPs. The HSR helps myeloma cells evade bortezomib-induced apoptosis.[32,122,123] Pre-clinical and clinical development of HSP inhibitors has failed to yield an FDA-approved inhibitor.[124] Inhibition of a single HSP can lead to upregulation of other HSPs.[125] Therefore, instead of inhibiting multiple HSPs individually, targeting the master HSR transcription factor, HSF1, is a potential therapeutic strategy.

This work shows that myeloma cells upregulate the HSR in response to bortezomib and that HSF1 knockdown can sensitize cells to PIs. We demonstrate that HSF1 knockdown leads to a greater additive effect on apoptosis than knockdown of multiple HSPs when combined with bortezomib. However, no direct HSF1 inhibitor has advanced to clinical studies, mainly due to inefficacy at therapeutically relevant concentrations or off-target effects.[126] An HSF1 inhibitor alternative is indirect inhibition by targeting HSF1 activation. To inform indirect HSF1 inhibition strategies, we detail regulation of HSF1 activation by PTMs. We show that bortezomib leads to HSF1 phosphorylation and that pS326 is an activating PTM. Additional characterization of pS326 necessitates generation of cell lines stably overexpressing either wildtype HSF1 or an amino acid substitution. These cell lines can inform HSF1 activation studies. We generated these cell lines and show that HSF1 overexpression results in downregulation of the bortezomib-induced heat shock response and sensitization to bortezomib-induced apoptosis. Therefore, to further characterize pS326, an alternative approach such as kinase inhibition studies is required.

Previous studies have detailed putative upstream and in-vitro kinases responsible for pS326, but none has been shown to be directly responsible for pS326 under conditions of proteasome inhibition in myeloma cells.[79,81] Therefore, we characterize candidate kinases and show that the kinase is cytosolic. In addition, we show that pS326 inhibition is a novel mechanism of action for the multikinase inhibitor TG02. A TG02 and PI combination treatment leads to an additive effect on apoptosis in myeloma cells, and this effect is due in part to inhibition of bortezomib-induced HSP upregulation.

We were unable to identify the specific kinase responsible for serine 326 phosphorylation, however, our data provide insight into inhibition of this PTM. We infer that the kinase is a currently uncharacterized cytosolic TG02 target. Future studies can follow up on our work to find this needle in a haystack. Kinase inhibitor introduction to PI-based therapy could result in inhibition of HSF1 activation and downregulation of the PI-induced HSR, leading to greater PI sensitization. PI-based therapy improvements and new drug development will increase patient overall and long-term progression-free survival, and could ultimately lead to the eradication of this disease which takes away hundreds of loved ones every day.

II. HSF1-MEDIATED REGULATION OF BORTEZOMIB-INDUCED HEAT SHOCK RESPONSE IN MULTIPLE MYELOMA

(*Originally published in Oncotarget, July 26, 2016*)

Bortezomib-Induced Heat Shock Response Protects Multiple Myeloma Cells and is Activated by Heat Shock Factor 1 Serine 326 Phosphorylation

Shardule P. Shah[1], Ajay K. Nooka[1], David L. Jaye[1,2], Nizar J. Bahlis[3], Sagar Lonial[1], and Lawrence H. Boise[1]

[1]Department of Hematology and Medical Oncology, Winship Cancer Institute of Emory University and the Emory University School of Medicine, Atlanta, GA; [2]Department of Pathology and Laboratory Medicine, Emory University School of Medicine, Atlanta, GA; and [3]Department of Medical Oncology and Hematology, Tom Baker Cancer Center, Calgary, AB, Canada

Correspondence:

Lawrence H. Boise

Department of Hematology and Medical Oncology

Winship Cancer Institute of Emory University, Emory University School of Medicine

1365 Clifton Road NE, Room C4012, Atlanta, GA 30322

Phone: 404-778-4724, Fax: 404-778-5530, E-mail: lboise@emory.edu

Keywords: Myeloma, bortezomib, heat shock, HSF1

Figures: 5 Tables: 1

Supplementary document: Methods, 1 figure, 1 table

Abstract

Proteasome inhibitors such as bortezomib are highly active in multiple myeloma by affecting signaling cascades and leading to a toxic buildup of misfolded proteins. Bortezomib-treated cells activate the cytoprotective heat shock response (HSR), including upregulation of heat shock proteins (HSPs). Here we inhibited the bortezomib-induced HSR by silencing its master regulator, Heat Shock Factor 1 (HSF1). HSF1 silencing led to bortezomib sensitization. In contrast, silencing of individual and combination HSPs, except HSP40β, did not result in significant bortezomib sensitization. However, HSP40β did not entirely account for increased bortezomib sensitivity upon HSF1 silencing. To determine the mechanism of HSF1 activation, we assessed phosphorylation and observed bortezomib-inducible phosphorylation in cell lines and patient samples. We determined that this bortezomib-inducible event is phosphorylation at serine 326. Prior clinical use of HSP inhibitors in combination with bortezomib has been disappointing in multiple myeloma therapy. Our results provide a rationale for targeting HSF1 activation in combination with bortezomib to enhance multiple myeloma treatment efficacy.

Introduction

In 2016, an estimated 30,330 people will be diagnosed with multiple myeloma, a plasma cell malignancy that historically affects older individuals[127]. Unlike most cancers, myeloma cells retain many of the same functions as their normal counterpart, long-lived bone marrow plasma cells, including immunoglobulin secretion[3]. Because plasma cells are constitutive immunoglobulin producers, they are dependent on the proteasome for quality control and survival, and myeloma cells also retain this dependence[3,16]. Bortezomib is a boronic acid-based proteasome inhibitor which inhibits the β5-subunit of the proteasome. Bortezomib has been a mainstay of myeloma therapy since its Food and Drug Administration (FDA) approval for refractory myeloma in 2003[7]. The use of bortezomib in combinatorial treatment regimens along with immunomodulatory drugs (IMiDs) has led to a dramatic improvement both in overall survival [OS] (46.6% five-year OS in 2005-2011 versus 29.7% in 1986-1990) and long-term progression-free survival [PFS] (36.0 months median PFS versus 29.7 months with bortezomib plus dexamethasone versus vincristine, doxorubicin, plus dexamethasone [VAD])[127,128]. Two additional proteasome inhibitors have recently been FDA-approved for myeloma therapy, highlighting the importance of this class of agents for the treatment of this disease[29,129-134].

Bortezomib-based regimens have led to remarkable improvement in myeloma patient outcomes. However, maximizing their utility may be difficult because myeloma cells can hijack cytoprotective processes used by normal plasma cells. Myeloma cells are able to counteract the pro-apoptotic effects of bortezomib through upregulation of pro-survival pathways, including the heat shock response (HSR)[11]. The HSR protects healthy

cells from stressors such as cold, UV light, and environmental toxins, and myeloma cells activate this cytoprotective mechanism to presumably protect themselves from bortezomib-mediated apoptosis. The HSR is mediated by heat shock proteins (HSPs). HSPs serve a wide variety of functions, but are primarily involved in protein folding and protein homeostasis regulation[32,135]. HSP inhibitors have been tested in myeloma clinical studies both as single agents and in combination with bortezomib[136,137]. However, none have been FDA-approved because HSP inhibitors suffer from low potency at clinically relevant levels and an induction in compensatory HSPs[37,45]. In addition, which HSPs are most critical to mounting a robust HSR is unknown. To counteract this, one strategy is to treat patients with multiple HSP inhibitors, a strategy limited by the presence of over 97 HSP-encoding genes[33]. Therefore, inhibition of bortezomib-mediated HSP induction may require dozens of inhibitors and is not a viable therapeutic approach.

Another strategy is to inhibit multiple HSPs simultaneously by targeting the master transcription factor of the HSR, Heat Shock Factor 1 (HSF1). Under baseline conditions, HSF1 is in an inactive cytoplasmic heterotetramer with HSP40, HSP70, and HSP90[63]. Maintenance of this heterotetramer is controlled by constitutive post-translational modifications (PTMs) such as phosphorylation of HSF1 at serine 303 (pS303) and pS307[91]. Upon proteotoxic stress such as proteasome inhibition, the HSR is induced, leading to dissociation of the inactive heterotetramer, HSF1 trimerization and nuclear translocation, and binding to the heat shock element (HSE) of HSP genes[138]. HSF1 pS419, pS230, pS320, and pS326, among other modifications, have been reported to positively regulate HSF1 activity[73,74,76,79,139,140]. During attenuation of the HSR, HSF1 exits the nucleus, and is either degraded or returns to its inactive state[58].

Here, we show that HSF1 knockdown sensitizes myeloma cells to bortezomib treatment. In addition, we demonstrate that targeting HSF1 is a more effective therapeutic approach than targeting multiple HSPs. Therefore, targeting HSF1 activation and associated bortezomib-induced PTMs is a potential therapeutic approach. We further demonstrate that bortezomib induces phosphorylation of HSF1 on serine 326. Together, these data provide evidence that in order to enhance the efficacy of proteasome inhibition in myeloma treatment, targeting HSF1 is an effective therapeutic strategy.

Results

Bortezomib-treated myeloma cell lines induce a cytoprotective HSR, characterized by HSP induction and HSF1 mediates this response. Therefore, we wanted to determine whether bortezomib treatment of myeloma patient samples led to HSP gene expression upregulation. RNA was extracted from isolated CD138+ cells from four different myeloma patients following bortezomib treatment (Figure 1A). cDNA was probed for changes in HSP and HSF1 gene expression using qPCR. Bortezomib did not lead to HSF1 gene expression induction. This finding is not surprising because HSF1 expression and activity are regulated at the post-transcriptional level[75,79,86,91,94,140-143]. Consistent with previous studies, HSP gene induction was observed in every patient sample and though there was a variable induction pattern between patient samples, HSPA1A was consistently the most upregulated gene followed by HSPA1B. Both of these isoforms code for HSP70. In addition, strong HSP90AA1 (HSP90α) and DNAJB1 (HSP40β) induction was observed.

We then wanted to characterize HSP and HSF1 protein expression before and after bortezomib treatment in four cell lines: MM.1S, KMS18, U266, and RPMI-8226 [8226] (Figure 1B). Consistent with previous findings, bortezomib treatment resulted in the induction of the HSR in all four lines, however the responses were somewhat varied. MM.1S cells showed strong HSP27, HSP40β, HSP70, and HSP105 induction. KMS18 cells showed strong HSP27, HSP40β, and HSP105 and modest HSP70 induction. U266 cells showed strong HSP40β and HSP70 induction while HSP105 was not detected. 8226 cells showed strong HSP40β and modest HSP70 induction and HSP105 was not detected. Baseline HSP90α levels were high in all four lines and none showed strong induction of HSP90α. Notably, baseline HSP27 and HSP70 levels were higher in 8226 cells than in the other cell lines. Also, though HSP induction varied between cell lines, none showed an increase in HSF1 expression. The observed HSF1 gel shift upon bortezomib treatment is consistent with HSF1 post-translational modification. We also probed for HSP and HSF1 expression in bortezomib-treated isolated CD138+ cells from four different myeloma patients (Figure 1C). Consistent with the results in cell lines, bortezomib induced various HSP and did not increase HSF1 expression.

Since HSPs are cytoprotective, a strategy to enhance bortezomib-mediated apoptosis is to reduce HSP induction. Previous studies have concluded that single HSP knockdown may not induce lethality in myeloma and as seen above, bortezomib leads to the induction of a variable pattern of multiple HSPs. Therefore, one approach to enhance bortezomib-mediated apoptosis is to target multiple HSPs either individually or simultaneously. However, identifying and targeting the correct HSP(s) has proven to be a challenge due to the variability observed in the HSR in different samples (Figure 1B-

C). Therefore, we used siRNA to knock down HSF1 (Figure 1D). We treated the four cell lines with HSF1 siRNA and bortezomib. HSF1 knockdown led to a decrease in bortezomib-mediated HSP induction to various degrees, with the exception of HSP90α, which showed minimal decrease in protein expression. HSF1 siRNA treatment resulted in minimal induction of cell death while bortezomib treatment resulted in cell-line and dose-dependent moderate to high apoptosis (Figure 1E). However, with an HSF1 siRNA and bortezomib combination, we observed a greater than additive apoptotic effect with MM.1S and KMS18 cells, an additive effect with U266 cells, and no effect with 8226 cells. Therefore, targeting the global response instead of individual HSPs may be a more effective means to sensitize myeloma cells to proteasome inhibition.

To determine if knockdown of expression of one or more HSP was responsible for the increased apoptosis observed with HSF1 knockdown, we used an 84-gene HSP gene expression array (Figure 2A). We treated MM.1S cells with bortezomib and HSF1 siRNA and probed for changes in HSP gene expression. We found several patterns of gene expression in this 84-gene panel, including genes that were induced by HSF1 silencing in the absence or presence of bortezomib (Supplementary Table 1). However we focused on genes that were induced by bortezomib (Figure 2A, zoomed region). Of the 17 genes induced at least twofold by bortezomib, the induction of 10 was inhibited by at least 50% by HSF1 silencing (Figure 2A). We independently confirmed these genes as HSF1-dependent by qRT-PCR (Figure 2B).

Next, to determine if one or more HSP was responsible for the observed HSF1 protective effect, we compared the effect of HSF1 silencing to silencing specific HSPs on bortezomib-induced apoptosis (Figures 2C and Supplementary Figure 1). Only the

silencing of DNAJB1 (HSP40β) showed a significant increase in bortezomib-induced apoptosis when compared to a control siRNA. However, the apoptosis seen with DNAJB1 siRNA and bortezomib was significantly lower than that of HSF1 siRNA and bortezomib. Therefore, no individual HSP can account for HSF1's observed protective effect. To further explore DNAJB1's role in the HSR, we treated MM.1S cells with DNAJB1 or HSF1 siRNA with bortezomib and probed for various HSP genes (Figure 2D). DNAJB1 knockdown led to significant reduction of HSP90AA1 and HSP90AB1 bortezomib-mediated induction, but not nearly to the same level as HSF1 knockdown. DNAJB1 knockdown and HSF1 knockdown resulted in similar reduction of DNAJB1 induction. However, DNAJB1 knockdown did not lead to reduction of CRYAB, HSPA1A, and HSPA1B gene induction. Thus while DNAJB1 knockdown influences the HSR, which likely accounts for its protective effects, it does not fully replicate the activity of HSF1.

Our data suggest that silencing HSF1 sensitizes cells to bortezomib through its regulation of multiple HSRs. Therefore, we next tested if simultaneous knockdown of multiple HSP genes could replicate the apoptotic or regulatory effects of HSF1 knockdown upon bortezomib treatment. We silenced the three most HSF1-dependent HSP genes as listed in Figure 2A; HSPA1A, HSPA1B, and DNAJB1 (simultaneous knockdown of all three = 3X), and determined the effect on gene expression (Figure 2E) and apoptosis (Figure 2F). At the gene expression level, there was no evidence that individual HSPA1A and HSPA1B knockdown had any regulatory effect on the expression of other HSPs. Silencing of all three HSPs did not significantly reduce HSP gene induction levels below individual siRNA treatment. Additionally, inducible HSP

levels remained significantly above that of HSF1 siRNA. Silencing of all three HSPs with bortezomib resulted in higher apoptosis than bortezomib alone, HSPA1A siRNA with bortezomib, and HSPA1B with bortezomib. Apoptosis was similar to DNAJB1 siRNA with bortezomib, and lower compared to HSF1 siRNA with bortezomib. Taken together these data suggest that expression of the three most bortezomib-induced HSF1-dependent HSP genes cannot account for the survival effects of HSF1 knockdown. These findings imply that targeting HSF1 would be a more effective approach than targeting HSPs to enhance proteasome inhibitor activity.

Currently, there are no HSF1 inhibitors that are FDA-approved or even in clinical trials, and published data for many inhibitors raise questions ranging from specificity to efficacy[99,140]. Therefore, we pursued an approach targeting HSF1 activation, and specifically, PTMs that mediate activation. Based on prior studies of HSF1 activation, we initially focused on bortezomib-induced changes in phosphorylation. To demonstrate that HSF1 is modified by phosphorylation, we used Phos-Tag™ electrophoresis[144]. We employed this technique to detect HSF1 constitutive and bortezomib-induced phosphorylation patterns in MM.1S and KMS18 cells. In these cell lines, under baseline conditions, there are two bands: one showing unphosphorylated HSF1 and one, which is sensitive to λ phosphatase treatment, demonstrating constitutive HSF1 phosphorylation. Bortezomib treatment led to the presence of an HSF1-inducible phosphorylation band while unphosphorylated and constitutively phosphorylated HSF1 expression decreased. In three different patient samples, bortezomib treatment also led to the presence of an inducible HSF1 phospho-species (Figure 3B). Two of these samples also showed strong bortezomib-inducible HSP upregulation (Figure 1C).

Next, we wanted to identify HSF1 phospho-species detected by Phos-Tag™. Therefore, we performed phosphoproteomic analysis to detect HSF1 phospho-species with and without bortezomib treatment in MM.1S and KMS18 (Figure 4). One inducible site, phosphoserine (pS) 326 was detected in both lines. Constitutive pS13, pS303, pS307, and pS363 was observed in both lines while constitutive pS368 was seen in KMS18 but not MM.1S cells. Notably pS13 and pS368 are previously undescribed HSF1 phosphorylation sites, and bortezomib treatment decreased pS363 expression in MM.1S cells. Inducible pS314 was observed in MM.1S but not KMS18 cells. Using these data, we tested available HSF1 phopshoantibodies, pS326 and pS303. We treated MM.1S, KMS18, and 8226 cells with bortezomib for 24h, collected protein lysates at various timepoints, and probed for pS326 and pS303 expression (Figure 5A). For all three lines, pS326 expression was minimally present at 0h and increased at each timepoint until 9h in MM.1S and KMS18 cells and 6h in 8226 cells. pS326 expression decreased to near baseline levels by 24h. This finding confirmed phosphoproteomics studies of MM.1S and KMS18 cells that detected S326 as a bortezomib-inducible phosphorylation site. Also, in MM.1S and KMS18 cells, there was a stronger pS326 peak than in 8226 cells, and taken together with data shown above, provides evidence of a more robust bortezomib-induced HSR in MM.1S and KMS18 than 8226 cells. For pS303, we confirmed a constitutive phosphorylation pattern in MM.1S, KMS18, and 8226 cells. However, pS303 expression decreased with bortezomib treatment in 8226 cells. This differential expression pattern may be due to the lack of a strong HSR in 8226 cells. As a result, 8226 HSF1 modifications associated with HSR negative regulation may not be as active. In addition, we used Phos-Tag™ and available HSF1

phosphoantibodies to determine the contribution of pS326 to total HSF1 inducible phosphorylation (Figure 5B). We observed that phosphorylation at serine 326 is responsible for HSF1 inducible phosphorylation. In agreement with data shown above, pS326 increases in all three lines, with a 9h peak in MM.1S and KMS18 cells and 6h in 8226 cells. Additional phosphorylation events, as visualized by the intermediate bands showing phospho-species in membranes probed for total HSF1, precede inducible pS326 phosphorylation. However, their identity could not be determined. HSP60 is a mitochondrial HSP and known as a "housekeeping protein". Here, it is used as a loading control. In a patient sample, pS326 is also responsible for HSF1 inducible phosphorylation (Figures 5C and 3B). In addition, we analyzed constitutive and inducible pS326 expression in MM.1S cells by immunocytochemistry (Figure 5D). Cells were stained with pS326 and counterstained with hematoxylin. We observed that bortezomib leads to a strong induction of nuclear pS326.

Discussion

Bortezomib has been a mainstay of myeloma therapy since its FDA approval in 2003 and is commonly used in combination with cyclophosphamide, melphalan, prednisone, IMiDs, and dexamethasone[145]. Bortezomib-based regimens have significantly improved patient survival, but bortezomib resistance is common and can lead to relapse[146]. Here, we confirmed that bortezomib treatment leads to upregulation of the cytoprotective HSR (Figure 1A-C). Strategies to downregulate the HSR in myeloma have not been successful in clinical trials. For example, HSP90 inhibitors have been tested in clinical trials but have not been effective in myeloma[136,137,147]. Interestingly, our

data show that bortezomib treatment did not lead to HSP90 induction in any of the four cell lines tested (Figure 1B). This result differs from previously published reports. However these early studies used very high concentrations of bortezomib that resulted in only modest changes at the protein level[11]. Therefore, one of the reasons why HSP90 inhibition may not be sufficient in combination with bortezomib is because myeloma cells have constitutively high HSP90 protein expression that does not significantly increase with bortezomib treatment.

Instead of attenuating the bortezomib-induced HSR with multiple HSP inhibitors, we hypothesized that knocking down HSF1 would inhibit bortezomib-induced upregulation of the HSR and sensitize myeloma cells to bortezomib treatment (Figure 1D). HSF1 knockdown led to inhibition of the HSR in all four cell lines tested, and bortezomib sensitization in three (Figure 1E). The fourth line, 8226, had higher baseline levels of HSP27 and 70 than the other cell lines, thus leading to the observation that HSF1 knockdown may not have as strong of an effect on survival because the bortezomib-induced HSR is more robust in the other cell lines compared to 8226. This result is consistent with our previous findings demonstrating that 8226 is more efficient at IgL secretion than MM.1S, which suggests that IgL production does not contribute as heavily to proteasome load in this cell line[16]. Clinical bortezomib resistance may arise when patient myeloma cells that were once responsive to bortezomib deregulate the HSR. This could lead to an increase in basal HSP levels and loss of bortezomib sensitivity.

Since HSPs have proven to be targetable by small molecule inhibitors, we next determined whether a single or multiple HSPs were responsible for HSF1-depdendent survival following proteasome inhibition. Consistent with the HSR being a systemic

response to stress, we demonstrated that 9 HSPs were upregulated in an HSF1-dependent fashion (Figure 2A). It is not surprising, therefore, that silencing of any single HSP or even the three most HSF1-dependent HSPs was not as effective as silencing HSF1 (Figure 2C-F). Taken together, these data suggest that targeting HSF1 would be a more promising approach to bortezomib sensitization than targeting individual or even multiple HSPs. Interestingly, while several small molecule inhibitors of HSF1 have been reported, most are not specific for HSF1[99,104,106,109,140,148,149]. Pre-clinical studies using HSF1 inhibitors alone or in combination with existing treatments such as bortezomib are limited and it remains unclear if these inhibitors can be developed into therapeutic agents [102,150]. In addition, previous studies have pointed to HSF1 activation as a critical component of the cellular response to proteasome inhibition[59,105]. Therefore we focused on targeting HSF1 activation upon proteasome inhibition in myeloma cells.

The activation of HSF1 occurs through post-translational modifications that allow this transcription factor to be released from HSP binding, move to the nucleus, bind DNA, and activate transcription from HSE-containing promoters. We showed that HSF1 is phosphorylated upon bortezomib treatment in cell lines and patient samples and identified and confirmed an inducible phosphorylation site, serine 326 (Figures 3-4). We also confirmed that bortezomib treatment leads to nuclear pS326 accumulation (Figure 5). pS326 has been shown to positively regulate HSF1 transactivation on HSE-containing promoters in HeLa cervical carcinoma cells and MDA-MB-231 breast cancer cells[81,151]. In addition, hyperphosphorylation of serine 326, which is upregulated in breast cancer compared with its normal counterparts, has been used as a biomarker to indicate HSF1 activation in immortalized primary mammary epithelial tumor cells[56,152].

DNA-PK, ERK1/2, MEK, mTOR, and PI3K have been shown to be responsible for serine 326 phosphorylation in various systems[79,81,93,139,152,153]. Knowledge of which kinase is responsible for this phosphorylation event upon bortezomib treatment in myeloma could facilitate development of effective kinase and proteasome inhibitor combination treatments. These treatments could dampen the bortezomib-induced HSR and increase myeloma cell apoptosis. We have initiated studies to determine the bortezomib-inducible HSF1 kinase and our preliminary data show that the responsible kinase is not JAK, JNK, or MEK (S.P.S. and L.H.B., unpublished data, April 2016).

Future studies should explore the role of other HSF1 phosphorylation sites in myeloma beyond serine 326, including sites of constitutive phosphorylation. Our data show constitutive phosphorylation on serine 13, 303, 307, and 363, and 368. In agreement, others have shown constitutive phosphorylation on serine 303 (catalyzed by GSK3α/β), 307 (ERK1/2, JNK), and 363 (JNK, PKC) in other systems[79,86,91,94]. Serine 13 and 368 are previously undescribed sites and require further exploration with regard to their role in HSF1 activation. Promoting constitutive phosphorylation events could keep HSF1 from becoming fully activated, thus leading to a downregulated HSR. Therefore, knowledge of constitutive phosphorylation events and their respective kinases could lead to additional types of combinatorial treatments, such as pairing phosphatase inhibitors with proteasome inhibitors.

Kinase and proteasome inhibitor combination treatments are currently being studied in myeloma, including combining aurora-A, Chk1, CDK, Akt, MEK, mTOR, PI3K, and p38 inhibitors with bortezomib[154,155]. Interestingly, the latter five kinases have been reported to phosphorylate HSF1[140]. Furthermore, a recent study found that

bortezomib treatment increases Pim half-life by prevention of Pim proteasomal degradation and therefore, the inclusion of a Pim kinase inhibitor in a bortezomib-based regimen could be effective in myeloma treatment[156]. In addition to phosphorylation, HSF1 PTMs include acetylation and sumoylation. A more detailed understanding of these modifications could provide rationale to test, for example, acetylase/deacetylase inhibitors and SUMOylation inhibitors in combination with bortezomib. For example, SIRT1, an NAD+-dependent deacetylase, has been reported to aid in HSF1 binding to HSE-containing promoters of HSP genes[65,88]. Therefore, a SIRT1 inhibitor could potentially downregulate the bortezomib-induced HSR.

The data presented in this study show that myeloma cells activate the HSR in response to bortezomib and that targeting HSF1 can downregulate the HSR and sensitize cells to bortezomib treatment. Here, we provide a rationale for pairing bortezomib with an HSF1 inhibitor or drugs that target HSF1 PTMs to enhance the efficacy of bortezomib-based treatment regimens. This novel therapeutic strategy could lead to improved progression-free and overall survival for myeloma patients.

Materials and Methods

Cell Lines

The MM.1S cell line was obtained from Dr. Steven Rosen (City of Hope, Duarte, CA) and Dr. P. Leif Bergsagel (Mayo Clinic, Scottsdale, AZ) provided the KMS-18 cell line. RPMI-8226 (8226/S) and U266 cell lines were purchased from American Type Culture Collection (Manassas, VA). Cells were cultured as previously described[157]. MM.1S and 8226 cell lines were tested and authenticated by sequencing. KMS18 cell line was tested

and authenticated by flow cytometry. U266 was not authenticated after purchase; however, phenotypic analysis is consistent with known features for this line, e.g., CCND1 overexpression and BRAF activation.

siRNA and Bortezomib Treatment

siRNA was obtained from Dharmacon RNA Technologies (GE Healthcare, Little Chalfont, United Kingdom), selecting the ON-TARGETplus SMARTpool duplexes as the RNAi-specific technology platform. ON-TARGETplus Non-targeting Control Pool was used as a control. 48h viability after ON-TARGETplus Non-targeting Control Pool electroporation was greater than 90% for MM.1S, KMS18, and U266 and greater than 75% for 8226 (data not shown). Cells were transfected using the Amaxa Nucleofector II (Lonza Group, Basel, Switzerland). The following cell lines, reagents, and programs were used: MM.1S: V reagent, program O-023; KMS18: C, T-001; U266: R, X-005; 8226: V, G-015. The following oligonucleotides were used: ON-TARGETplus Non-targeting Control Pool: D-001810-10-20 and ON-TARGETplus SMARTpool: L-009743-00-0005 (CRYAB), L-012735-01-0005 (DNAJB1), L-021141-01-0005 (DNAJC17), L-012109-00-0010 (HSF1), L-005168-00-0005 (HSPA1A), L-003501-00-0005 (HSPA1B), L-005186-00-0005 (HSPCA [HSP90AA1]), L-005187-00-0005 (HSPCB [HSP90AB1]), L-005269-00-0005 (HSPB1), and L-004972-00-0005 (HSPH1). Bortezomib was obtained from LC Laboratories (Woburn, MA).

Flow Cytometry Cell Death Detection

Cells were collected at indicated timepoints. $1.0x10^5$-$2.5x10^5$ million cells were washed with 1X phosphate buffered saline (PBS) and resuspended in 500 µL FACS buffer (1% BSA in PBS containing 0.01% sodium azide) containing BioVision 1001-1000 Annexin

V-FITC (BioVision, San Francisco, CA) and 1 mg/ml propidium iodide (Sigma-Aldrich, St. Louis, MO). Cell death was then measured with a BD FACSCanto II as previously described[158]. Data were analyzed using FlowJo software (TreeStar, Ashland, OR).

Immunoblotting

Protein lysate preparation and western blotting were performed as previously described with the following change[157]. PVDF membranes were used and membranes were pre-wet in methanol for two minutes and then incubated in transfer buffer for five minutes. The following primary antibodies were used: rat anti-HSF1 mAb (Enzo Lifesciences, Farmingdale, NY), rabbit anti-HSP27 pAb (Enzo), rabbit anti-DNAJB1/HSP40β pAb (Enzo), rabbit anti-DNAJC17/HSP40C pAb (Abcam, Cambridge, United Kingdom), mouse anti-HSP70/72 mAb (Enzo), rat anti-HSP90α mAb (Enzo), mouse anti-HSP90β mAb, rabbit anti-HSP105/110 pAb (Enzo), rabbit anti-HSF1 phospho-serine (pS) 326 (Abcam), and rabbit anti-HSF1 pS303 (Abcam). The following secondary antibodies were used: ECL Rabbit IgG HRP-linked whole Ab (from donkey) (GE Healthcare), ECL Mouse IgG HRP-linked fragment Ab (from sheep) (GE Healthcare) [for all mouse antibodies except anti-HSP90β], goat anti-mouse IgG HRP (PerkinElmer Life Sciences, Boston, MA) [for anti-HSP90β], and goat anti-rat IgG HRP (Santa Cruz Biotechnology, Santa Cruz, CA).

Patient Samples

A patient sample diagnostics table is provided (Table 1). Ficoll isolated buffy coat from myeloma patient bone marrow aspirates were collected and washed with RPMI 1640 complete medium. CD138+ plasma cells were isolated using CD138 microbeads and MACS Columns as per manufacturer's instructions (Miltenyi Biotec, Bergisch Gladbach,

Germany), placed in RPMI 1640 complete medium, and bortezomib-treated at indicated concentrations. All samples were collected from patients who gave prior written consent as per an Institutional Review Board-approved protocol.

RT-PCR and qPCR

cDNA was prepared from RNA using the ABI high capacity cDNA kit (Thermo Fisher Scientific, Waltham, MA). qPCR was performed using TaqMan gene expression master mix (ABI 4368814) with an ABI 9600 Fast thermocycler as previously described[157]. The following ABI probes were used (Thermo Fisher Scientific): BAG3 (Hs00188713_m1), CRYAB (Hs00157107_m1), DNAJB1 (Hs00428680_m1), DNAJC17 (Hs01118821_g1), HSF1 (Hs00232134_m1), HSP90AA1 (Hs00743767_sH), HSP90AB1 (Hs01546471_g1), HSPA1A (Hs00359163_s1), HSPA1B (Hs01040501_sH), HSPB1 (Hs03044127_g1), HSPH1 (Hs00971475_m1) and GAPDH (Hs02758991_g1). For the 84-gene HSP expression array, the QIAGEN© Human Heat Shock Array qPCR Panel (PAHS-076C) was used according to manufacturer's instructions.

Phos-Tag™

Protein lysates in 1X Protein MetalloPhosphatases (PMP) and 1X $MnCl_2$ were treated with 64 units lambda (λ) phosphatase (New England Biolabs, Ipswich, MA) as per manufacturer's instructions. Protein was resolved on 50μM Phos-Tag™ (Wako Pure Chemical Industries, Osaka, Japan), 8% SDS-polyacrylamide gels as per manufacturer's instructions. Subsequent protein transfer and expression analysis was performed as described above.

Immunoprecipitation and Phosphoproteomics

Protein lysates were collected as described above. Lysates were precleared using Protein G Agarose, FastFlow (Millipore, Temecula, CA) as per manufacturer's instructions and antibody complex was formed using Preclearing Matrix B-rabbit: sc-45059 (Santa Cruz) and rabbit anti-HSF1 (Enzo) as per manufacturer's instructions. Precleared lysate was incubated with the antibody complex, and bound eluate was either resolved on a Mini-PROTEAN® precast gel (Bio-Rad) and subsequently Coomassie stained (Bio-Rad) as per manufacturer's instructions, or the antibody complex was collected. Excised gel bands of interest or the antibody complex were sent to the Emory University School of Medicine Integrated Proteomics Core for liquid chromatography tandem mass spectrometry (LC-MS/MS) analysis (Supplementary Methods)[159].

Immunocytochemistry

MM.1S cell pellets underwent formalin fixation and paraffin embedding. Immunostaining of cell block sections was performed essentially as described on a Dako autostainer[160]. Antigen unmasking employed Target Retrieval Solution citrate buffer (Dako). Anti-pS326-HSF1 was used at a 1:2000 dilution and bound antibody was detected with Envision dual link kit with standard DAB reactions (Dako). Hematoxylin counterstained sections were mounted for light microscopy.

Acknowledgments

We thank Duc Duong, Dr. Nick Seyfried, and the Emory University Integrated Proteomics Core for their technical assistance with phosphoproteomics. We thank Dianne Alexis and the Winship Pathology Core Lab for their technical assistance with immunocytochemistry.

Conflict-of-interest disclosure

A.K.N is a consultant/advisory board member for Spectrum Pharmaceuticals, Novartis, and Amgen. S.L. is a consultant/advisory board member for Millennium, The Takeda Oncology, Celgene, Novartis, Bristol-Myers Squibb, Onyx Pharmaceuticals, and Janssen Pharmaceutical Companies, The Pharmaceutical Companies of Johnson & Johnson. L.H.B. is a consultant/advisory board member for Onyx Pharmaceuticals and Novartis. The other authors disclosed no potential conflicts of interest.

Grant Support

R01 CA127910 (LHB), P30 CA138292 (Emory Proteomics Core and Cancer Tissue and Pathology Shared Resource of the Winship Cancer Institute of Emory University) and funding from the TJ Martell Foundation (LHB) supported this work. LHB is a GRA Distinguished Cancer Scientist.

Table 1. Patient Sample Clinical Diagnostics

Sample	Diagnostic sample	Analysis performed	Age	Sex	ISS stage	CTG	FISH	Prior lines	LEN ref	BTZ ref	CFZ ref	POM ref
10001139	Myeloma	qPCR	61	M	1	46,XY[20]	None	5	Yes	Yes	No	No
10001152-2	Myeloma	qPCR	65	M	3	45,X,-Y[3]/46,XY[26]	gain of 1q, monosomy 13 and 17, del (17p)	3	Yes	Yes	Yes	Yes
10001252	Myeloma	qPCR	69	F	3	46,XX,del(16)(q22)[9]/46,XX[13]	gain of IgH; monosomy 13, t(4;14)	0	No	No	No	No
10001279-2	Myeloma	qPCR	42	F	3	47-49,XX,+1,dic(1;16)(p12;q24),add(8)(p23),t(11;14)(q13;q32),t(13;18)(q14;q21.3),add(17)(p11.1),-19,+2-4mar[cp14]/46,XX[6]	gain of 1q, gain of 13q, t(11;14)	5	Yes	Yes	No	No
10001171	Myeloma	Western	68	M	1	55,XY,t(1;17)(q21;q21),add(4)(p16),+5,+7,+9,+11,+15,+15,-16,+19,+21,+21,+mar[4]/46,XY[29]	trisomy 7, 9, 11	2	No	No	No	No
10001183	Myeloma	Western, Phos-Tag Western	54	F	Unk	48-51,X,-X,del(1)(q32),+3,der(3)add(3)(p21)t(1;3)(q27;q25),+9,+11,add(18)(p11.2),+20,+2-3mar[cp4]/46,XX[16]	gain of IgH, trisomy 3, 9, 11	3	Yes	Yes	No	No
10001184	EMD	Western, Phos-Tag Western	64	F	1	46,XX[30]	trisomy 9	3	Yes	Yes	No	No
10001208	Myeloma	Western	71	M	3	54-59,Y,der(X)t(X;11)(p22.1;q13),del(2)(p13),+3,der(3)t(1;3)(q21;p25),+4,+5,add(5)(q13),+7,add(8)(p11.2)x2,+9,del(10)(q22q24),del(11)(p13p14),del(13)(q12q22),+15,add(15)(q22),+17,add(17)(p12),+18,+19,add(20)(p13),+21,+21,+21,del(22)(q11.2),+2-4mar[cp16]/46,XY[4]	gain of 1q, loss of IgH, monosomy 13, del 13q, del (17p), trisomy 3,7,9,11,17	2	Yes	Yes	No	No
01	Myeloma	Phos-Tag Western	54	M	2	Unk	t(4;14); del 17p	3	Yes	Yes	Yes	Yes

EMD: extramedullary myeloma; M: Male; F: Female; ISS: International Staging System; CTG: cytogenetics; FISH: Fluorescent in-situ hybridization; LEN: lenalidomide; BTZ: bortezomib; CFZ: carfilzomib; POM: pomalidomide; ref: refractory; unk: unknown

Figure 1

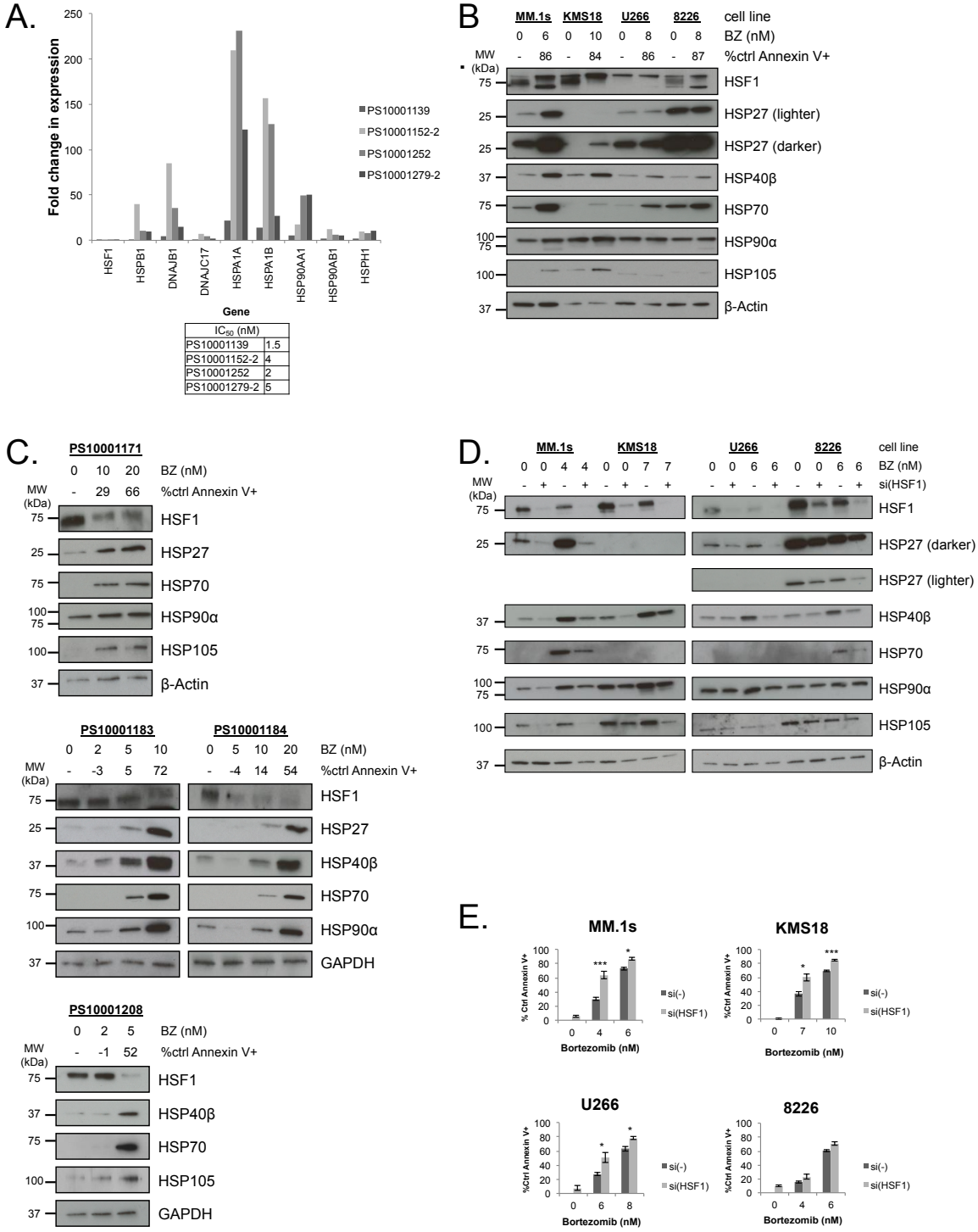
A.
Fold change in expression
250
200
150
100
50
0
HSF1
HSPB1
DNAJB1
DNAJC17
HSPA1A
HSPA1B
HSP90AA1
HSP90AB1
HSPH1
Gene
PS10001139
PS10001152-2
PS10001252
PS10001279-2
IC50 (nM)
PS10001139 1.5
PS10001152-2 4
PS10001252 2
PS10001279-2 5
B
MM.1s KMS18 U266 8226 cell line
0 6 0 10 0 8 0 8 BZ (nM)
MW (kDa) - 86 - 84 - 86 - 87 %ctrl Annexin V+
HSF1
HSP27 (lighter)
HSP27 (darker)
HSP40β
HSP70
HSP90α
HSP105
β-Actin
C.
PS10001171
0 10 20 BZ (nM)
MW (kDa) - 29 66 %ctrl Annexin V+
HSF1
HSP27
HSP70
HSP90α
HSP105
β-Actin
PS10001183
PS10001184
0 2 5 10 0 5 10 20 BZ (nM)
MW (kDa) - -3 5 72 - -4 14 54 %ctrl Annexin V+
HSF1
HSP27
HSP40β
HSP70
HSP90α
GAPDH
PS10001208
0 2 5 BZ (nM)
MW (kDa) - -1 52 %ctrl Annexin V+
HSF1
HSP40β
HSP70
HSP105
GAPDH
D.
MM.1s KMS18 U266 8226 cell line
0 0 4 4 0 0 7 7 0 0 6 6 0 0 6 6 BZ (nM)
MW (kDa) - + - + - + - + - + - + - + - + si(HSF1)
HSF1
HSP27 (darker)
HSP27 (lighter)
HSP40β
HSP70
HSP90α
HSP105
β-Actin
E.
MM.1s
KMS18
U266
8226
% Ctrl Annexin V+
Bortezomib (nM)
si(-)
si(HSF1)

Figure 1: Bortezomib Induces HSP Expression in Multiple Myeloma Cells, and HSF1 Silencing Sensitizes Multiple Myeloma Cells to Bortezomib Treatment. (A) CD138+ cells were purified (>90%) from freshly isolated myeloma patient samples and treated with bortezomib for 24h. Cells were collected at 12h for qRT-PCR gene expression analysis and analyzed at 24h for apoptosis. Gene expression is expressed relative to untreated cells and normalized to GAPDH endogenous control. A table lists bortezomib IC_{50} values. (B) Myeloma cell lines were treated with bortezomib for 24h. Protein lysates were collected at 12h for western blot analysis and cells were analyzed at 24h for apoptosis. Apoptosis was measured by Annexin V and PI staining and flow cytometry. Data are representative of three independent experiments. Western blot images have been cropped for presentation clarity. (C) CD138+ cells were purified (>90%) from freshly isolated myeloma patient samples and treated with bortezomib for 24h. Protein lysates were collected at 12h for western blot analysis and cells were analyzed at 24h for apoptosis. Western blot images have been cropped for presentation clarity (D) HSF1 was silenced in myeloma cell lines for 24h and cells were treated with bortezomib for an additional 24h. Protein lysates were collected afterward for western blot analysis. Data are representative of four independent experiments. Western blot images have been cropped for presentation clarity. (E) Experimental setup was as described in (D). Bortezomib-induced apoptosis was measured by Annexin V and PI staining and flow cytometry. P-value is calculated by paired t-test. (*P<0.05, **P<0.01, ***P<0.001)

Figure 2

A.

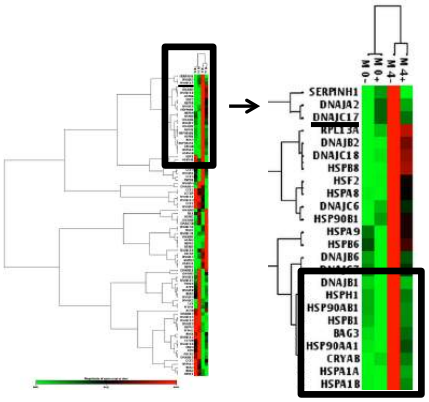

Genes whose mRNA induction by bortezomib is >50% HSF1-dependent	
Gene	**%HSF1-dependence**
HSPA1A (HSP70)	83.4
DNAJB1 (HSP40B)	80.3
HSPA1B (HSP70)	76.7
DNAJC17 (HSP40C)*	67.3
CRYAB (HSPB5)	66.3
BAG3*	63.8
HSPH1 (HSP105)	63.3
HSPB1 (HSP27)	56.5
HSP90AA1	56.4
HSP90AB1	55.4

B.

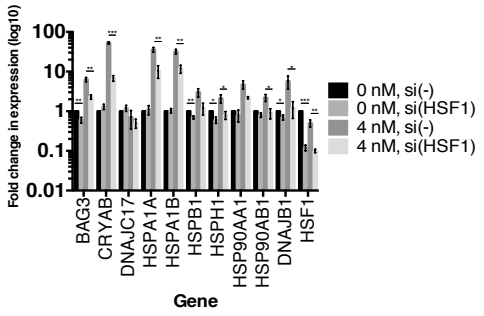

C.

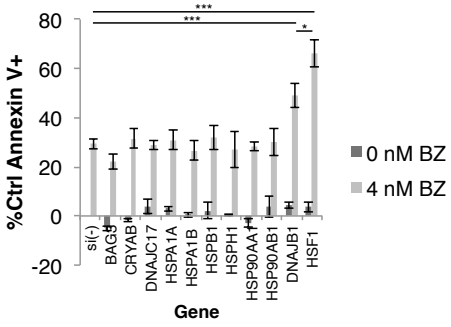

D.

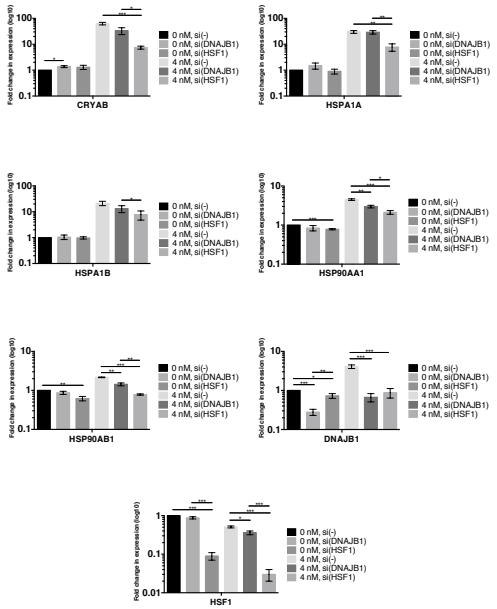

E.

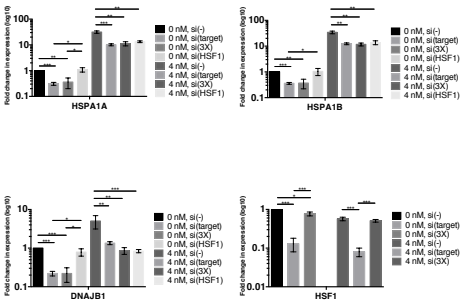

F.

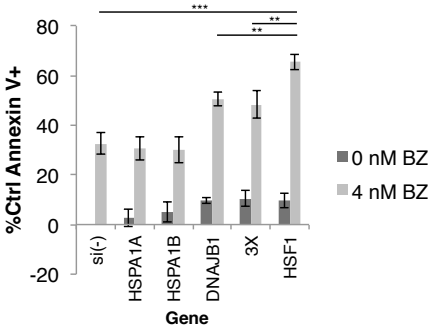

Figure 2: In Combination with Bortezomib Treatment, HSF1 Silencing is More Effective than HSP Silencing at HSR Downregulation. (A) (Left) MM.1S cells were treated with a non-silencing control (-) or HSF1 (+) siRNA for 24h followed by 0 or 4 nM bortezomib for an additional 24h. RNA was extracted afterward from whole cell lysates, reverse transcribed to cDNA, and probed for changes in gene expression using the QIAGEN© Human Heat Shock Array qPCR Panel. Gene expression is expressed relative to MM.1S(-), 0 nM and normalized to the mean of five housekeeping genes (B2M, HPRT1, RPL13A, GAPDH, and ACTB). Green indicates lower expression, black indicates no change, and red indicates higher expression. (Right) A table listing all genes whose bortezomib-induced mRNA induction is >50% HSF1-dependent. (B) Independent confirmation of bortezomib-induced HSF1-dependent genes. Experimental setup was as described in (A). Gene expression is expressed relative to untreated cells and normalized to GAPDH endogenous control. Data are presented as the mean±s.e. of three independent experiments. (C) MM.1S cells were treated with a non-silencing control [si(-)] or HSP or HSF1 siRNA for 24h followed by 0 or 4 nM bortezomib for an additional 24h. Cells were analyzed at 48h for apoptosis. Apoptosis was measured by Annexin V and PI staining and flow cytometry. Data are presented as the mean±s.e. of three independent experiments. (D) MM.1S cells were treated with a non-silencing control [si(-)] or single gene (DNAJB1 or HSF1) siRNA for 24h followed by 0 or 4 nM bortezomib for an additional 24h. RNA was extracted from whole cell lysates, reverse transcribed to cDNA, and probed for changes in gene expression. Gene expression is expressed relative to untreated cells and normalized to GAPDH endogenous control. Data are presented as the mean±s.e. of three independent experiments. (E) MM.1S cells were treated with a non-silencing control [si(-)], single gene (HSPA1A, HSPA1B, DNAJB1, HSF1) or combination (3X: HSPA1A + HSPA1B + DNAJB1) siRNA for 24h and 0 or 4 nM bortezomib for an additional 24h. RNA was extracted at 48h from whole cell lysates, reverse transcribed to cDNA, and probed for changes in gene expression. Gene expression is expressed relative to untreated cells and normalized to GAPDH endogenous control. Data are presented as the mean±s.e. of three independent experiments. (F) Setup was as described in (E). Bortezomib-induced apoptosis was measured by Annexin V and PI staining and flow cytometry. P-value is calculated by paired t-test. (*P<0.05, **P<0.01, ***P<0.001)

Figure 3

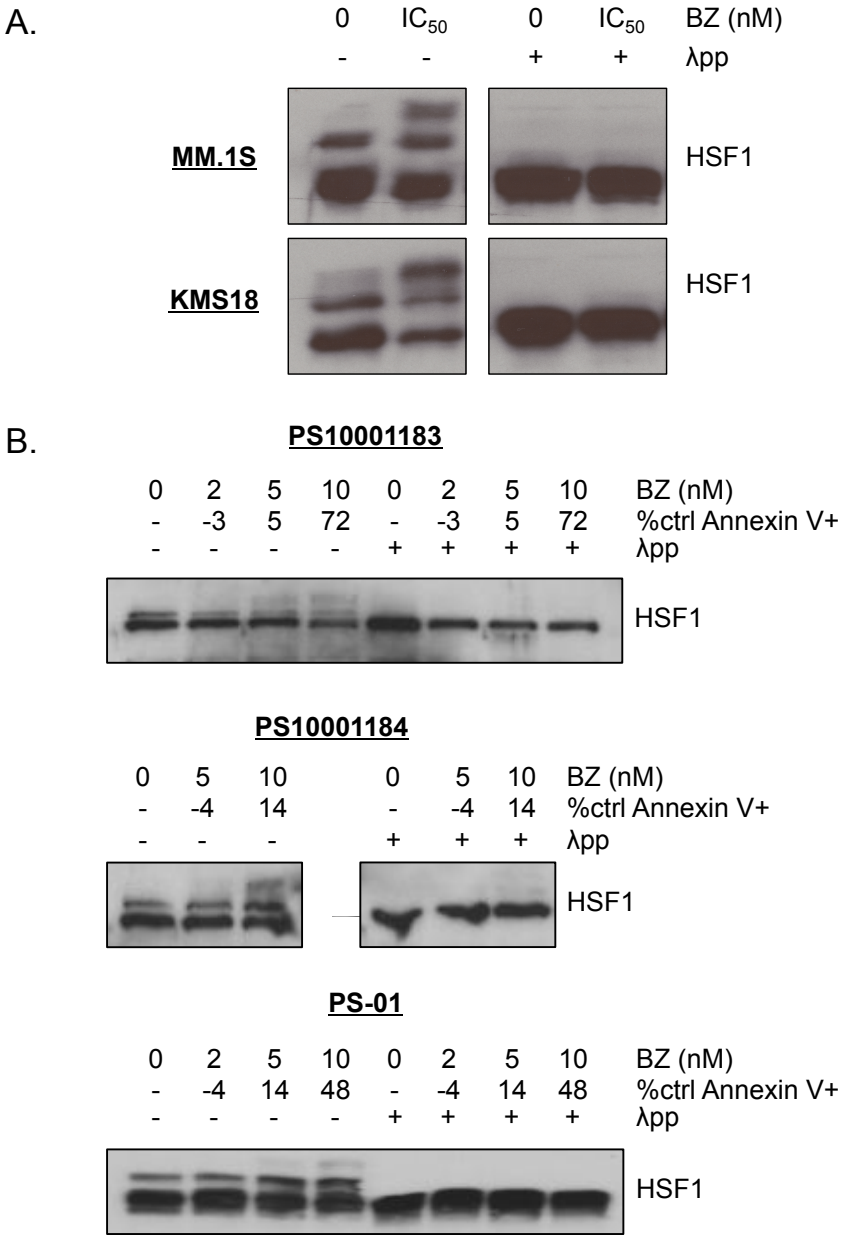

Figure 3: HSF1 is Phosphorylated Upon Bortezomib Treatment in Multiple Myeloma Cells. (A) MM.1S and KMS18 cells or (B) CD138+ cells from freshly isolated patient samples were treated with bortezomib (MM.1S: 5 nM, KMS18: 8 nM) for 24h. Protein lysates were collected at 12h for western blot analysis and cells were analyzed at 24h for apoptosis. Phos-Tag™ western blotting was performed on prepared lysates followed by HSF1 detection. (λ phosphatase was used to determine which bands were due to phosphorylation.) Bortezomib-induced apoptosis at 24h is indicated by percent control Annexin V+. Cell line data is representative of seven independent experiments. Western blot images have been cropped for presentation clarity.

Figure 4

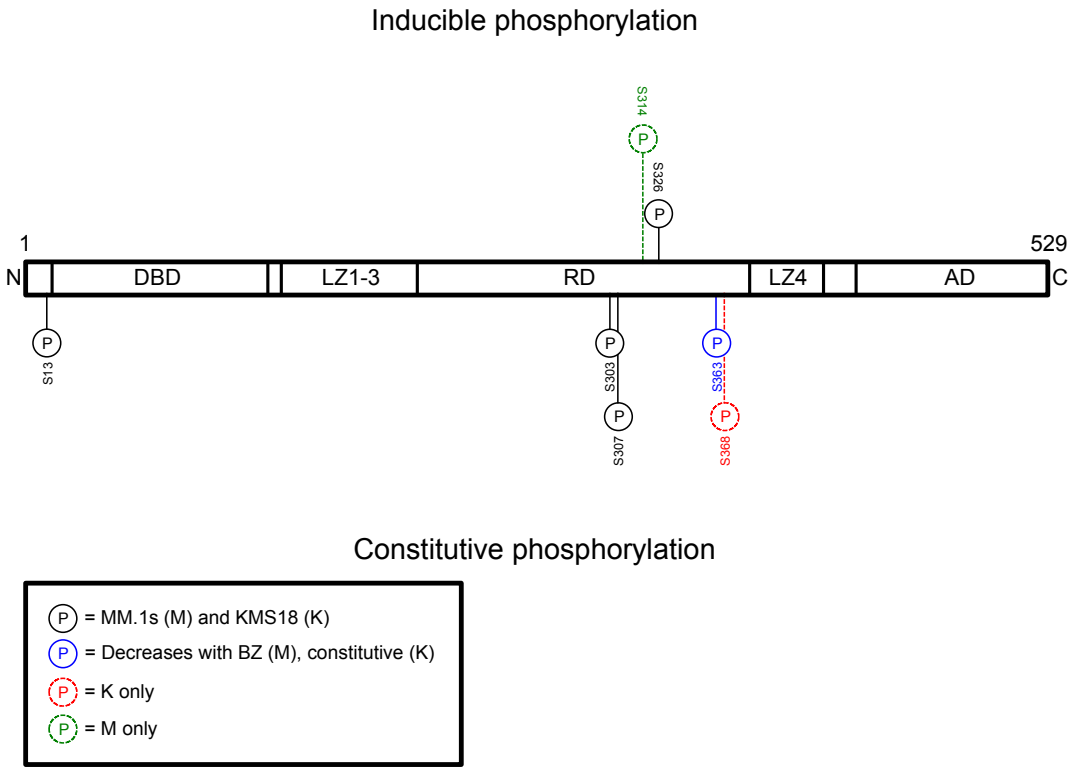

Figure 4: Phosphoproteomics Reveals that HSF1 Serine 326 is a Bortezomib-inducible Phosphorylation Site and Serine 303 is a Constitutive Phosphorylation Site. MM.1S and KMS18 cells were treated with bortezomib for 9h and cells were lysed. Immunoprecipitated or gel excised HSF1 was sent to the Emory University Proteomics Core for phosphoproteomics analysis. Detected constitutive and inducible PTMs are represented here.

Figure 5

A.

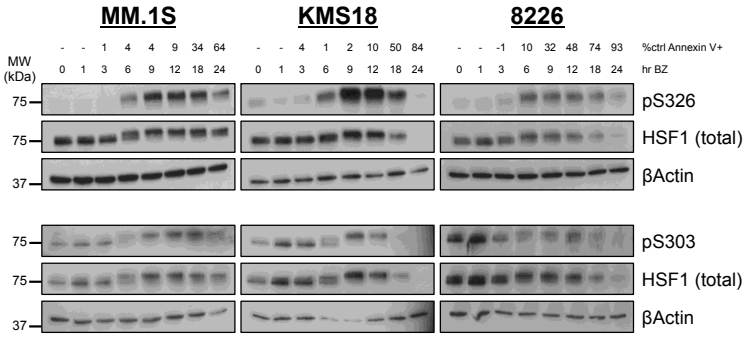

B.

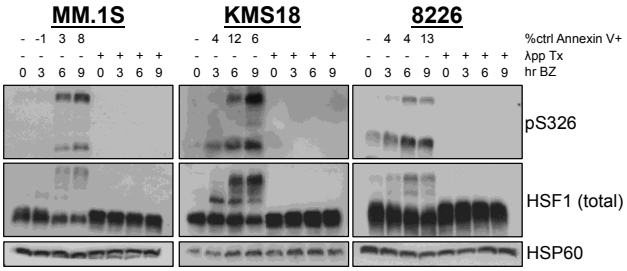

C.

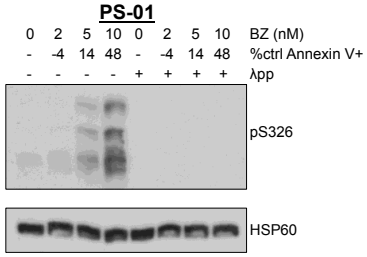

D.

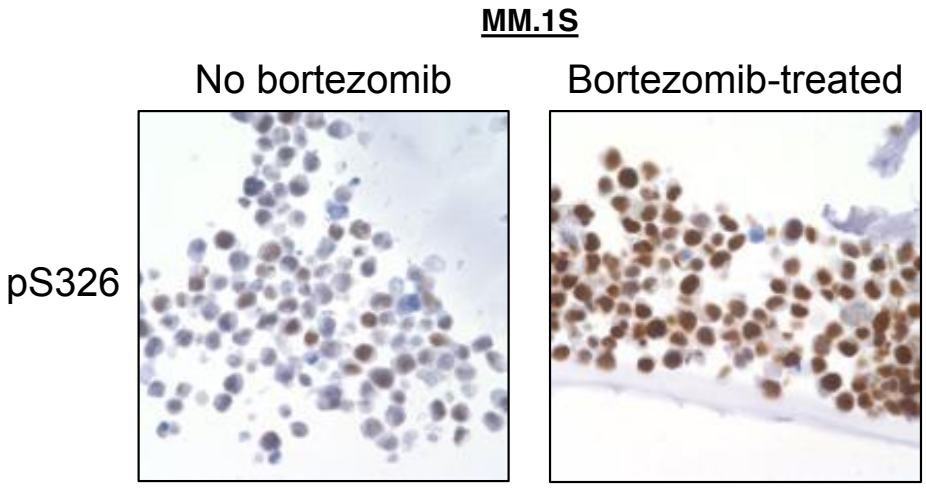

Figure 5: Phospho-specific Antibodies Confirm that HSF1 Serine 326 is a Bortezomib-inducible Phosphorylation Site and Serine 303 is a Constitutive Phosphorylation Site. (A) MM.1S, KMS18, and 8226 cells were treated with bortezomib (MM.1S: 5 nM, KMS18: 10 nM, 8226: 8 nM) for up to 24h and lysed at various timepoints. Bortezomib-induced apoptosis is indicated by percent control Annexin V+. Western blot analysis was performed on prepared lysates. Western blot images have been cropped for presentation clarity. (B) MM.1S. KMS18, and 8226 cells were treated with bortezomib (MM.1S: 5 nM, KMS18: 10 nM, 8226: 8 nM) for up to 9h and lysed at various timepoints. Bortezomib-induced apoptosis is indicated by percent control Annexin V+. Phos-Tag^{TM} western blotting was performed on prepared lysates. (λ phosphatase was used to determine which bands were due to phosphorylation.) Western blot images have been cropped for presentation clarity. (C) CD138+ cells from freshly isolated patient samples were treated with bortezomib for 24h and cells were lysed at 9h. Bortezomib-induced apoptosis at 24h is indicated by percent control Annexin V+. Phos-Tag^{TM} western blotting was performed on prepared lysates. Western blot images have been cropped for presentation clarity. (D) MM.1S cells were treated with bortezomib for 9h and fixed. Slides were stained with pS326 (1:2000 dilution), counterstained with hematoxylin, and visualized by immunocytochemistry

Supplementary Methods - Mass Spectrometry

In-gel Sample Digestion

Gel bands were diced into ~1 mm cubes, destained with 50% acetonitrile (ACN) in 50 mM ammonium bicarbonate (ABC), dehydrated with ACN, and dried down using a SpeedVac (Thermo). Trypsin was added at a concentration of 10 ng/µL and samples were placed on ice for 30 minutes. The gel cubes were then covered with ABC buffer and digestion was allowed to proceed overnight. Peptides were extracted twice with 5% formic acid in 50/50 ABC/ACN solution. Each extraction consisted of 10 minutes of low vortexing in extraction buffer and 3 cycles of centrifugation with 1 min on and 1 min off per cycle. A final step of 100% ACN was used to extract all solution from the gel cubes and the entire peptide solution was dried completely by SpeedVac.

In-solution Sample Digestion

IP beads were resuspended in 50mM ammonium bicarbonate and treated with 1 mM dithiothreitol (DTT) at 25°C for 30 minutes, followed by 5 mM iodoacetimide (IAA) at 25°C for 30 minutes in the dark. Proteins were digested with 1 **µ**g of lysyl endopeptidase (Wako) at room temperature for 2 hours and further digested overnight with 1:50 (w/w) trypsin (Promega) at room temperature. Resulting peptides were desalted with a Sep-Pak C18 column (Waters) and dried under vacuum.

LC-MS/MS Orbitrap XL analysis

The dried peptides were resuspended in 10 **µ**L of loading buffer (0.1% formic acid, 0.03% trifluoroacetic acid, 1% acetonitrile). Peptide mixtures (2 **µ**L) were separated on a self-packed C18 (1.9 **µ**m Dr. Maisch, Germany) fused silica column (15 cm x 75 **µ**m internal diameter (ID); New Objective, Woburn, MA) by a double split liquid

chromatography (LC) system consisting of an Agilent 1100 binary pump and a Famos autosampler. The LC system was interfaced to an Orbitrap XL mass spectrometer (ThermoFisher Scientific, San Jose, CA). Elution was performed over a 90 or 120 minute gradient at a rate of 300 nL/min (measured at the tip using a micropipette) with buffer B ranging from 3% to 80% (buffer A: 0.1% formic acid in water, buffer B: 0.1 % formic in acetonitrile). The mass spectrometer cycle was programmed to collect 1 precursor scan in the Orbitrap followed by 10 ion trap CID tandem (MS/MS) scans per cycle. The MS scans (300-1800 m/z range, 1,000,000 AGC, 150 ms maximum ion time) were collected at a resolution of 30,000 at m/z 200. Both the MS and CID MS/MS (2 m/z isolation width, 35% collision energy) scans were detected in centroid mode. Dynamic exclusion was set to exclude previous sequenced precursor ions for 20 seconds within a 10 ppm window.

LC-MS/MS Q-Exactive analysis

The dried peptides were resuspended in 10 **µ**L of loading buffer (0.1% formic acid, 0.03% trifluoroacetic acid, 1% acetonitrile). Peptide mixtures (2 **µ**L) were separated on a self-packed C18 (1.9 **µ**m Dr. Maisch, Germany) fused silica column (15 cm x 75 **µ**m internal diameter (ID); New Objective, Woburn, MA) by a NanoAcquity UPLC (Waters) and monitored on a Q-Exactive Plus mass spectrometer (ThermoFisher Scientific, San Jose, CA). Elution was performed over a 90 minute gradient at a rate of 300nl/min with buffer B ranging from 3% to 80% (buffer A: 0.1% formic acid in water, buffer B: 0.1% formic acid in acetonitrile). The mass spectrometer cycle was programmed to collect 1 precursor scan followed by 10 HCD tandem (MS/MS) scan per cycle. The MS scans (300-1800 m/z range, 1,000,000 AGC, 150 ms maximum ion

time) were collected at a resolution of 70,000 at m/z 200 in profile mode and the HCD MS/MS spectra (2 m/z isolation width, 30% collision energy, 50,000 AGC target, 50 ms maximum ion time) were detected at a resolution of 17,500 at m/z 200 in centroid mode. Dynamic exclusion was set to exclude previous sequenced precursor ions for 30 seconds within a 10 ppm window. Precursor ions with +1, and +6 or higher charge states were excluded from sequencing.

Database search parameters

Spectra were searched using the same parameters on one of two software programs (A) Spectra were searched using Sequest Sorcerer version 4.3 (Sage-N Research) against a decoy supplement human REFSEQ database (version 62 with 68,742 target sequences). Searching parameters included fully tryptic restriction and a parent ion mass tolerance (± 50 ppm). Methionine oxidation (+15.99492Da) and serine, threonine, and tyrosine phosphorylation (+79.966331Da) were variable modifications (up to 3 allowed per peptide); cysteine was assigned a fixed carbamidomethyl modification (+57.021465 Da). The peptides were classified by charge state and filtered dynamically by increasing XCorr and ΔCn values to reduce protein false discovery rate to less than 1%, according to the target-decoy strategy. (B) Spectra were searched using Proteome Discoverer 1.4 against a decoy supplement human REFSEQ database (version 62 with 68,742 target sequences). Searching parameters included fully tryptic restriction and a parent ion mass tolerance (± 50 ppm). Methionine oxidation (+15.99492Da) and serine, threonine, and tyrosine phosphorylation (+79.966331Da) were variable modifications (up to 3 allowed per peptide); cysteine was assigned a fixed carbamidomethyl modification (+57.021465 Da). The peptide matches were filtered in using percolator to a psm level fdr of 1%.

Supplementary Table 1

Gene	Fold change M 0+	Fold change M 4-	Fold change M 4+	% reduction of BZ-based induction
HSPA1A	0.13	129.90	21.56	83.4
HSF1	0.18	1.02	0.20	80.4
DNAJB1	0.57	6.63	1.31	80.3
HSPA1B	0.53	32.03	7.46	76.7
DNAJC17	4.67	13.15	4.31	67.3
CRYAB	1.51	8.73	2.04	66.3
BAG3	0.69	6.29	2.27	63.8
HSPH1	0.56	3.69	1.35	63.3
HSPB1	0.76	2.75	1.20	56.5
HSP90AA1	0.85	5.77	2.51	56.4
HSP90AB1	0.74	2.50	1.12	55.4
HSPD1	0.74	1.46	0.75	49.0
HSPA8	0.92	5.61	3.23	42.5
HSPA4L	0.75	1.04	0.61	41.3
CCT6A	0.78	0.84	0.53	36.5
DNAJC6	1.20	2.63	1.67	36.3
DNAJA1	0.73	1.48	0.96	34.8
HSPE1	0.78	0.93	0.62	33.3
DNAJC14	1.03	0.76	0.51	32.7
DNAJC11	0.96	0.73	0.52	29.7
HPRT1	0.77	0.49	0.35	28.9
HSPB6	0.50	1.93	1.40	27.6
CCT7	0.91	0.86	0.63	26.4
DNAJA3	0.93	0.81	0.60	25.9
BAG2	0.85	0.50	0.38	24.5
DNAJB6	0.91	1.42	1.08	23.7
DNAJB2	1.02	4.26	3.33	21.8
DNAJA2	1.09	1.32	1.05	20.2
SERPINH1	1.04	1.24	1.00	19.6
HSPB8	1.22	84.69	68.42	19.2
CCT2	0.90	0.91	0.74	17.9
HSPA9	0.85	1.41	1.16	17.7
DNAJC7	0.91	1.29	1.07	17.4
DNAJA4	1.16	1.17	0.98	16.2
HSF2	1.01	1.52	1.28	16.2
HSP90B1	1.09	1.53	1.29	15.4
DNAJC18	1.07	2.90	2.46	15.0
CCT3	0.89	1.09	0.93	14.7
CCT4	0.88	1.10	0.97	12.3
DNAJC9	1.02	0.58	0.51	11.4
HSPA4	0.95	0.50	0.44	10.8
DNAJB14	1.17	1.11	1.01	9.5
TCP1	0.82	1.01	0.91	9.4
DNAJB12	1.06	0.83	0.77	7.0
PFDN2	0.96	0.74	0.70	5.5
RPL13A	1.05	1.41	1.35	4.3
DNAJC5	1.28	1.05	1.02	2.8
BAG4	0.83	0.65	0.64	0.8
TOR1A	1.14	0.93	0.94	-0.5
HSF4	1.04	0.94	0.96	-2.8
B2M	1.13	0.82	0.85	-2.9
DNAJC16	1.17	1.25	1.28	-3.1
DNAJC13	1.01	0.66	0.68	-3.6
DNAJC19	1.02	0.54	0.56	-3.8
PFDN1	1.51	1.13	1.18	-4.9
CCS	1.24	1.04	1.10	-5.9
GAPDH	1.02	2.39	2.55	-6.7
ATF6	1.19	0.88	0.94	-7.0
DNAJC3	1.09	1.26	1.35	-7.3
DNAJC1	1.28	0.90	0.97	-8.4
HSPA14	0.89	0.69	0.76	-10.6
BAG5	1.23	0.80	0.89	-11.3
ADCK3	1.11	0.58	0.65	-11.3
DNAJC15	1.41	0.92	1.06	-14.8
DNAJC21	1.05	1.03	1.20	-16.3
CRYAA	1.18	1.76	2.11	-19.9
DNAJC4	1.39	0.59	0.71	-20.1
HSPA5	1.09	2.66	3.24	-21.7
DNAJB11	1.25	0.97	1.22	-25.3
DNAJC8	1.45	0.68	0.87	-27.7
DNAJB13	1.19	0.43	0.56	-29.3
ACTB	1.08	0.74	0.99	-33.8
HSPA1L	1.20	7.32	9.97	-36.3
BAG1	1.09	0.59	0.82	-39.0
DNAJC12	1.01	0.44	0.61	-39.8
SIL1	1.14	0.86	1.21	-40.8
CCT5	0.87	0.58	0.82	-41.1
DNAJC10	1.38	0.53	0.76	-43.1
DNAJB5	1.72	0.92	1.33	-44.0
DNAJC5G	1.01	1.30	1.88	-44.5
DNAJB9	1.48	1.20	1.88	-57.2
CCT6B	1.38	0.45	0.79	-77.1
RTC	1.52	2.85	5.20	-82.0
HGDC	0.92	1.55	2.82	-82.7
RTC	1.40	2.55	5.05	-97.8
PPC	1.20	1.34	2.66	-97.8
RTC	1.41	2.69	5.36	-99.6
DNAJC5B	1.48	0.86	1.81	-109.7
PPC	1.16	1.30	2.80	-116.0
PPC	1.22	1.29	2.84	-119.2
HSPA2	1.03	1.24	2.83	-128.3
HSPB7	0.92	1.15	2.82	-145.5
HSPB2	2.13	0.94	2.78	-197.6
HSPB3	1.06	1.15	3.51	-205.5
DNAJB8	2.31	0.76	3.08	-303.4
DNAJB7	1.05	0.90	3.96	-341.3

M = MM.1S cell line; 0, 4 = 0, 4 nM bortezomib treatment;
- = non-silencing control siRNA; + = HSF1 siRNA

Supplementary Figure 1

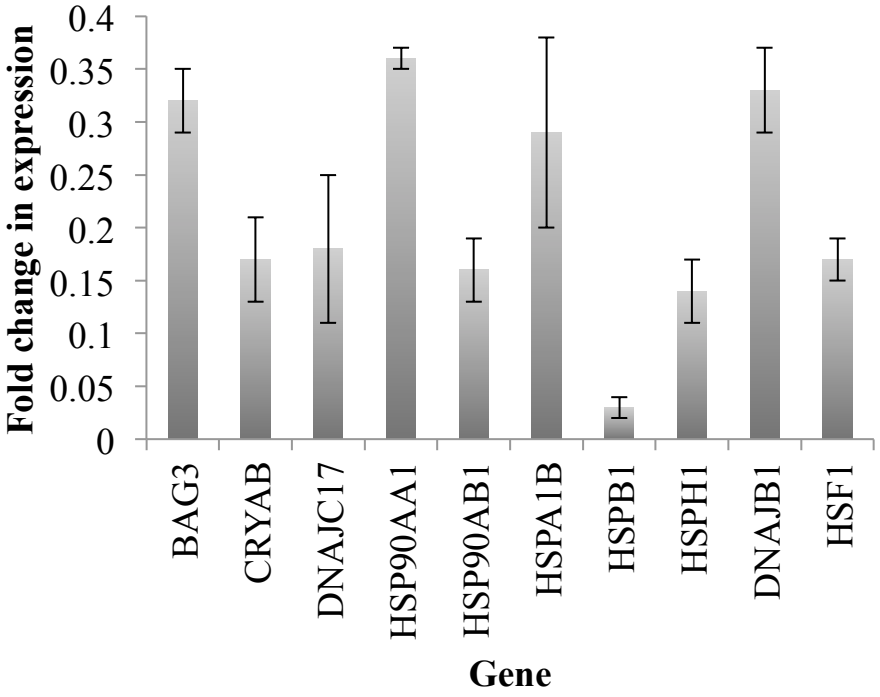

Supplementary Figure 1: HSP or HSF1 Silencing Leads to Robust Knockdown 48h After Transfection. MM.1S cells were treated with a non-silencing control [si(-)] or HSP or HSF1 siRNA for 24h followed by 0 (untreated) or 4 nM bortezomib for an additional 24h. Gene expression is shown for untreated cells relative to si(-) and normalized to GAPDH endogenous control. Data are presented as the mean±s.e. of three independent experiments.

III. HSF1 OVEREXPRESSION AND PROTEASOME INHIBITOR STUDIES IN MULTIPLE MYELOMA

Introduction

We have shown that bortezomib treatment induces HSF1 serine 326 phosphorylation in myeloma cells, and have also reviewed previous studies which have detailed the role of this post-translational modification. Previous studies have shown that a serine-to-alanine mutation downregulates HSF1 activation and target HSP upregulation[79,81,161]. Therefore, we sought to understand the biological effects of altering this modification in myeloma cells in conjunction with proteasome inhibition.

Hypothesis

(1) Introducing a serine-to-alanine substitution at serine 326 inhibits HSF1 activation and sensitizes cells to bortezomib treatment

(2) Introducing a serine-to-glutamate substitution at serine 326 results in a constitutively active heat shock response (HSR) and protects myeloma cells from bortezomib treatment

Materials and methods

Mutant cell line generation: Agilent QuikChange Lightning kit was used to introduce a single amino acid mutation into a pBabe-HSF1-Flag high copy number SV40 viral promoter plasmid (Figure 1 and ref [162]). pBabe-HSF1-Flag plasmid was a gift from Robert Kingston. We confirmed HSF1 cDNA, flag, and EcoRI sequences. This plasmid confers puromycin resistance. We transfected constructs into 293T cells using

Lipofectamine 2000 as per manufacturer's instructions and verified construct expression via Western blot analysis after 48h. We then performed transfection of Phoenix cells, which are a transfection-optimized modification of the 293T cell line, filter purified viral supernatant, and infected the MM.1s cell line with the assistance of polybrene. We then selected for puromycin at 1 μg/mL, which is a lethal dose for MM.1s cells lacking the resistance gene. Parental (without puromycin selection) and pBabe vector control cell lines were used for experimental controls.

Bortezomib treatment: Bortezomib treatment was performed as previously described 24h after puromycin was removed from the medium[163]. 5 nM was determined to be IC_{50} for bortezomib-induced cell death in parental cells.

Western blot analysis: Western blot analysis for protein expression was performed as previously described[163].

Cell viability analysis: Cell viability analysis was performed by Annexin V/PI staining and flow cytometry as previously described[163].

Results

We treated the following MM.1s cell lines with 5 nM bortezomib: parental, pBabe vector control (empty vector control), pBabe wildtype HSF1 (wt), serine-to-alanine 326 mutation (S326A), and serine-to-glutamate 326 mutation (S326E). Protein lysates were collected at 9h for western blot analysis and cells were analyzed for viability at 24h

(Figures 2 and 3). As anticipated, parental and empty vector MM.1s cells (collectively referred to hereafter as "control") showed the same amount of apoptosis (~IC_{50}). Surprisingly, wt, S326A, and S326E cells (collectively referred to hereafter as "overexpressors") all showed approximately a 50% increase in cell death compared to parental and empty vector cells.

Western blot analysis showed that baseline heat shock protein 27 (HSP27) was expressed in overexpressors and not detected in control. S326E showed the highest baseline HSP27 of the overexpressors and wt showed the lowest. Interestingly, bortezomib treatment led to HSP27 induction in control but a decrease to uniform expression in overexpressors. HSP40 expression was not detected at baseline in any cell lines, moderately induced by bortezomib in control, but very modestly induced in overexpressors with almost no induction in S326E. In a reversal of the HSP27 baseline expression pattern, there was modest HSP70 expression in control but no HSP70 expression in overexpressors. Bortezomib treatment led to strong HSP70 induction in controls, no induction in wt, very modest induction in S326A, and induction in S326E. Consistent with previous findings, HSP90 expression was consistent across all cell lines and bortezomib did not induce expression. HSP105/110 expression was similar across all cell lines at baseline and no consistent induction pattern was observed.

Baseline phospho-serine 326 was very highly present in wt but not in any other cell lines. Bortezomib treatment led to an increase in phospho-serine 326 in all cell lines. Total phospho-serine 326 expression in wt was significantly higher than that of the other cell lines but there was a similar magnitude of increase between all cell lines. Total HSF1 was very highly expressed in all overexpressors and consistent with previous

findings, no induction was observed. The antibody against total HSF1 can detect both phosphorylated and unphosphorylated forms as represented by the presence of a higher band. We observed that both baseline and bortezomib-induced total HSF1 in S326E was represented in a phosphorylated form. wt bortezomib-induced total HSF1 showed a shift from the unphosphorylated to the phosphorylated form. The data are unclear on a S326A shift but we believe that baseline and induced phospho-serine 326 expression is similar between S326A and S326E.

Discussion

Here we show that HSF1 overexpression results in increased sensitivity to bortezomib treatment, and decreased baseline and bortezomib-induced HSP expression (Figures 2 and 3), regardless of whether serine 326 is mutated or not. Overexpression may physically disrupt the inactive HSP40/70/90-HSF1 heterotetramer even in the absence of bortezomib, leading the cell to mount a false HSR. In this scenario, HSF1 would translocate into the nucleus, leading to an increase in baseline HSP27 expression. Bortezomib treatment may lead to an inducible HSR, but high baseline HSP27 expression may rapidly negatively feedback upon bortezomib treatment and therefore decrease induced HSP27 expression (Figure 4).

Interestingly, overexpressors show higher baseline HSP27, but lower (HSP40) or equal (HSP70) than control. The connection between HSP40 and HSP70 being a part of the inactive heterotetramer while HSP27 is not may provide clues toward an explanation for overexpressor baseline protein expression. In addition, high baseline HSP27 may negatively regulate HSP40 and HSP70 induction upon bortezomib treatment, though this

is unlikely given the different chaperone niches HSP27 and HSP40/HSP70 occupy as detailed elsewhere. There may be a role for negative feedback crosstalk for an as yet uncharacterized bortezomib-induced HSP occupying the same niche as HSP40/70.

HSP70 expression in S326E is higher than in the other overexpressors. This gives rise to the possibility that a phosphomimetic may allow for more HSF1 nuclear translocation and *HSP70* gene transcription compared to other overexpressors. Regardless, its cell death is unexpectedly high given the original hypothesis that a constitutive heat shock response would protect cells from proteasome inhibitor-induced apoptosis. In agreement with our apoptosis data, a recent study showed that HSF1 hyperactivation, intended to protect cells from proteotoxic stress, may actually result in growth inhibition[5].

Future studies should perform subcellular localization for all five cell lines under conditions of proteasome inhibition, to determine if overexpression changes total HSF1, phospho-serine 326, or downstream HSP localization. In addition, future studies can also attempt to mimic baseline parental HSF1 expression, even in overexpressors, in order to perform a better controlled comparison. These proposed studies will help us better understand why (a) HSF1 overexpressors show different biology compared to control and (b) there is minimal difference with regard to bortezomib sensitivity between overexpressors and control and between the overexpressors themselves.

Figure 1

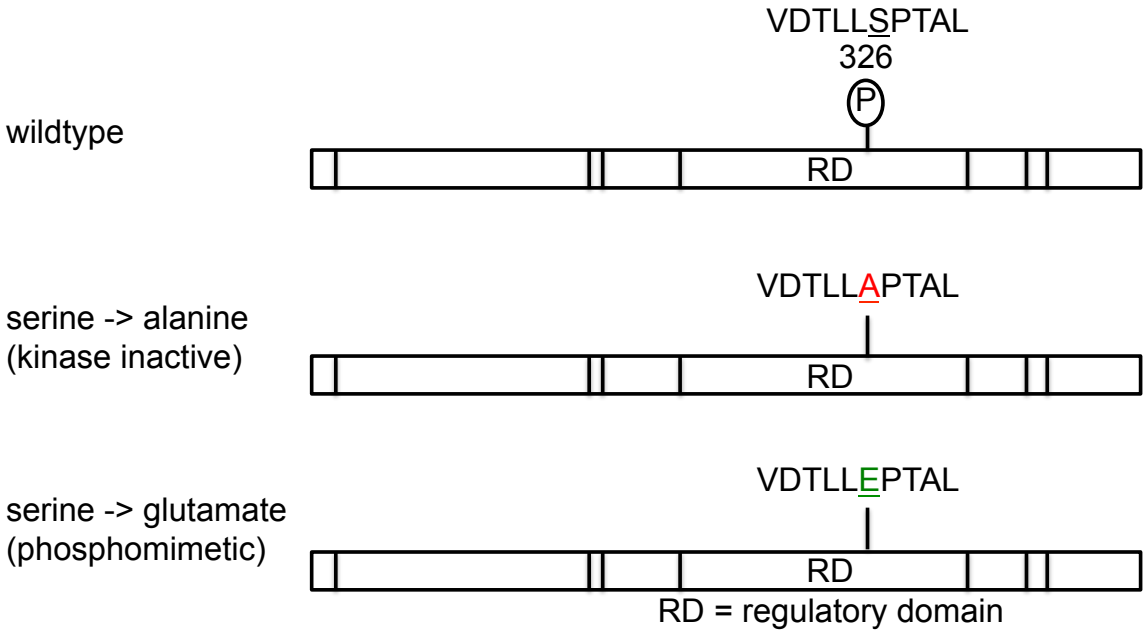

Figure 1: Schematic of HSF1 Overexpressors
pBabe HSF1 was overexpressed in MM.1s cells as detailed in Materials and Methods. (Top) No alteration was made to pBabe HSF1. (Middle) A serine-to-alanine mutation at amino acid position 326 was made using the Agilent QuikChange Lightning kit. (Bottom) A serine-to-glutamate mutation at amino acid position 326 was made using the Agilent QuikChange Lightning kit. Abbreviations; P = phosphorylation, RD = regulatory domain

Figure 2

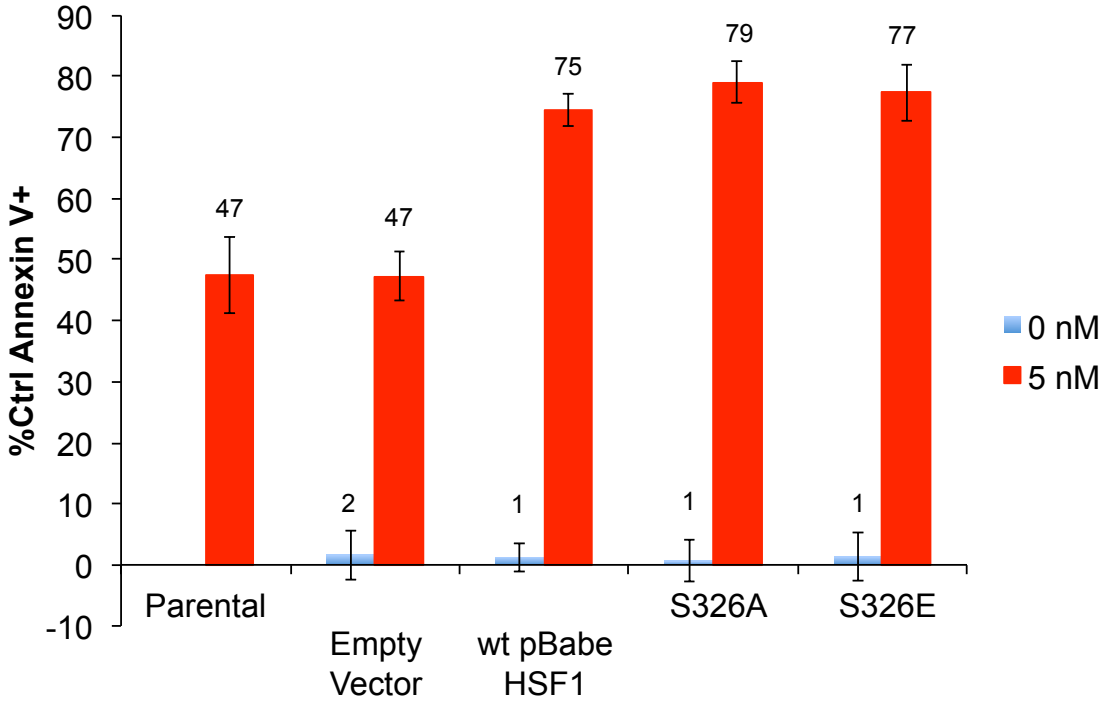

Figure 2: HSF1 Overexpression Sensitizes Myeloma Cells to Bortezomib Treatment Cell lines were generated as detailed in Materials and Methods. Cells were treated with 5 nM bortezomib and analyzed at 24h for apoptosis. Apoptosis was measured by Annexin V and PI staining and flow cytometry. Data are represented as a mean ± standard error of four independent experiments.

Figure 3

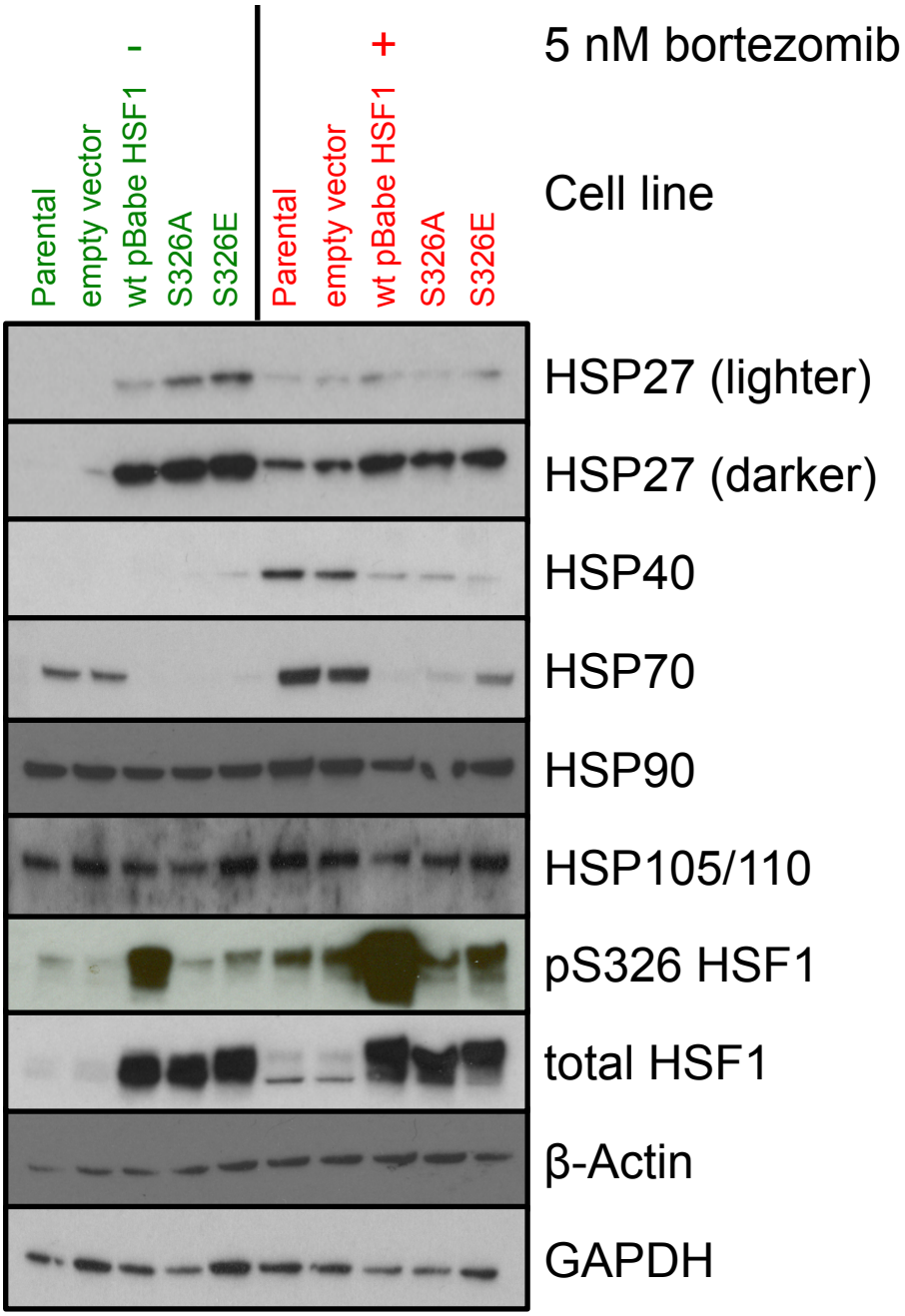

Figure 3: HSF1 Overexpression Inhibits the Bortezomib-inducible HSR
Cell lines were generated as detailed in Materials and Methods. Cells were treated with 5 nM bortezomib. Protein lysates were collected at 9h for western blot analysis. Western blot data are representative of four independent experiments.

Figure 4

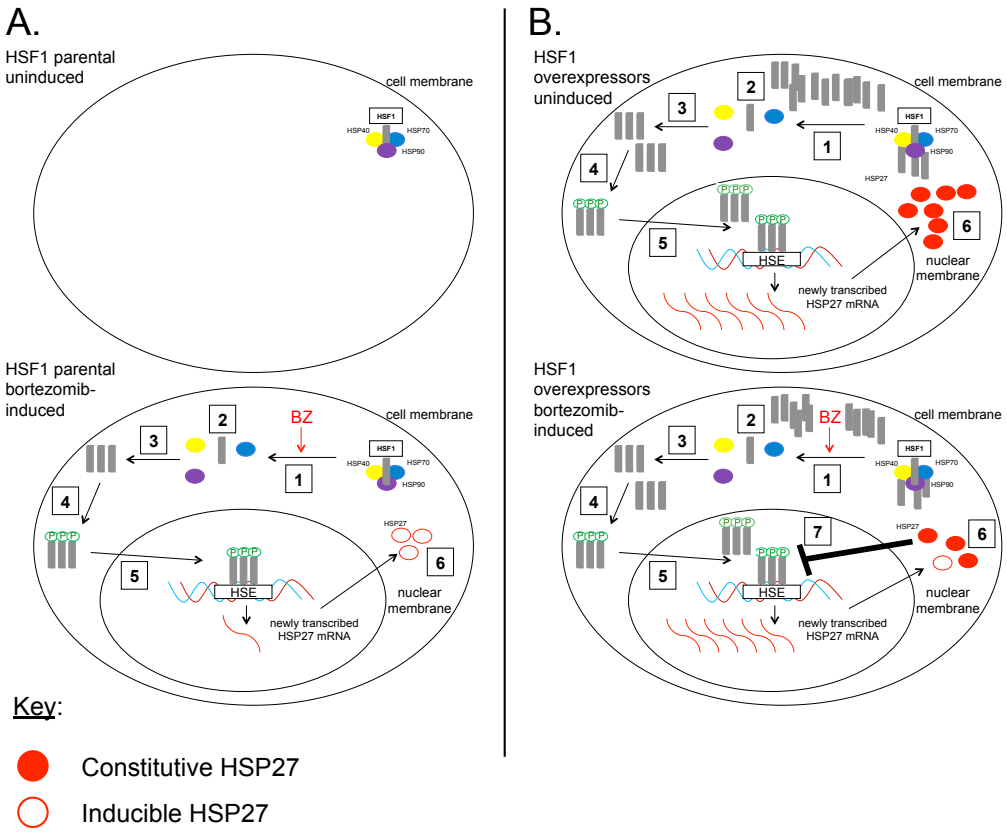

Figure 4: HSF1 Overexpression Falsely Activates the HSR and Inhibits the Bortezomib-inducible HSR

(A, top) Heat Shock Factor 1 (HSF1) is shown in the cytosol in an inactive heterotetramer with heat shock protein (HSP) 40/70/90 in parental or empty pBabe vector myeloma cell lines. (A, bottom) (1,2) Bortezomib treatment leads to heterotetramer dissociation. (3,4) HSF1 trimerizes and is modified by activating phosphorylation events. (5) The activated HSF1 trimer translocates to the nucleus where it binds to the heat shock element (HSE) of target HSP genes such as HSP27 and promotes transcription. (6) Newly transcribed HSP mRNAs exit the nucleus and are translated into HSPs. (B) HSF1 is overexpressed, either wildtype, or containing a serine-to-alanine or serine-to-glutamate mutation at amino acid position 326. Some HSF1 monomers are bound in an inactive heterotetramer with HSP40/70/90 and some are unbound in the cytosol. (B, top) (1,2) HSF1 overexpression leads to heterotetramer dissociation and activation of a false heat shock response. (3,4) HSF1 trimerizes and is modified by activating phosphorylation events. Increased HSF1 activation is represented by additional trimers. (5,6) Same as (A, bottom). Increased HSP27 mRNA transcription is represented by additional mRNA. (B, bottom) (1) Bortezomib treatment leads to heterotetramer dissociation. (2-6) Same as (B, top) (7) Baseline HSP27 inhibits bortezomib-induced upregulation of HSP27 expression in a negative feedback loop. Abbreviations; BZ = bortezomib, HSE = heat shock element, HSF = heat shock factor, HSP = heat shock protein, P = phosphorylation, S = serine

IV. TG02 REGULATION OF PROTEASOME INHIBITOR-INDUCED HSF1 ACTIVATION IN MULTIPLE MYELOMA

(*Originally submitted to Leukemia, November 10, 2016*)

Title:
TG02 inhibits proteasome inhibitor-induced HSF1 serine 326 phosphorylation and heat shock response in multiple myeloma

Running Title:
TG02 inhibits the heat shock response in myeloma

Shardule P Shah[1], Ajay K Nooka[1], Sagar Lonial[1], Lawrence H Boise[1]

[1]Department of Hematology and Medical Oncology, Winship Cancer Institute of Emory University and the Emory University School of Medicine, Atlanta, GA

Correspondence:
Lawrence H. Boise
Department of Hematology and Medical Oncology
Winship Cancer Institute of Emory University, Emory University School of Medicine
1365 Clifton Road NE, Room C4012, Atlanta, GA 30322
Phone: 404-778-4724, Fax: 404-778-5530, E-mail: lboise@emory.edu

Conflict of Interest Statement:
A.K.N is a consultant/advisory board member for Spectrum Pharmaceuticals, Novartis, and Amgen. S.L. is a consultant/advisory board member and receives research support from Millennium, The Takeda Oncology Company, Celgene, Bristol-Myers Squibb, and Janssen Pharmaceutical Companies, The Pharmaceutical Companies of Johnson & Johnson, and is a consultant/advisory board member for Novartis and Onyx Pharmaceuticals.

Grant Support:
R01 CA127910 (LHB), R01 CA192844 (LHB), P30 CA138292 (LHB, Emory Proteomics Core and Cancer Tissue and Pathology Shared Resource of the Winship Cancer Institute of Emory University) and funding from the TJ Martell Foundation (LHB) supported this work

Multiple myeloma (MM) is a plasma cell malignancy with an estimated 30 330 new cases and the cause of 12 650 deaths in the United States in 2016.[164] Mechanisms of MM therapies such as the proteasome inhibitors (PIs) bortezomib and carfilzomib have been widely studied, and broadly target either normal or malignant plasma cell biology.[3] Plasma cells are reliant on the proteasome for quality control due to their roles as constitutive secretors of immunoglobulin.[16] Therefore, PIs function in part by inhibiting a vital component of normal plasma cell biology, resulting in increased myeloma cell apoptosis. The advent of PIs has led to a dramatic increase in patient survival, largely due to their use in combination with therapies such as immunodulatory drugs (IMiDs) and autologous stem cell transplant.[146] However, nearly all patients will develop PI resistance. One of the first responses of a myeloma cell treated with PIs is to upregulate the cytoprotective heat shock response (HSR) in order to avoid apoptosis, and the HSR has been linked to PI resistance.[11,165]

The HSR consists of heat shock protein (HSP) upregulation and Heat Shock Factor 1 (HSF1) is the master transcription factor that regulates the bortezomib-induced HSR.[126,163] Several HSF1 drug screens have failed to lead to an FDA-approved inhibitor, largely due to off-target effects or lack of efficacy at therapeutically relevant concentrations.[126] We have recently shown that HSF1-mediated bortezomib-induced HSP upregulation is dependent on HSF1 serine 326 (S326) phosphorylation.[163] Therefore, we sought to identify and inhibit the kinase(s) responsible for PI-induced S326 phosphorylation (PI-pS326), and observe PI-pS326 phosphorylation and apoptotic effects.

We previously determined that neither AKT, CaMKII, JAK, JNK, nor MAPK/ERK is the responsible kinase (ref 163 and data not shown). To help identify the kinase, we performed subcellular fractionation in order to determine whether the kinase is cytoplasmic or nuclear (Figure 1A). We treated two myeloma cell lines, MM.1s and KMS18, with bortezomib for 9h, collected protein lysate, and performed either total cell lysis or subcellular fractionation. We then performed SDS-PAGE using equal cell numbers for each fraction and western blot analysis for pS326 and total HSF1. We also probed for β-Actin, GAPDH, Lamin A/C, and PGAM1 for localization controls. In MM.1s cells, we observe minimal cytoplasmic and no detectable nuclear baseline pS326. Bortezomib leads to a strong increase in both cytoplasmic and nuclear pS326 at 9h. KMS18 cells show increased baseline cytoplasmic pS326 compared to MM.1s cells, but similarly, no detectable baseline nuclear pS326. Cytoplasmic pS326 remains high in bortezomib-treated KMS18 cells and bortezomib also leads to increased nuclear pS326 as with MM.1s cells. From these data we infer that the kinase responsible for PI-pS326 is cytoplasmic.

Next, to identify potential kinases, we used a phosphokinase antibody array to identify kinases activated by bortezomib (Figure 1B). We treated MM.1s cells with bortezomib and quantified phosphokinase induction (Supplemental Table 1). Kinases responsible for these changes could lead to identification of the kinase responsible for PI-pS326. Bortezomib led to a >1.5-fold increase in p53 (S392), HSP27, and c-Jun phosphorylation. Bortezomib also led to a 1.2-1.5-fold increase in JNK1/2/3, Akt1/2/3, p53 (S46), and p27 phosphorylation. The kinases responsible for these phosphorylation

events include cyclin-dependent kinases (CDKs), amongst other families (Supplemental Table 1).[166]

Given the number of potential HSF1 kinases identified by the phosphokinase array, we elected to probe the response using a multikinase inhibitor that has activity in combination with PIs. Therefore, we treated cells with TG02, whose single nanomolar range targets are CDKs.[167] TG02 also inhibits other kinases at higher concentrations.[167] We have recently shown that the combination of TG02 and carfilzomib leads to a greater than additive effect on apoptosis in MM cell lines and patient samples.[168] In addition, two Phase I studies of TG02 in hematological malignancies were recently completed and showed activity in relapsed/refractory MM.[169-171] First, we tested three MM cell lines of varying PI sensitivity and degrees of PI-induced HSF1-mediated HSR. In MM.1s cells, a TG02 and bortezomib or carfilzomib combination leads to inhibition of both HSF1 phosphorylation and HSF1-mediated PI-induced HSP upregulation (Figure 2A). TG02 strongly inhibits constitutive and PI-induced HSP70 and HSP40 upregulation, and bortezomib-induced HSP27 and HSP105/110 upregulation. Consistent with previous findings, the combination of TG02 and bortezomib results in a strong additive effect on apoptosis, and we confirm our previous findings that the combination of TG02 and carfilzomib results in an additive effect in MM.1s cells (Figure 2B).[168,172] Furthermore, we observe that TG02 strongly inhibits PI-pS326, PI-induced HSP27 upregulation, and PI-induced HSP40 upregulation in H929 cells (Figure 2C, left). TG02 also inhibits PI-pS326 in U266 cells but does not lead to HSP inhibition (Figure 2C, right). An additive effect on apoptosis is observed in H929 cells with TG02 and low-dose bortezomib treatment (Figure 2D, upper). However, no additive effect on apoptosis is observed in

U266 cells, which is consistent with the lack of HSR induction in this cell line (Figure 2D, lower).

We treated two freshly isolated CD138+ patient samples with the combination of TG02 and carfilzomib (Figure 2E). One sample (PS10001496) showed sensitivity to both carfilzomib and TG02, leading to an additive effect on apoptosis. Consistent with the cell line data, TG02 inhibited both PI-pS326 and HSR induction (Figure 2E, top panel). The other sample (PS10001225-2) showed sensitivity to TG02, but was resistant to carfilzomib and no additive effect on apoptosis was observed (Figure 2E, bottom panel). This sample had higher constitutive HSP levels, which were inhibited by TG02. Interestingly, while the cells were resistant to carfilzomib-induced apoptosis, PI-pS326 and HSP induction was observed. This suggests an alternate mechanism of carfilzomib resistance that is likely downstream of the HSR, rendering these cells resistant to its inhibition.

CDK9 is the most sensitive TG02 target.[167] Therefore, we performed CDK9 siRNA knockdown in MM.1s cells but did not observe any change in induced pS326 levels or any additive effect with bortezomib (Figures 2F). This is consistent with our previous findings with carfilzomib.[168] Taken together, our data show that TG02 inhibits pS326 in MM cell lines and patient samples.

In summary, we show that the PI-pS326 kinase is cytoplasmic and inhibited by TG02. We show a novel mechanism by which TG02 combines with PIs to increase MM apoptosis: downregulation of the PI-induced HSR by inhibition of HSF1 activation. While we were unable to identify the HSF1 kinase we showed that it is inhibitable by a kinase inhibitor that has shown preclinical and clinical activity in combination with

proteasome inhibitors. These findings support the further development of TG02 in combination with PIs for the treatment of MM.

Note:

Supplementary information is available at Leukemia's website

Methods and Materials

Cell lines

MM.1s, KMS18, and U266 cell line characteristics and procurement details have been previously described[163]. H929 cell line was obtained from ATCC (Manassas, VA).

Patient samples

CD138+ cells (>75%) were purified from myeloma patient bone marrow aspirates as previously described[163].

Bortezomib treatment

Bortezomib was obtained from LC Labs and treatment was performed as previously described[163].

Carfilzomib treatment

Carfilzomib was generously provided by Onyx Pharmaceuticals (San Francisco, CA) as part of their PRISM-NTP program. Carfilzomib was prepared in DMSO and diluted in complete RPMI 1640 medium to desired concentrations. Additional treatment details are same as with bortezomib treatment.

Subcellular localization

Cells were treated with 0 or 8 nM bortezomib for 9h and washed twice with 1X PBS at 500g for 5 min at RT. Cell pellets were divided in two equal parts, one for total cell lysis and the other for subcellular localization. Cell pellet for total cell lysis was lysed in RIPA buffer containing 1% each protease inhibitor, PMSF, and phosphatase inhibitor cocktail for 1h on ice. Supernatant was collected after 14,000g centrifugation for 10 min at 4C. Cell pellet for subcellular localization was treated with 1X cytoplasmic extract (CE) buffer, composed of 10 mM HEPES, 60 mM KCl, 1 mM EDTA, 0.075% (v/v) NP40, 1 mM DTT, 1 mM PMSF, 1% each protease inhibitor and phosphatase inhibitor, adjusted to pH 7.6. Cytoplasmic supernatant was collected after 10,000g centrifugation for 10 min at 4C and nuclear pellet was washed with CE buffer without NP-40 at 8,000 RPM for 5 min at 4C. Nuclear pellet was lysed with RIPA buffer containing 1% each protease inhibitor, PMSF, and phosphatase inhibitor cocktail for 20 min on ice, and nuclear supernatant was collected after 14,000g centrifugation for 10 min at 4C. Equal cell number was used for western blot analysis.

Western blot analysis

Western blot analysis was performed as previously described[163].

R&D Biosystems ARY003B phosphoprotein microarray

$5*10^6$ MM.1s cells were treated with either 0 or 8 nM bortezomib for 9h. Microarray was performed as per manufacturer's instructions.

TG02 treatment

TG02 was generously provided by Tragara Pharmaceuticals, prepared in DMSO, and diluted in complete RPMI 1640 medium to listed concentrations.

siRNA treatment

siRNA treatment was performed using either a non-targeting control, CDK9 siRNA, or HSF1 siRNA as previously described[163].

Cell death analysis

Cell death analysis was performed by using Annexin V/PI and flow cytometry as previously described[163].

Figure 1

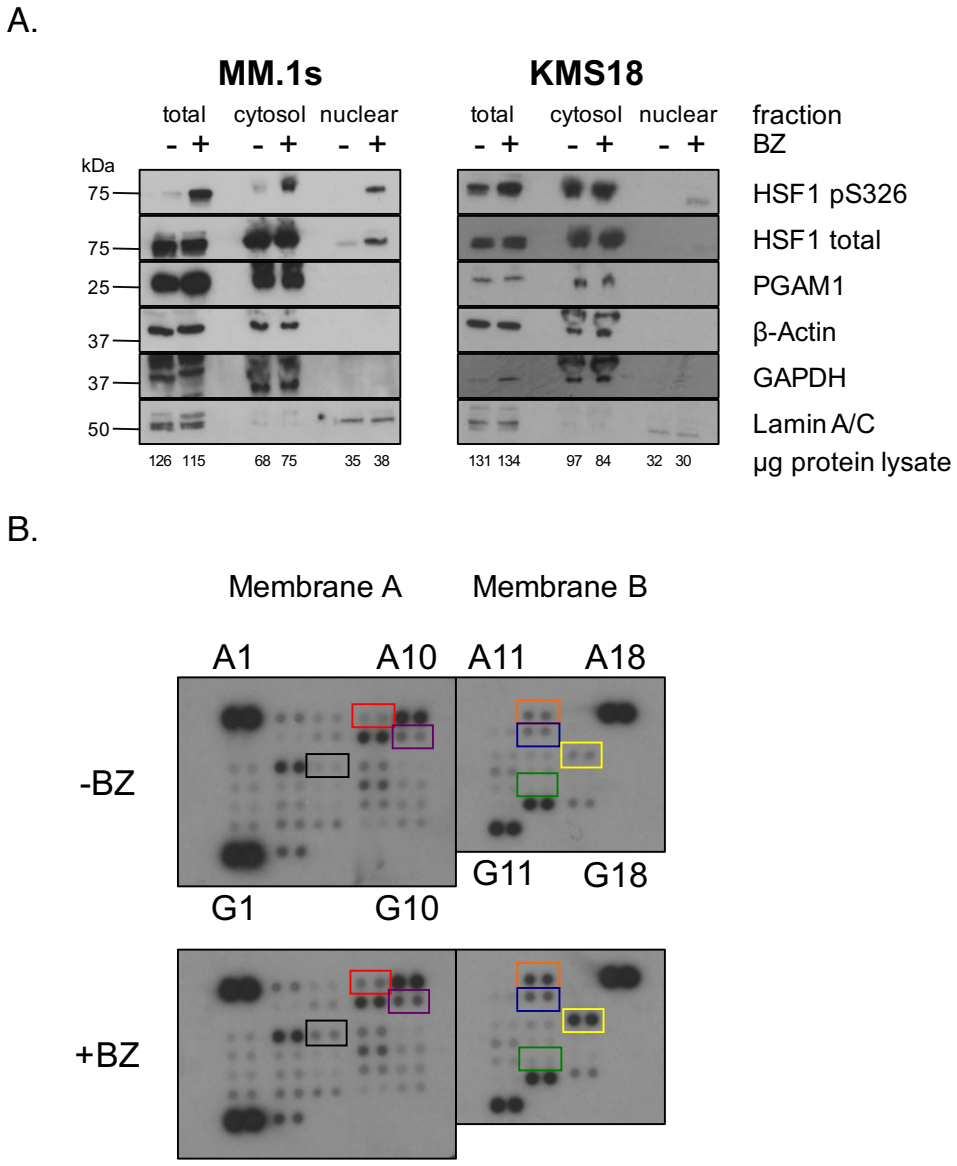

Figure 1: (A) HSF1 Serine 326 is Phosphorylated in the Cytoplasm. MM.1s and KMS18 cells were treated with 8 nM bortezomib for 9h followed by either total lysis or subcellular fractionation and equal cell number western blot analysis. Data are representative of four independent experiments. **(B) Human Kinome Phosphoprotein Microarray Identifies BZ-induced Targets.** MM.1s cells were treated with 8 nM bortezomib for 9h. Protein lysis and all subsequent steps were performed using the R&D Systems Human Phospho-Kinase Antibody Array as per manufacturer's instructions. Coordinate pairs and box colors are matched with their respective targets as follows: red, A7/8 = JNK1/2/3; orange, A13/14 = p53 (S392); purple, B9/10 = Akt1/2/3; blue, B13/14 = p53 (S46); black, C5/6 = HSP27; yellow, C15/16 = c-Jun; green, E13/14 = p27. Data are representative of two independent experiments.

Figure 2

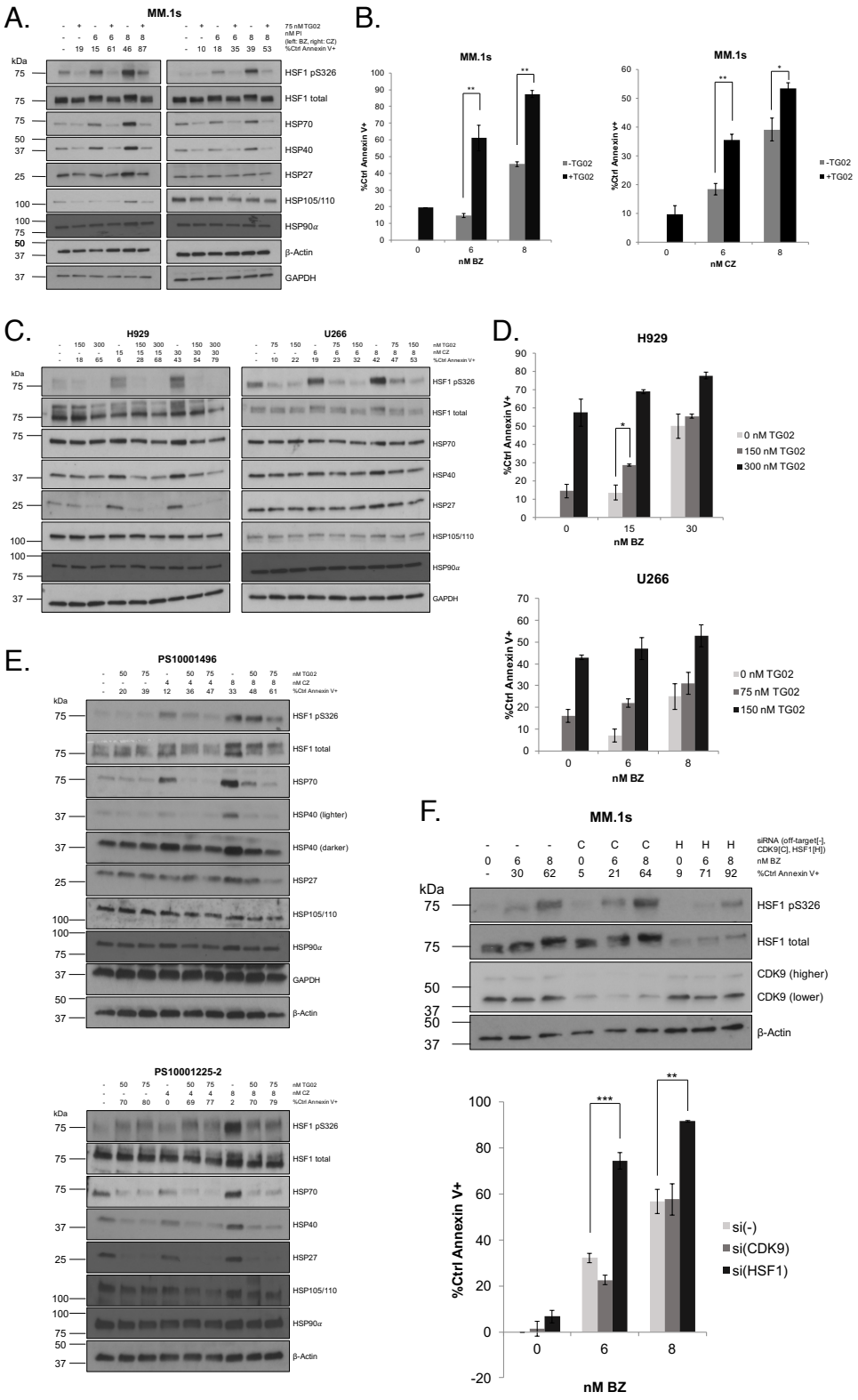
A.
MM.1s
HSF1 pS326
HSF1 total
HSP70
HSP40
HSP27
HSP105/110
HSP90α
β-Actin
GAPDH
B.
MM.1s
%Ctrl Annexin V+
nM BZ
nM CZ
-TG02
+TG02
C.
H929
U266
D.
H929
U266
0 nM TG02
150 nM TG02
300 nM TG02
75 nM TG02
E.
PS10001496
PS10001225-2
HSP40 (lighter)
HSP40 (darker)
F.
MM.1s
siRNA (off-target[-], CDK9[C], HSF1[H])
CDK9 (higher)
CDK9 (lower)
si(-)
si(CDK9)
si(HSF1)

Figure 2: **(A) TG02 Inhibits Proteasome-inhibitor Induced HSF1 Serine 326 Phosphorylation and Proteasome Inhibitor-induced HSR in Myeloma Cells.** MM.1s cells were co-treated with TG02 and either bortezomib (left) or carfilzomib (right). Protein lysates were collected at 9h for western blot analysis and cells were analyzed at 24h for apoptosis. Apoptosis was measured by Annexin V and PI staining and flow cytometry. Western blot data are representative of four independent experiments. **(B) TG02 and Proteasome Inhibitor Combination Leads to an Additive Effect on Apoptosis in MM.1s Cells.** Experimental setup was as described in (A). **(C) TG02 Inhibits Bortezomib-induced HSF1 Serine 326 Phosphorylation and Bortezomib-induced HSR in H929 Cells and HSF1 Serine 326 Phosphorylation in U266 cells.** H929 or U266 cells were co-treated with TG02 and bortezomib. Western blot data are representative of four independent experiments. **(D) TG02 and Bortezomib Combination Leads to an Additive Effect on Apoptosis in H929 cells but not U266 Cells.** Experimental setup was as described in (C). **(E) TG02 Inhibits Carfilzomib-induced HSF1 Serine 326 Phosphorylation and Bortezomib-induced HSR in Patient Samples.** CD138+ (>90%: PS10001496, >75%: PS10001225-2) cells from freshly isolated patient samples were co-treated with TG02 and carfilzomib. Experimental design as above. **(F) CDK9 is not Responsible for Bortezomib-induced S326 Phosphorylation and its Silencing does not Sensitize Cells to Bortezomib-induced Apoptosis.** MM.1s cells were treated with a non-silencing control (-), CDK9 (C), or HSF1 (H) siRNA for 24h followed by bortezomib treatment for either an additional 9h for western blot analysis (top) or 24h for flow cytometry analysis (bottom). Data are representative of three independent experiments. Apoptosis was measured as described above. *p*-values are calculated by paired t-test. (*$p<0.05$, **$p<0.01$).

Supplemental Table

Array Coordinate	Protein	Phosphorylation Site	Fold Increase in Induction (n=2)	Putative Upstream Kinases	In Vitro Kinases
C15/16	c-Jun	S63	2.7	CDK3, ERK7, JNK1, JNK2, PBK, PLK3, VRK1	CDK3, ERK7, JNK1, JNK2, PBK, PRKD1, VRK1
C5/6	HSP27	S78/S82	1.75	Akt1, P70S6KB, PRKD1	Akt1, MAPKAPK2, PKACA, PKG1 iso2, PRKD1
A13/14	p53	S392	1.54	LKB1, NuaK1	CDK7, CDK9, CK2A (CKII), ERK1, LKB1, PKR
B9/10	Akt1/2/3	S473	1.46	IKKE, ILK, LRRK2, mTOR, PDK1, PIKFYVE, PRKD1, TBK1	DNAPK, ILK, LRRK2, MAPKAPK2, mTOR, PDK1, PKCA/B, PDK1, TBK1
A7/8	JNK1/2/3	T183/Y185, T221/Y223	1.38	ASK1, MEKK6, MKK7	MKK4, MKK7
B13/14	p53	S46	1.38	ATM, CDK5, DYRK2, HIPK2, P38A, PKCD	ATM, CDK5, DNAPK, DYRK2, HIPK2, P38A, PKCD
E13/14	p27	T198	1.22	Akt1, CAMK1A, Pim1	Akt1, AMPK1, Pim1, SGK1

Identification and characterization of BZ-induced targets and their respective kinases as described in Figure 1B. Fold increase quantification was performed using Fiji (ImageJ). Putative upstream kinases have been determined in intact cells or organisms. In-vitro kinases have been determined outside of intact cells or organisms. Both putative upstream and in-vitro kinases for respective targets are displayed as listed in the PhosphoSitePlus® database.

V. DISCUSSION

A. Implications from Bortezomib-Induction of Heat Shock Factor 1 Serine 326 Phosphorylation Studies

1. Characterization of the MPH

In our studies of the HSF1-mediated bortezomib-induced HSR in MM, we characterized what we will term the MM PI-induced HSR (MPH), which is the HSP subset whose bortezomib-induction is HSF1-dependent. Individual HSF1-dependent bortezomib-induced HSPs have been previously identified, but the novelty of the MPH is the use of multiple cell lines and patient samples to establish a complete HSP catalog.[11,32,150] HSF1-dependent bortezomib-induced HSP characterization provides a unique look into a subset of the HSR. The entirety of the HSR consists of over 100 HSPs, and many are upregulated when cells face any driver of stress, including stress unrelated to PI, such as extreme temperatures, environmental toxins, and radiation.[173] Therefore, MPH structural and functional characterization based on our data can inform future drug design studies.

We have stated earlier that single HSP inhibition is clinically ineffective and inhibiting several HSPs by using multiple inhibitors to target individual HSPs is impractical. In addition, there is no FDA-approved HSF1 inhibitor and indirect HSF1 inhibition studies are ongoing. Therefore, pharmacological inhibition of conserved MPH protein-protein interactions is a potential therapeutic strategy, and could serve as an alternate therapeutic strategy to direct and indirect HSF1 inhibition. For example, inhibition of HSP-chaperone binding could lead to excess misfolded protein aggregation and ultimately apoptosis.

One caveat regarding the MPH is that it was formed from MM.1s cell line data. We have confirmed a similar MPH in four additional cell lines and two patient samples using western blotting and qRT-PCR, however, broad scale MPH data remain limited. Future studies should perform HSP arrays on additional bortezomib-treated cell lines and patient samples to include HSPs that might not have been upregulated in the MM.1s cell line. These data would strengthen understanding of the MPH.

In addition, the MPH could inform functional studies. Interestingly, 75% of the MPH is large HSPs (≥40 kDa) and 25% is smaller HSPs (<40 kDa). Larger HSPs (HSP40, HSP70, HSP90) tend to have roles in protein refolding whereas the majority of smaller HSPs (HSP27, HSPB5) guide misfolded proteins toward proteasomal degradation. The skewing of the MPH toward larger HSPs show a possible feedback mechanism by which myeloma cells can tailor the MPH toward upregulation of larger HSPs due to the inability of myeloma cells to perform proteasomal degradation (Figure 1). This mechanism would prevent unnecessary upregulation of HSPs whose functions cannot be properly executed and would explain why PI leads to HSF1 preferential binding to the HSE of larger HSPs in contrast to smaller HSPs.

2. The Role of the MPH and HSF1 Activation in Combination Therapy

Our studies have detailed bortezomib-induced HSP upregulation and HSF1 activation. Future studies should investigate carfilzomib-induced HSP upregulation and HSF1 activation. A comparable HSF1 PTM and HSR pattern would indicate that the mechanism of HSF1 activation and upregulation of downstream HSPs is independent of PI structure. Our findings detailed elsewhere show that several HSF1-dependent HSPs

induced by bortezomib are also induced by carfilzomib but these data are only from one cell line and two patient samples. Consistency of the MPH across multiple PIs would further validate the previously proposed protein structure and functional studies.

One caveat regarding our MPH studies is that PIs are almost never administered alone but more often as part of combination therapy. Therefore, the MPH in IMiD + PI combination therapy should be further investigated. We hypothesize that combination therapy would increase HSP expression, and skew toward larger HSPs if the data support our previous model. This is because IMiDs work in part by binding to CRBN, the substrate adaptor of the $CRL4^{CRBN}$ E3 ubiquitin ligase. IMiDs induce recruitment of the substrates IKZF1 (Ikaros), IKZF3 (Aiolos), and CK1α (Casein Kinase) to $CRL4^{CRBN}$ and their ubiquitination by this ligase. An IMiD + PI combination could lead to a ubiquitinated substrate buildup and may further intensify the HSR, therefore validating the addition of a broad scale HSP inhibition to this drug combination. Interestingly, dexamethasone, a steroid administered as part of frontline MM combination therapy, has been shown to induce the HSR in animal models of Huntington's disease, demonstrating the need for further investigation into HSP upregulation by dexamethasone-containing MM combination therapies.[174]

In addition, future studies should compare bortezomib and carfilzomib-induced HSF1 PTMs in order to strengthen our understanding of PI-induced HSF1 activation. Also, a comparison of PI-only and IMiD + PI combination therapy with regard to PTMs that regulate HSF1 activation should be performed. Proteomics studies of cell line or patient sample combination therapy-induced PTMs can provide deeper insight into inhibition of HSF1 activation. Additional MM therapies commonly co-administered with

PIs, such as dexamethasone, prednisone, or melphalan, can also be incorporated. Taken together, these studies could show that HSF1 or broad scale HSP inhibition may be necessary to increase sensitivity to IMiD or dexamethasone-containing therapies.

3. Non-HSR HSF1 Functionality in MM

Our data show that HSF1 inhibition results in greater sensitization to bortezomib than individual HSP inhibition alone, and than simultaneously inhibiting the three most HSF1-dependent targets. To paraphrase German psychologist, Kurt Koffka, our data is the first to show that the whole (HSF1 inhibition) is other than the sum of the parts (multiple HSP inhibition). We believe it is likely because HSF1 plays a multifaceted role in stressed and non-stressed conditions, including cell-cycle regulation, signaling, metabolism, adhesion and translation.[56] Of these roles, the study of glucose metabolism has recently garnered significant interest. Previous studies have shown that glucose, the dominant tumor energy supplement, participates in regulating HSF1 activation in hepatocellular carcinoma cell lines.[175] Interestingly, glucose, but not 2D-glucose, can induce the phosphorylation of HSF1 at S326 and upregulate the expression of hspb5 and hsp70 as well as the non-heat shock proteins CSK2 and RBM23.[175] HSPs and HSF1 separately positively regulate glucose metabolism.[175,176] Therefore, HSF1 inhibition could effect both proteostasis and glucose metabolism (Figure 2). Which potential HSF1 roles listed above specifically relates to myeloma cell biology remains to be fully elucidated but is a topic of great interest to the cancer biology field.[56,57,110,175-177]

4. Non-pS326 HSF1 PI-induced Phosphorylation in MM

Activation is an additional component of our rapidly evolving understanding of HSF1 biology. Our studies were the first to show that bortezomib induces HSF1 phosphorylation in MM cell lines and patient samples, and previous studies have shown that HSF1 activation is also regulated by acetylation and sumoylation.[126] While we have detailed pS326 elsewhere and characterized pS303, a more comprehensive account of HSF1 activation is required to better understand the MM HSF1 lifecycle. This examination can provide further insight into HSF1 inhibition strategies aside from pS326 inhibition. One limitation of a pS326 inhibition strategy is that transactivation associated with pS326 occurs in the middle of the HSF1 lifecycle, after heterotetramer release, trimerization, and nuclear translocation. An alternative to allowing HSF1 to progress through the early part of its lifecycle is kinase inhibitor inhibition of early activating events. This may prevent the proverbial fox from running loose in the henhouse, when it may be too late to fully inhibit HSF1 activity. Future studies should identify the kinases responsible for activating PTMs associated with aforementioned early lifecycle events such as pS195, pS320, pS333, and pS419.

In addition, our proteomics studies revealed that bortezomib induces pS314 in the MM.1s cell line. The functional role of pS314 is unknown as is its regulation. There is the possibility that pS314 and pS326 are co-dependent, similar to the manner by which pS303 is required for pS307. Alternatively, these two activating PTMs could be functionally redundant. One potential cytoprotective mechanism could be that inhibition of either pS314 or pS326 is not enough to fully inhibit PI-induced HSF1 transactivation and inhibition of both may be required for total HSF1 inactivation. The proximity of

these two activating events, raises the possibility that these two amino acids are located in a phosphorylation hotspot and regulated by similar kinases.

Novel details about HSF1 activation may arise from further characterization of pS13, a novel phosphorylation event discovered during our proteomics studies. We are working with an immunochemical company to develop a pS13 antibody and will perform functional characterization of pS13 and observe any change in pS13 expression before and after bortezomib treatment. A difference would warrant further investigation into the kinase responsible for this inducible phosphorylation event.

In addition, further studies are necessary to detail the late lifecycle events of HSF1, specifically after newly translated HSPs commence HSR downregulation and HSF1 nuclear presence is no longer required. Whether HSF1 is degraded or returns to its inactive heterotetramer state upon returning to the cytoplasm is unknown and requires further study. Acetylation may play a role in the late stages of HSF1 activation as described below.

5. Acetylation Regulation of HSF1 Activation

In addition to phosphorylation, HSF1 PTMs include sumoylation and acetylation. While we will not detail sumoylation here, investigation of its role in maintaining HSF1 constitutive phosphorylation may inform strategies targeting inhibition of HSF1 activation. Inhibition of activating acetylation events such as K208 and K298 as detailed by previous studies may contribute to MPH downregulation.[87] Furthermore, our proteomics data reveal that K62, a novel HSF1 PTM, is constitutively acetylated and shows higher acetylation levels upon bortezomib treatment in KMS18 cells. We have not

pursued additional characterization of this PTM but believe that future studies should characterize the role of K62 in activation. In addition, SIRT1, a deacetylase and sirtuin family member, has been shown to prolong HSF1 binding to the hsp70 HSE by maintaining HSF1 in a deacetylated, DNA-binding competent state.[65,88,97,178] We have performed preliminary sirtuin inhibition studies by treating myeloma cells with a combination of bortezomib and nicotinamide, a pan-sirtuin inhibitor. Interestingly, nicotinamide protected against bortezomib-induced apoptosis though it lead to downregulation of the bortezomib-induced HSR. One explanation for this is that nicotinamide is a pan-sirtuin inhibitor whereas SIRT1 is the specific deacetylase that regulates the HSF1 DNA-binding state. Therefore, inhibition of non-SIRT1 sirtuins could have counteracted the effects of SIRT1 inhibition. Characterization of acetylation in the HSF1 lifecycle using mass spectrometry in combination with a specific SIRT1 inhibitor, or SIRT1 CRISPR knockdown may elucidate how HSF1 dissociates from HSE and provide insight into downregulation of the middle and late stages of the HSF1 lifecycle.

6. pS326 as a MM Biomarker

Our studies are the first to characterize PI-induced pS326 in MM, and we believe that pS326 is a vital biomarker in MM. This is because of its potential role in IMiD and dexamethasone-induced HSF1 activation in addition to its demonstrated function in PI-induced HSF1 activation. Our cell line western blot and immunocytochemistry data and patient sample western blot data show that pS326 is strongly induced upon proteasome inhibition. Patient sample immunocytochemistry could support our data and strengthen

our understanding of PI-pS326. We have performed preliminary immunocytochemistry studies of MM patients before and after single agent treatment of oprozomib, an oral carfilzomib derivative (Figure 3). We stained frozen bone marrow sections with a pS326 antibody to detect pS326 expression before and after treatment. We were able to detect pS326 staining in 80% of patient samples and strong staining in 20%, but were unable to find a sample in which there was an expression change between before and after. Two confounding factors are that the sample size was five and therefore a greater number of samples are required for these studies, and also prior treatment was not considered before sample selection. These five patients could already have been treated with bortezomib or carfilzomib beforehand, thus priming the HSR before oprozomib treatment. We believe that future pS326 biomarker studies should investigate patient pS326 before induction therapy and after administration of proteasome inhibition to see if patients mount a HSR. Patients with low constitutive HSP expression and pS326 inducibility are predicted to be good responders to PI therapy, while high constitutive HSP expression and inducibility could indicate poor response (Figure 4). Patients who show high inducible pS326 expression could be potential candidates for HSF1 or HSF1-inhibition kinase inhibitor therapy. Taken together, we have shown evidence in cell lines and patient samples that pS326 is a potential biomarker which can be used to detect patient sensitivity to proteasome inhibition.

7. Summary

Myeloma cells hijack cytoprotective mechanisms used by normal plasma cells to maintain homeostasis such as the HSR. Our data show the first complete representation

of the MM bortezomib-induced HSF1-mediated HSR. We show evidence that HSF1 inhibition is a more effective therapeutic strategy than individual or multiple HSP inhibition and detail HSF1 activation and associated PTMs including pS326. Therapeutically, HSP induction has been linked to PI resistance, and PI resistance occurs in almost all MM patients. Therefore, eliminating the ability of myeloma cells to activate the HSR by direct or indirect inhibition of HSF1 could increase sensitivity to PI-based combination therapy and increase MM patient overall and long-term progression-free survival.

B. Implications from TG02 and Proteasome Inhibitor Studies

1. The PI-pS326 Kinase is Cytosolic

Previous sections have detailed the role of pS326 in HSF1 activation upon proteasome inhibition. However, we have been unable to identify the kinase responsible for PI-pS326. Identification could inform HSF1 inhibition strategies, leading to downregulation of the PI-induced HSR. Therefore, we performed subcellular fractionation to determine if PI-pS326 occurs in the cytosol or nucleus. These are the first studies detailing PI-induced pS326 localization. Our data show that S326 is phosphorylated in the cytosol followed by pS326 translocation into the nucleus and reveal additional possibilities about the role of pS326 and its regulation. Previous studies have shown that the kinetics of HSF1 PTMs do not match HSF1 activation kinetics.[88] Therefore, we propose that S326 phosphorylation occurs in the cytosol but its functional role in the nucleus is not executed until later in the HSF1 lifecycle (Figure 5). Another hypothesis is that in contrast to several previous studies, S326 has a role in the early part of the HSF1 lifecycle, such as facilitating heterotetramer breakup from HSP40/70/90, trimerization, or translocation. Therefore, future studies should use fluorescence microscopy or subcellular fractionation to detect pS326 localization earlier than 9h. There is also the unlikely possibility that the responsible kinase is nuclear and pS326 shuttles between the nucleus and cytoplasm between the inception of phosphorylation and peak phosphorylation. Addition of a nuclear exportin blocker to localization studies could provide more insight into target kinase localization.

2. TG02 Sensitizes MM Cell Lines and Patient Samples to Proteasome Inhibition and Inhibits PI-pS326

We have previously shown that TG02 causes a decrease in Mcl-1 protein levels and can work in an additive manner with carfilzomib to increase apoptosis in MM cell lines and patient samples.[168] A previous study also showed that TG02 synergizes with bortezomib in the MM.1s cell line and in an in-vivo mouse MM xenograft model.[172] Our studies here demonstrate a novel mechanism of inhibition of PI-induced HSF1 activation and HSP upregulation. We show that the kinase responsible for PI-pS326 is inhibited by TG02 in MM cell lines and patient samples. We also confirm that a TG02 and bortezomib or carfilzomib combination has an additive effect on apoptosis in the MM.1s cell line. In addition, we show that a TG02 and bortezomib combination has an additive effect on apoptosis in the H929 cell line and a myeloma patient sample.

We performed TG02 and PI co-treatment, which led to PI-pS326 inhibition in all three MM cell lines and both patient samples tested. Interestingly, this inhibition was ubiquitous though HSR inducibility and the additive effect on apoptosis varied. Therefore, our data show that TG02 can inhibit PI-pS326 independent of PI sensitivity and HSR inducibility. Despite this lack of correlation between TG02, an additive effect, and PI-pS326 inhibition, there was a distinct trend in our data. An additive effect on apoptosis was seen when TG02 treatment led to HSP induction inhibition, not just PI-pS326 inhibition. Both the MM.1s cell line and patient sample that showed a TG02 and bortezomib additive effect on apoptosis showed a strong TG02-mediated decrease in HSP70 and HSP40 expression and moderate HSP27 decreased expression. The H929 cell line, which showed a TG02 and bortezomib additive effect on apoptosis only at a low

dose, displayed TG02-mediated inhibition of HSP40 upregulation and HSP27 upregulation but not HSP70 upregulation. The U266 cell line and other patient sample did not show HSP upregulation as detected by western blot or an additive effect on apoptosis. However, several constitutive HSPs for the TG02-sensitive carfilzomib-resistant patient sample were still inhibited, indicating a role for carfilzomib resistance downstream of the HSR. For U266 cells, one possibility is that a low-level HSR not detectable by western blot was induced, explaining PI-pS326, but negative feedback mediated by newly transcribed HSPs rapidly led to HSR downregulation.

Our studies here are preliminary and require follow-up in order to strengthen our understanding of the data. Our hypothesis is that the threshold for PI-pS326 is lower than that for PI-induced HSP upregulation, and the latter must occur in order for TG02 to inhibit HSF1-dependent HSP upregulation, leading to PI sensitization (Figure 6). Additional studies to confirm this model should include a broad array of MM cell lines, patient samples, and should use both bortezomib and carfilzomib to show that TG02 inhibition of PI-pS326 and HSF1-mediated HSP upregulation is independent of PI structure.

3. Have We Moved Closer to Identifying the PI-pS326 Kinase?

Our use of TG02 was guided by its function as a multikinase inhibitor in order to help identify the kinase responsible for PI-pS326. As detailed earlier, we used several inhibitors against putative pS326 kinases but were unable to show PI-pS326 inhibition. However, our phosphokinase antibody array data indicated that either ERK5 or one of the CDK family members might be responsible and TG02 inhibits both ERK5 and CDK

family members. After observing that TG02 targets the kinase responsible for PI-pS326, we began to inhibit putative kinases. TG02 has <10 nM specificity for CDK1/2/3/5/9, 43 nM specificity for ERK5, and low nanomolar range specificity for additional targets. ERK5 was an attractive candidate because it is the only demonstrated TG02 cytosolic serine/threonine kinase.[167,172] However, our preliminary data show that ERK5 is not activated by bortezomib and is therefore not the responsible kinase. We then performed siRNA knockdown to inhibit CDK9 but did not detect a change in PI-pS326 nor any additive effect on apoptosis. This is consistent with our previous findings showing that CDK9 silencing does not change carfilzomib sensitivity in the same manner as TG02 addition.[168] We then tested a CDK1/5 inhibitor to determine if either is the responsible kinase. Preliminary data show neither inhibits PI-pS326 nor has an additive effect on apoptosis. A caveat is that we tested this inhibitor in MM.1s cells at indicated concentrations but were unable to observe G2/M cell cycle arrest, which is a downstream effect of CDK1 inhibition. One potential reason for this is because the 9h timeframe used in these studies may not have been long enough to induce G2/M arrest. A 24h or 48h timeframe may be needed to induce G2/M arrest, however, PI-pS326 phosphorylation peaks at 6-9h in MM cell lines and patient samples at IC_{50}-IC_{90}. Further studies should use lower PI concentrations over a longer time period more compatible with CDK inhibition detection. Taken together, neither ERK5 nor CDK1/5/9 is likely to be the kinase responsible for PI-pS326. Our TG02 and fractionation data lead us to believe that the kinase is a cytoplasmic TG02 target. Therefore, we can infer that the TG02 target responsible for PI-pS326 has not yet been elucidated.

4. Early Detection of TG02-Mediated PI-pS326 Inhibition in MM.1s Cells

Exploring HSF1 activation dynamics as detailed earlier may lead to additional insight into its activation and ultimately the kinase responsible for PI-pS326. Our preliminary data show that pS326 in MM cell lines and patient samples can be detected by western blot as early as 3h after PI treatment. We observe TG02 inhibition of pS326 at 3h but no effect on constitutive or inducible HSP expression in MM.1s cells. These data support our earlier conclusion that TG02 inhibition of PI-pS326 does not require HSR induction. Therefore, to find the responsible kinase for PI-pS326, kinetic and other functional studies should also be performed at earlier timepoints before other activating PTMs potentially obscure the HSF1 PTM landscape.

5. Summary

Here we have shown that PI-pS326 inhibition is a novel TG02 function. We have observed this in all MM cell lines and patient samples tested, though an additive effect an apoptosis was seen only when PIs induced HSP upregulation. The TG02-target kinase responsible for PI-pS326 has yet to be identified but our fractionation data show that it is cytoplasmic. Future studies should specifically identify this kinase and test the effects of its inhibition on the PI-induced HSR and also its additive effect on apoptosis. Further interrogation into the TG02 and PI combination will inform HSF1 regulation studies and provide clues into downregulating the HSR in order to sensitize cells to proteasome inhibition.

Figure 1

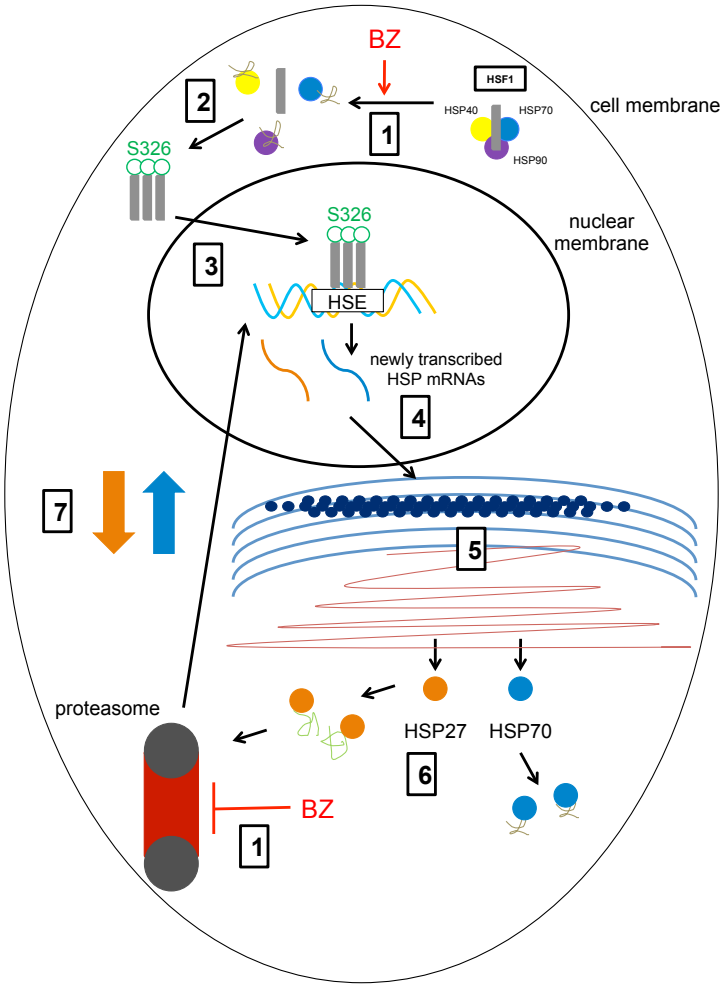

Figure 1: Proteasome Inhibition Skews HSF1-Dependent HSP Upregulation Toward Large (≥40 kDa) HSPs. Heat Shock Factor 1 (HSF1) is shown in the cytosol in an inactive heterotetramer with heat shock protein (HSP) 40/70/90. (1, top) Bortezomib treatment leads to heterotetramer dissociation. HSP40/70/90 chaperone misfolded proteins toward refolding. (1, bottom) Bortezomib treatment leads to β5 proteasomal subunit inhibition and 26S proteasome inactivation. (2) HSF1 trimerizes and is phosphorylated at serine 326 though in which order this occurs is not yet known. (3) The activated HSF1 trimer translocates to the nucleus where it binds to the heat shock element (HSE) of target HSP genes and promotes transcription. (4,5) Newly transcribed HSP mRNAs exit the nucleus and are translated and modified in the ER (blue) and Golgi (maroon), respectively. (6) Small HSPs (<40 kDa) bind misfolded proteins or protein aggregates and guide them toward proteasomal degradation while large HSPs (≥40 kDa) chaperone misfolded proteins toward refolding. (7) A currently uncharacterized feedback mechanism senses that the proteasome is no longer available for degradation, leading to downregulation of smaller HSP transcription and upregulation of larger HSP transcription. Abbreviations: BZ = bortezomib, HSE = heat shock element, HSF = heat shock factor, HSP = heat shock protein, P = phosphorylation, S = serine

Figure 2

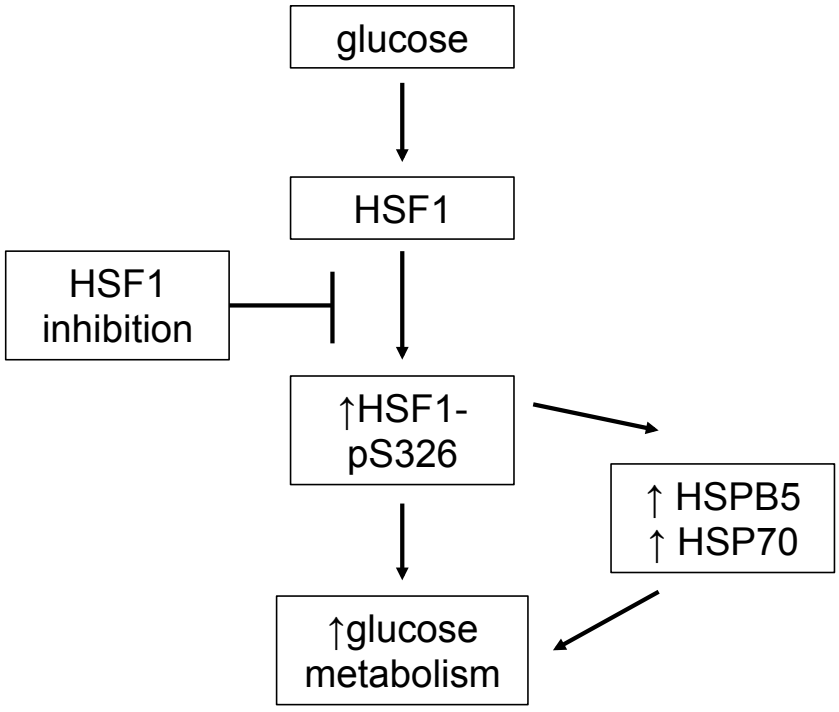

Figure 2: HSF1 Inhibition Can Lead to Dual Inhibition of Glucose Metabolism. Glucose leads to Heat Shock Factor 1 (HSF1) serine 326 phosphorylation, which in turn leads to upregulation of Heat Shock Protein (HSP) B5 and HSP70. HSF1 and HSPB5/HSP70 separately upregulate glucose metabolism. Inhibition of serine 326 phosphorylation can lead to dual inhibition of glucose metabolism.

Figure 3

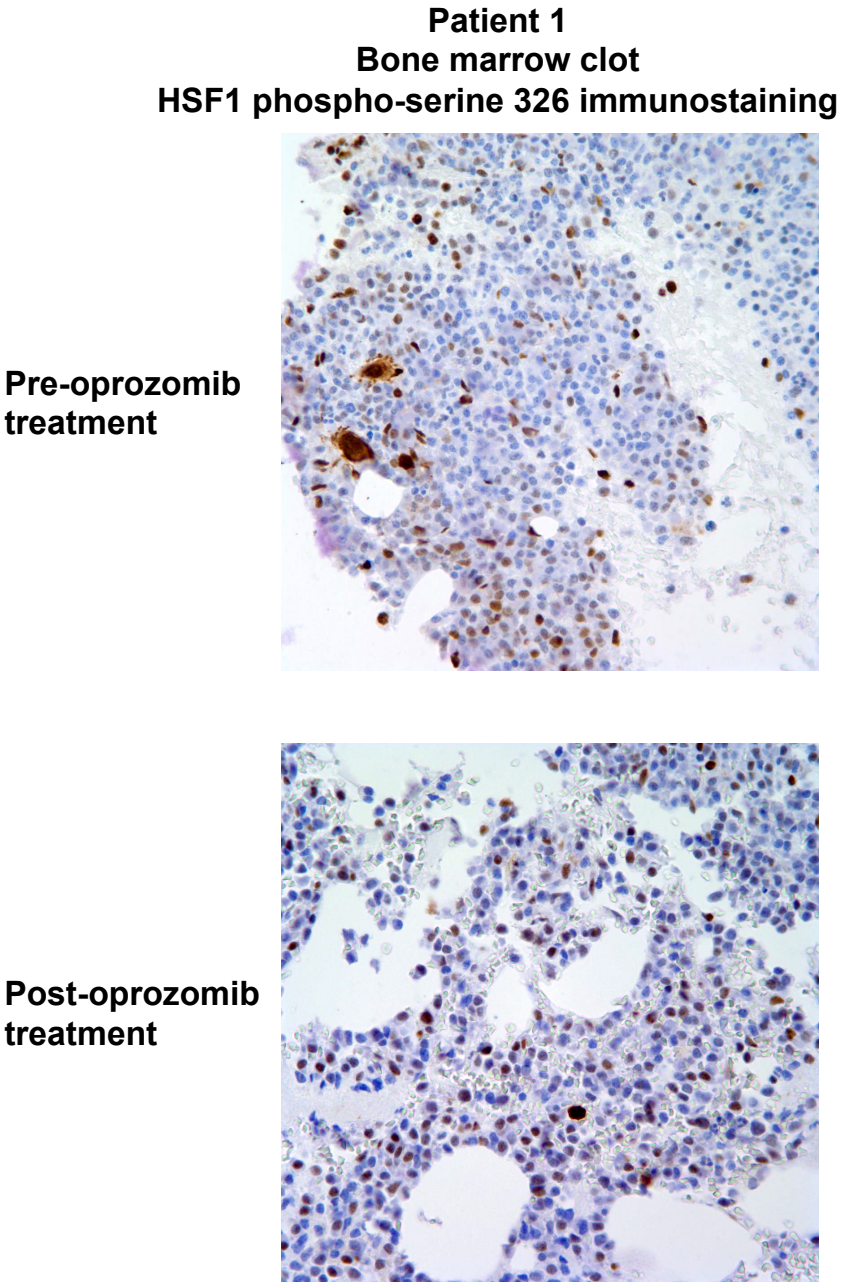

Figure 3: HSF1 Phospho-serine 326 Staining is Observed in a Patient Sample Both Pre- and Post-Oprozomib Treatment. Immunostaining of cell block sections was performed essentially as described on a Dako autostainer.[160] Antigen unmasking employed Target Retrieval Solution citrate buffer (Dako). Anti-pS326-HSF1 was used at a 1:2000 dilution and bound antibody was detected with Envision dual link kit with standard DAB reactions (Dako). Hematoxylin counterstained sections were mounted for light microscopy. Courtesy: David L Jaye, MD

Figure 4

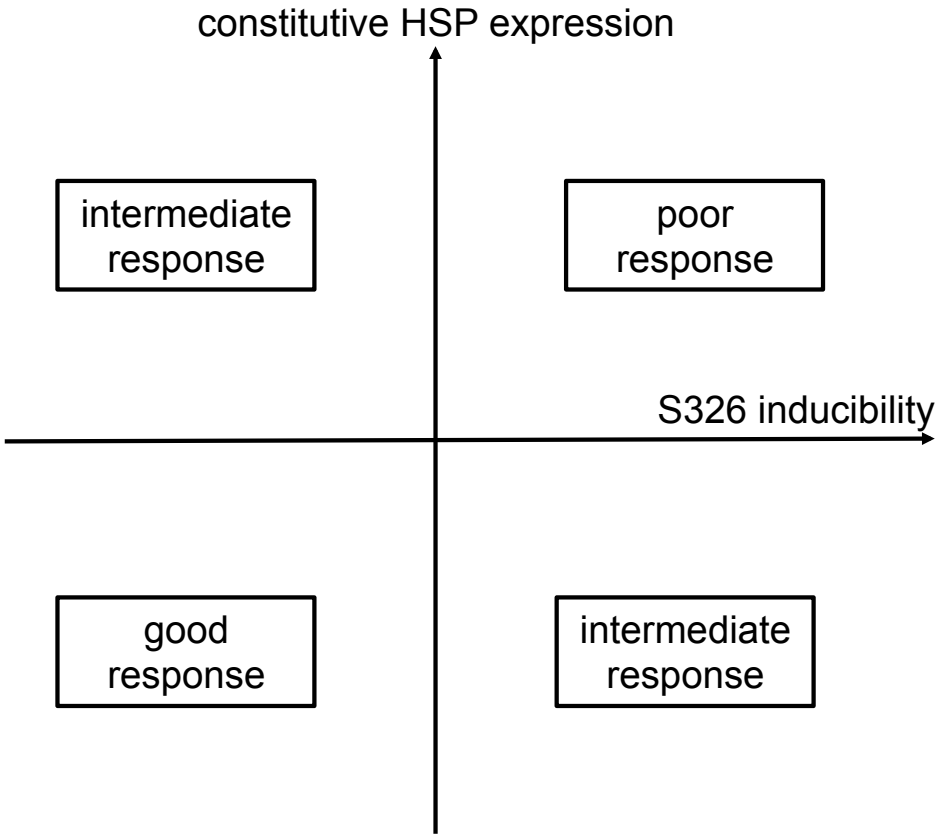

Figure 4: A Proposed Schematic for HSF1 Biomarker Studies to Predict Proteasome Inhibitor Response. (Lower left quadrant) Patients who show low Heat Shock Factor 1 (HSF1) serine 326 inducibility in response to proteasome inhibitor (PI) treatment and low constitutive heat shock protein (HSP) expression are predicted to be good responders to PI treatment. (Lower right and upper left quadrant) High levels of either HSF1 serine 326 inducibility or constitutive HSP expression predict intermediate PI response. (Upper right quadrant) High levels of both HSF1 serine 326 inducibility and constitutive HSP expression predict poor PI response.

Figure 5

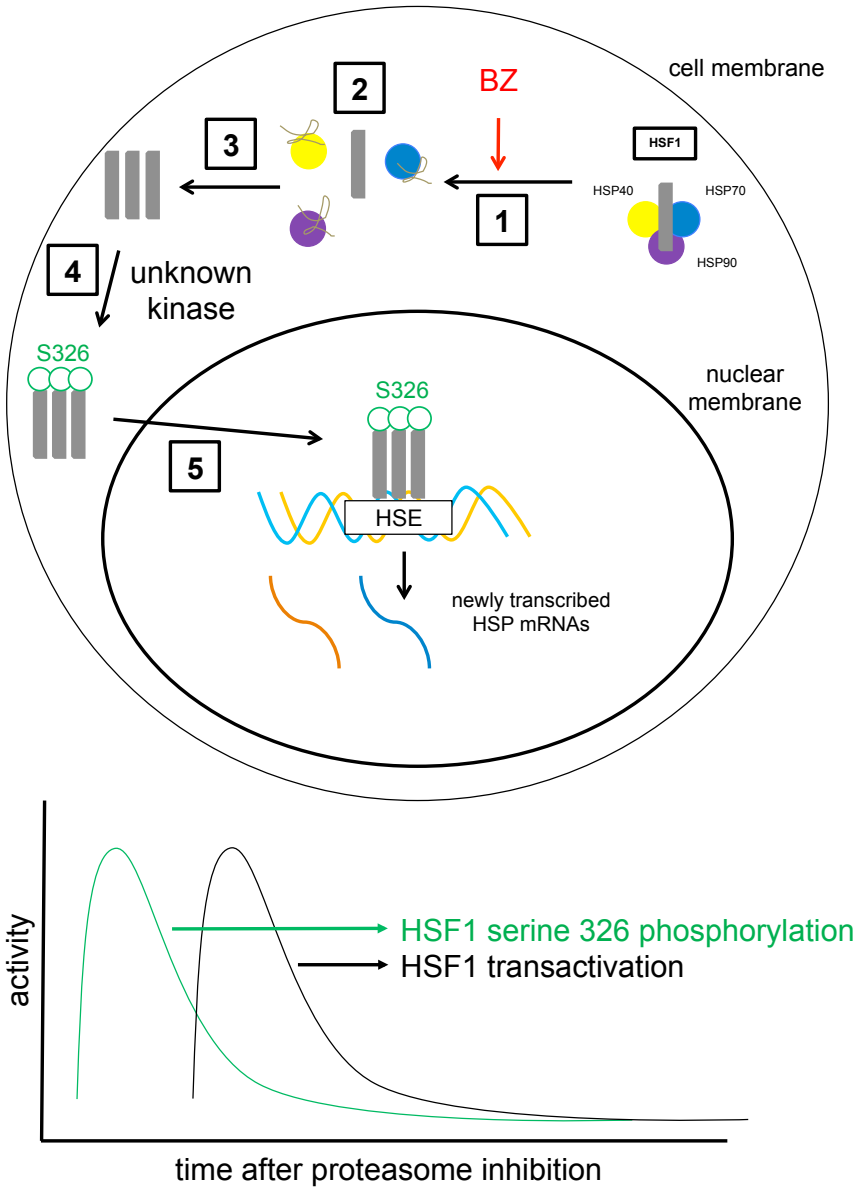

Figure 5: HSF1 Serine 326 Phosphorylation Occurs in the Cytosol Followed by HSF1 Nuclear Translocation. (Top) Heat Shock Factor 1 (HSF1) is shown in the cytosol in an inactive heterotetramer with heat shock protein (HSP) 40/70/90. (1) Bortezomib treatment leads to heterotetramer dissociation. (2) HSP40/70/90 chaperone misfolded proteins toward refolding. (3,4) HSF1 trimerizes and is phosphorylated at serine 326 by an unknown kinase, though which occurs first is not yet known. (5) The activated HSF1 trimer translocates to the nucleus where it binds to the heat shock element (HSE) of target HSP genes and promotes transcription. (Bottom) A proposed graph of activity versus time after proteasome inhibition for HSF1 serine 326 phosphorylation and HSF1 transactivation. HSF1 transactivation is defined as the period of HSP gene transcription promoted by HSF1-HSE binding.

Figure 6

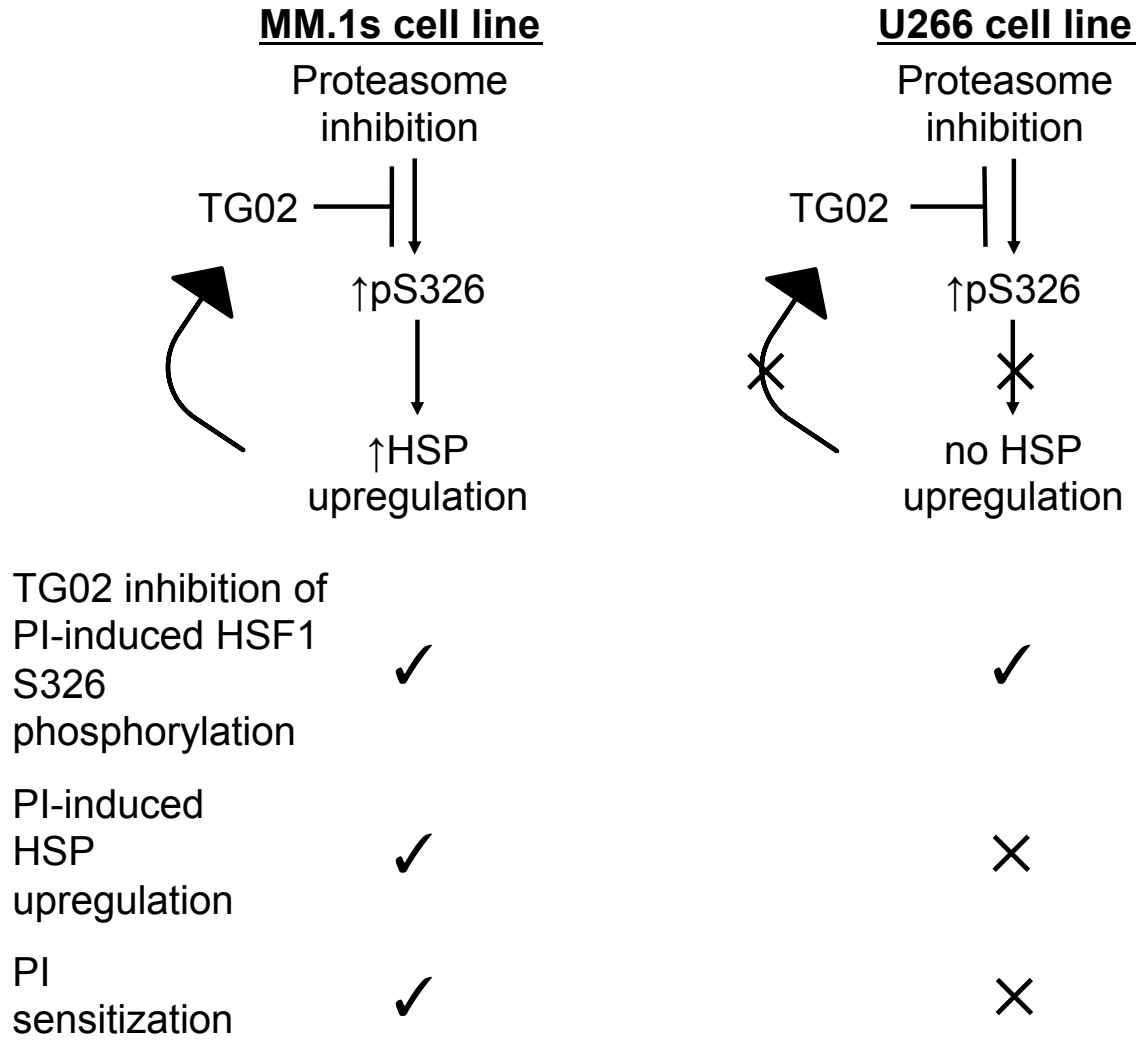

Figure 6: The Threshold for PI-induced HSF1 Serine 326 Phosphorylation is Lower than that of HSP Upregulation. In both the MM.1s and U266 cell lines, proteasome inhibitor (PI) treatment leads to Heat Shock Factor 1 (HSF1) serine 326 phosphorylation. TG02 inhibits serine 326 phosphorylation in both cell lines. (Left) In the MM.1s cell line, PI treatment induces HSP upregulation. Therefore, TG02 also inhibits PI-induced HSP upregulation, leading to sensitization to proteasome inhibitors. (Right) In the U266 cell line, PI treatment does not induce HSP upregulation, and no PI sensitization is observed.

VI. REFERENCES

1. Kumar SK, Rajkumar SV, Dispenzieri A, et al. Improved survival in multiple myeloma and the impact of novel therapies. *Blood*. 2008;111(5):2516-2520.

2. Singhal S, Mehta J, Desikan R, et al. Antitumor activity of thalidomide in refractory multiple myeloma. *N Engl J Med*. 1999;341(21):1565-1571.

3. Boise LH, Kaufman JL, Bahlis NJ, Lonial S, Lee KP. The Tao of myeloma. *Blood*. 2014;124(12):1873-1879.

4. Weathington NM, Mallampalli RK. Emerging therapies targeting the ubiquitin proteasome system in cancer. *J Clin Invest*. 2014;124(1):6-12.

5. Sahasrabuddhe AA, Elenitoba-Johnson KSJ. Role of the ubiquitin proteasome system in hematologic malignancies. *Immunological Reviews*. 2015;263(1):224-239.

6. Hideshima T, Anderson KC. Biologic impact of proteasome inhibition in multiple myeloma cells--from the aspects of preclinical studies. *Semin Hematol*. 2012;49(3):223-227.

7. Moreau P, Richardson PG, Cavo M, et al. Proteasome inhibitors in multiple myeloma: 10 years later. *Blood*. 2012;120(5):947-959.

8. Palombella VJ, Conner EM, Fuseler JW, et al. Role of the proteasome and NF-kappaB in streptococcal cell wall-induced polyarthritis. *Proc Natl Acad Sci U S A*. 1998;95(26):15671-15676.

9. Adams J, Palombella VJ, Sausville EA, et al. Proteasome inhibitors: a novel class of potent and effective antitumor agents. *Cancer Res*. 1999;59(11):2615-2622.

10. Hideshima T, Richardson P, Chauhan D, et al. The proteasome inhibitor PS-341 inhibits growth, induces apoptosis, and overcomes drug resistance in human multiple myeloma cells. *Cancer Res*. 2001;61(7):3071-3076.

11. Mitsiades N, Mitsiades CS, Poulaki V, et al. Molecular sequelae of proteasome inhibition in human multiple myeloma cells. *Proc Natl Acad Sci U S A*. 2002;99(22):14374-14379.

12. Richardson PG, Barlogie B, Berenson J, et al. A phase 2 study of bortezomib in relapsed, refractory myeloma. *N Engl J Med*. 2003;348(26):2609-2617.

13. Hideshima T, Mitsiades C, Akiyama M, et al. Molecular mechanisms mediating antimyeloma activity of proteasome inhibitor PS-341. *Blood*. 2003;101(4):1530-1534.

14. Iwakoshi NN, Lee AH, Vallabhajosyula P, Otipoby KL, Rajewsky K, Glimcher LH. Plasma cell differentiation and the unfolded protein response intersect at the transcription factor XBP-1. *Nat Immunol*. 2003;4(4):321-329.

15. Lee AH, Iwakoshi NN, Anderson KC, Glimcher LH. Proteasome inhibitors disrupt the unfolded protein response in myeloma cells. *Proc Natl Acad Sci U S A*. 2003;100(17):9946-9951.

16. Obeng EA, Carlson LM, Gutman DM, Harrington WJ, Jr., Lee KP, Boise LH. Proteasome inhibitors induce a terminal unfolded protein response in multiple myeloma cells. *Blood*. 2006;107(12):4907-4916.

17. Meister S, Schubert U, Neubert K, et al. Extensive immunoglobulin production sensitizes myeloma cells for proteasome inhibition. *Cancer Res*. 2007;67(4):1783-1792.

18. Bianchi G, Oliva L, Cascio P, et al. The proteasome load versus capacity balance determines apoptotic sensitivity of multiple myeloma cells to proteasome inhibition. *Blood*. 2009;113(13):3040-3049.

19. Ling SC, Lau EK, Al-Shabeeb A, et al. Response of myeloma to the proteasome inhibitor bortezomib is correlated with the unfolded protein response regulator XBP-1. *Haematologica*. 2012;97(1):64-72.

20. Leung-Hagesteijn C, Erdmann N, Cheung G, et al. Xbp1s-Negative Tumor B Cells and Pre-Plasmablasts Mediate Therapeutic Proteasome Inhibitor Resistance in Multiple Myeloma. *Cancer cell*. 2013;24(3):289-304.

21. Moriya S, Komatsu S, Yamasaki K, et al. Targeting the integrated networks of aggresome formation, proteasome, and autophagy potentiates ER stress-mediated cell death in multiple myeloma cells. *International Journal of Oncology*. 2015;46(2):474-486.

22. Selimovic D, Porzig BB, El-Khattouti A, et al. Bortezomib/proteasome inhibitor triggers both apoptosis and autophagy-dependent pathways in melanoma cells. *Cell Signal*. 2013;25(1):308-318.

23. Catley L, Weisberg E, Kiziltepe T, et al. Aggresome induction by proteasome inhibitor bortezomib and alpha-tubulin hyperacetylation by tubulin deacetylase (TDAC) inhibitor LBH589 are synergistic in myeloma cells. *Blood*. 2006;108(10):3441-3449.

24. Kale AJ, Moore BS. The molecular mechanisms of acquired proteasome inhibitor resistance. *Journal of medicinal chemistry*. 2012;55(23):10317-10327.

25. Ri M, Iida S, Nakashima T, et al. Bortezomib-resistant myeloma cell lines: a role for mutated PSMB5 in preventing the accumulation of unfolded proteins and fatal ER stress. *Leukemia*. 2010;24(8):1506-1512.

26. Oerlemans R, Franke NE, Assaraf YG, et al. Molecular basis of bortezomib resistance: proteasome subunit β5 (PSMB5) gene mutation and overexpression of PSMB5 protein. *Blood*. 2008;112(6):2489-2499.

27. Kubiczkova L, Pour L, Sedlarikova L, Hajek R, Sevcikova S. Proteasome inhibitors - molecular basis and current perspectives in multiple myeloma. *J Cell Mol Med*. 2014;18(6):947-961.

28. Triphase Research and Development Corporation. Combination Study of Pomalidomide, Marizomib, and Low-Dose Dexamethasone in Relapsed and Refractory Multiple Myeloma. Bethesda (MD) National Library of Medicine. 2000- [cited 2016 Nov 13]. Available from: https://clinicaltrials.gov/ct2/show/NCT02103335 NLM Identifier: NCT02103335.

29. Richardson PG, Baz R, Wang M, et al. Phase 1 study of twice-weekly ixazomib, an oral proteasome inhibitor, in relapsed/refractory multiple myeloma patients. *Blood*. 2014;124(7):1038-1046.

30. Kumar SK, Bensinger WI, Zimmerman TM, et al. Phase 1 study of weekly dosing with the investigational oral proteasome inhibitor ixazomib in relapsed/refractory multiple myeloma. *Blood*. 2014;124(7):1047-1055.

31. Hofmeister C, Lonial S. "Is a Cure for Myeloma on the Horizon?" Online video clip. Patient Power. YouTube, Dec 2014. Web. Dec 2012.

32. Zhang L, Fok JH, Davies FE. Heat shock proteins in multiple myeloma. *Oncotarget*. 2014;5(5):1132-1148.

33. Kampinga HH, Hageman J, Vos MJ, et al. Guidelines for the nomenclature of the human heat shock proteins. *Cell Stress Chaperones*. 2009;14(1):105-111.

34. Qi W, White MC, Choi W, et al. Inhibition of inducible heat shock protein-70 (hsp72) enhances bortezomib-induced cell death in human bladder cancer cells. *PLoS One*. 2013;8(7):e69509.

35. Richardson PG, Mitsiades CS, Laubach JP, Lonial S, Chanan-Khan AA, Anderson KC. Inhibition of heat shock protein 90 (HSP90) as a therapeutic strategy for the treatment of myeloma and other cancers. *Br J Haematol*. 2011;152(4):367-379.

36. Ishii T, Seike T, Nakashima T, et al. Anti-tumor activity against multiple myeloma by combination of KW-2478, an Hsp90 inhibitor, with bortezomib. *Blood Cancer Journal*. 2012;2:e68.

37. Usmani SZ, Chiosis G. HSP90 inhibitors as therapy for multiple myeloma. *Clin Lymphoma Myeloma Leuk*. 2011;11 Suppl 1:S77-81.

38. Jhaveri K, Ochiana SO, Dunphy MP, et al. Heat shock protein 90 inhibitors in the treatment of cancer: current status and future directions. *Expert Opin Investig Drugs*. 2014;23(5):611-628.

39. Whitesell L, Lindquist SL. HSP90 and the chaperoning of cancer. *Nat Rev Cancer*. 2005;5(10):761-772.

40. Powers MV, Workman P. Inhibitors of the heat shock response: Biology and pharmacology. *FEBS Letters*. 2007;581(19):3758-3769.

41. Schmitt E, Maingret L, Puig PE, et al. Heat shock protein 70 neutralization exerts potent antitumor effects in animal models of colon cancer and melanoma. *Cancer Res*. 2006;66(8):4191-4197.

42. Braunstein MJ, Scott SS, Scott CM, et al. Antimyeloma Effects of the Heat Shock Protein 70 Molecular Chaperone Inhibitor MAL3-101. *J Oncol*. 2011;2011:232037.

43. Davenport EL, Zeisig A, Aronson LI, et al. Targeting heat shock protein 72 enhances Hsp90 inhibitor-induced apoptosis in myeloma. *Leukemia*. 2010;24(10):1804-1807.

44. Murphy ME. The HSP70 family and cancer. *Carcinogenesis*. 2013;34: 1181–8.

45. Goloudina AR, Demidov ON, Garrido C. Inhibition of HSP70: A challenging anti-cancer strategy. *Cancer Letters*. 2012;325(2):117-124.

46. Sauvageot CM, Weatherbee JL, Kesari S, et al. Efficacy of the HSP90 inhibitor 17-AAG in human glioma cell lines and tumorigenic glioma stem cells. *Neuro Oncol*. 2009;11(2):109-121.

47. Erlichman C. Tanespimycin: the opportunities and challenges of targeting heat shock protein 90. *Expert Opin Investig Drugs*. 2009;18(6):861-868.

48. McCollum AK, Teneyck CJ, Sauer BM, Toft DO, Erlichman C. Up-regulation of heat shock protein 27 induces resistance to 17-allylamino-demethoxygeldanamycin through a glutathione-mediated mechanism. *Cancer Res*. 2006;66(22):10967-10975.

49. Powers MV, Clarke PA, Workman P. Dual targeting of HSC70 and HSP72 inhibits HSP90 function and induces tumor-specific apoptosis. *Cancer Cell*. 2008;14(3):250-262.

50. Clarke PA, Hostein I, Banerji U, et al. Gene expression profiling of human colon cancer cells following inhibition of signal transduction by 17-allylamino-17-demethoxygeldanamycin, an inhibitor of the hsp90 molecular chaperone. *Oncogene*. 2000;19(36):4125-4133.

51. Maloney A, Clarke PA, Naaby-Hansen S, et al. Gene and protein expression profiling of human ovarian cancer cells treated with the heat shock protein 90 inhibitor 17-allylamino-17-demethoxygeldanamycin. *Cancer Res*. 2007;67(7):3239-3253.

52. Yasui H, Hideshima T, Ikeda H, et al. BIRB 796 enhances cytotoxicity triggered by bortezomib, heat shock protein (Hsp) 90 inhibitor, and dexamethasone via inhibition of p38 mitogen-activated protein kinase/Hsp27 pathway in multiple myeloma cell lines and inhibits paracrine tumour growth. *Br J Haematol*. 2007;136(3):414-423.

53. Acquaviva J, He S, Sang J, et al. mTOR inhibition potentiates HSP90 inhibitor activity via cessation of HSP synthesis. *Mol Cancer Res*. 2014;12(5):703-713.

54. Vihervaara A, Sistonen L. HSF1 at a glance. *J Cell Sci*. 2014;127(Pt 2):261-266.

55. Anckar J, Sistonen L. Regulation of HSF1 function in the heat stress response: implications in aging and disease. *Annu Rev Biochem*. 2011;80:1089-1115.

56. Mendillo ML, Santagata S, Koeva M, et al. HSF1 drives a transcriptional program distinct from heat shock to support highly malignant human cancers. *Cell*. 2012;150(3):549-562.

57. Scherz-Shouval R, Santagata S, Mendillo ML, et al. The reprogramming of tumor stroma by HSF1 is a potent enabler of malignancy. *Cell*. 2014;158(3):564-578.

58. Åkerfelt M, Morimoto RI, Sistonen L. Heat shock factors: integrators of cell stress, development and lifespan. *Nat Rev Mol Cell Biol*. 2010;11(8):545-555.

59. Rossi A, Riccio A, Coccia M, Trotta E, La Frazia S, Santoro MG. The proteasome inhibitor bortezomib is a potent inducer of zinc finger AN1-type domain 2a gene expression: role of heat shock factor 1 (HSF1)-heat shock factor 2 (HSF2) heterocomplexes. *J Biol Chem*. 2014;289(18):12705-12715.

60. Inouye S, Katsuki K, Izu H, et al. Activation of heat shock genes is not necessary for protection by heat shock transcription factor 1 against cell death due to a single exposure to high temperatures. *Mol Cell Biol*. 2003;23(16):5882-5895.

61. Zou J, Guo Y, Guettouche T, Smith DF, Voellmy R. Repression of heat shock transcription factor HSF1 activation by HSP90 (HSP90 complex) that forms a stress-sensitive complex with HSF1. *Cell*. 1998;94(4):471-480.

62. Ali A, Bharadwaj S, O'Carroll R, Ovsenek N. HSP90 interacts with and regulates the activity of heat shock factor 1 in Xenopus oocytes. *Mol Cell Biol*. 1998;18(9):4949-4960.

63. Neef DW, Jaeger AM, Thiele DJ. Heat shock transcription factor 1 as a therapeutic target in neurodegenerative diseases. *Nat Rev Drug Discov*. 2011;10(12):930-944.

64. Tomanek L, Somero GN. Interspecific- and acclimation-induced variation in levels of heat-shock proteins 70 (hsp70) and 90 (hsp90) and heat-shock transcription factor-1 (HSF1) in congeneric marine snails (genus Tegula): implications for regulation of hsp gene expression. *J Exp Biol*. 2002;205(Pt 5):677-685.

65. Verma P, Pfister JA, Mallick S, D'Mello SR. HSF1 protects neurons through a novel trimerization- and HSP-independent mechanism. *J Neurosci*. 2014;34(5):1599-1612.

66. Wang HY, Fu JC, Lee YC, Lu PJ. Hyperthermia stress activates heat shock protein expression via propyl isomerase 1 regulation with heat shock factor 1. *Mol Cell Biol*. 2013;33(24):4889-4899.

67. Devaney E. Molecular and Physiological Basis of Nematode Survival. Oxfordshire, UK: CAB International; 2011. Perry RN and Wharton DA (eds). pp. 238–9.

68. Takii R, Fujimoto M, Tan K, et al. ATF1 Modulates the Heat Shock Response by Regulating the Stress-Inducible Heat Shock Factor 1 Transcription Complex. *Mol Cell Biol*. 2015;35(1):11-25.

69. Gilmour DS, Lis JT. In vivo interactions of RNA polymerase II with genes of Drosophila melanogaster. *Mol Cell Biol*. 1985;5(8):2009-2018.

70. Taylor DM, Tradewell ML, Minotti S, Durham HD. Characterizing the role of Hsp90 in production of heat shock proteins in motor neurons reveals a suppressive effect of wild-type Hsf1. *Cell Stress Chaperones*. 2007;12(2):151-162.

71. Pockley AG, Calderwood SK, Santoro MG. Prokaryotic and Eukaryotic Heat Shock Proteins in Infectious Disease: Dordrecht: Springer; 2009.

72. Sourbier C, Scroggins BT, Ratnayake R, et al. Englerin A stimulates PKCθ to inhibit insulin signaling and simultaneously activate HSF1: An example of pharmacologically induced synthetic lethality. *Cancer cell*. 2013;23(2):228-237.

73. Kim SA, Yoon JH, Lee SH, Ahn SG. Polo-like kinase 1 phosphorylates heat shock transcription factor 1 and mediates its nuclear translocation during heat stress. *J Biol Chem*. 2005;280(13):12653-12657.

74. Murshid A, Chou SD, Prince T, Zhang Y, Bharti A, Calderwood SK. Protein kinase A binds and activates heat shock factor 1. *PLoS One*. 2010;5(11):e13830.

75. Soncin F, Zhang X, Chu B, et al. Transcriptional activity and DNA binding of heat shock factor-1 involve phosphorylation on threonine 142 by CK2. *Biochem Biophys Res Commun*. 2003;303(2):700-706.

76. Holmberg CI, Hietakangas V, Mikhailov A, et al. Phosphorylation of serine 230 promotes inducible transcriptional activity of heat shock factor 1. *Embo j*. 2001;20(14):3800-3810.

77. Calderwood SK, Xie Y, Wang X, et al. Signal Transduction Pathways Leading to Heat Shock Transcription. *Sign Transduct Insights*. 2010;2:13-24.

78. Xie Y, Zhong R, Chen C, Calderwood SK. Heat shock factor 1 contains two functional domains that mediate transcriptional repression of the c-fos and c-fms genes. *J Biol Chem*. 2003;278(7):4687-4698.

79. Guettouche T, Boellmann F, Lane WS, Voellmy R. Analysis of phosphorylation of human heat shock factor 1 in cells experiencing a stress. *BMC Biochem*. 2005;6:4.

80. Li D, Yallowitz A, Ozog L, Marchenko N. A gain-of-function mutant p53-HSF1 feed forward circuit governs adaptation of cancer cells to proteotoxic stress. *Cell Death Dis*. 2014;5:e1194.

81. Chou SD, Prince T, Gong J, Calderwood SK. mTOR is essential for the proteotoxic stress response, HSF1 activation and heat shock protein synthesis. *PLoS One*. 2012;7(6):e39679.

82. Tang Z, Dai S, He Y, et al. MEK Guards Proteome Stability and Inhibits Tumor-Suppressive Amyloidogenesis via HSF1. *Cell*. 2015;160(4):729-744.

83. Dai C, Santagata S, Tang Z, et al. Loss of tumor suppressor NF1 activates HSF1 to promote carcinogenesis. *The Journal of Clinical Investigation*. 2012;122(10):3742-3754.

84. Kim S-Y, Lee H-J, Nam J-W, Seo E-K, Lee Y-S. Coniferyl Aldehyde Reduces Radiation Damage Through Increased Protein Stability of Heat Shock Transcriptional Factor 1 by Phosphorylation. *International Journal of Radiation Oncology*Biology*Physics*. 2015;91(4):807-816.

85. Hong Y, Rogers R, Matunis MJ, et al. Regulation of heat shock transcription factor 1 by stress-induced SUMO-1 modification. *J Biol Chem*. 2001;276(43):40263-40267.

86. Hietakangas V, Ahlskog JK, Jakobsson AM, et al. Phosphorylation of serine 303 is a prerequisite for the stress-inducible SUMO modification of heat shock factor 1. *Mol Cell Biol*. 2003;23(8):2953-2968.

87. Raychaudhuri S, Loew C, Korner R, et al. Interplay of acetyltransferase EP300 and the proteasome system in regulating heat shock transcription factor 1. *Cell*. 2014;156(5):975-985.

88. Westerheide SD, Anckar J, Stevens SM, Jr., Sistonen L, Morimoto RI. Stress-inducible regulation of heat shock factor 1 by the deacetylase SIRT1. *Science*. 2009;323(5917):1063-1066.

89. Liu PC, Thiele DJ. Modulation of human heat shock factor trimerization by the linker domain. *J Biol Chem*. 1999;274(24):17219-17225.

90. Wang X, Khaleque MA, Zhao MJ, Zhong R, Gaestel M, Calderwood SK. Phosphorylation of HSF1 by MAPK-activated protein kinase 2 on serine 121, inhibits transcriptional activity and promotes HSP90 binding. *J Biol Chem*. 2006;281(2):782-791.

91. Chu B, Soncin F, Price BD, Stevenson MA, Calderwood SK. Sequential phosphorylation by mitogen-activated protein kinase and glycogen synthase kinase 3 represses transcriptional activation by heat shock factor-1. *J Biol Chem*. 1996;271(48):30847-30857.

92. Batista-Nascimento L, Neef DW, Liu PC, Rodrigues-Pousada C, Thiele DJ. Deciphering human heat shock transcription factor 1 regulation via post-translational modification in yeast. *PLoS One*. 2011;6(1):e15976.

93. Wang X, Grammatikakis N, Siganou A, Calderwood SK. Regulation of molecular chaperone gene transcription involves the serine phosphorylation, 14-3-3 epsilon binding, and cytoplasmic sequestration of heat shock factor 1. *Mol Cell Biol*. 2003;23(17):6013-6026.

94. Chu B, Zhong R, Soncin F, Stevenson MA, Calderwood SK. Transcriptional activity of heat shock factor 1 at 37 degrees C is repressed through phosphorylation on two distinct serine residues by glycogen synthase kinase 3 and protein kinases Calpha and Czeta. *J Biol Chem*. 1998;273(29):18640-18646.

95. Dai R, Frejtag W, He B, Zhang Y, Mivechi NF. c-Jun NH2-terminal kinase targeting and phosphorylation of heat shock factor-1 suppress its transcriptional activity. *J Biol Chem*. 2000;275(24):18210-18218.

96. Brunet Simioni M, De Thonel A, Hammann A, et al. Heat shock protein 27 is involved in SUMO-2/3 modification of heat shock factor 1 and thereby modulates the transcription factor activity. *Oncogene*. 2009;28(37):3332-3344.

97. Raynes R, Pombier KM, Nguyen K, Brunquell J, Mendez JE, Westerheide SD. The SIRT1 modulators AROS and DBC1 regulate HSF1 activity and the heat shock response. *PLoS One*. 2013;8(1):e54364.

98. Fu Q, Wang J, Boerma M, et al. Involvement of heat shock factor 1 in statin-induced transcriptional upregulation of endothelial thrombomodulin. *Circ Res*. 2008;103(4):369-377.

99. Whitesell L, Lindquist S. Inhibiting the transcription factor HSF1 as an anticancer strategy. *Expert Opin Ther Targets*. 2009;13(4):469-478.

100. Zaarur N, Gabai VL, Porco JA, Jr., Calderwood S, Sherman MY. Targeting heat shock response to sensitize cancer cells to proteasome and Hsp90 inhibitors. *Cancer Res*. 2006;66(3):1783-1791.

101. Kupchan SM, Court WA, Dailey RG, Jr., Gilmore CJ, Bryan RF. Triptolide and tripdiolide, novel antileukemic diterpenoid triepoxides from Tripterygium wilfordii. *J Am Chem Soc*. 1972;94(20):7194-7195.

102. Heimberger T, Andrulis M, Riedel S, et al. The heat shock transcription factor 1 as a potential new therapeutic target in multiple myeloma. *Br J Haematol*. 2013;160(4):465-476.

103. Titov DV, Gilman B, He QL, et al. XPB, a subunit of TFIIH, is a target of the natural product triptolide. *Nat Chem Biol*. 2011;7(3):182-188.

104. Yoon YJ, Kim JA, Shin KD, et al. KRIBB11 inhibits HSP70 synthesis through inhibition of heat shock factor 1 function by impairing the recruitment of positive transcription elongation factor b to the hsp70 promoter. *J Biol Chem*. 2011;286(3):1737-1747.

105. Wiita AP, Ziv E, Wiita PJ, et al. Global cellular response to chemotherapy-induced apoptosis. *Elife*. 2013;2:e01236.

106. Kim JA, Kim Y, Kwon BM, Han DC. The natural compound cantharidin induces cancer cell death through inhibition of heat shock protein 70 (HSP70) and Bcl-2-associated athanogene domain 3 (BAG3) expression by blocking heat shock factor 1 (HSF1) binding to promoters. *J Biol Chem*. 2013;288(40):28713-28726.

107. Li W, Xie L, Chen Z, et al. Cantharidin, a potent and selective PP2A inhibitor, induces an oxidative stress-independent growth inhibition of pancreatic cancer cells through G2/M cell-cycle arrest and apoptosis. *Cancer Sci*. 2010;101(5):1226-1233.

108. Dubertret L, Bertaux B, Fosse M, Touraine R. Psoriasis: a defect in the regulation of epidermal proteases, as shown by serial biopsies after cantharidin application. *Br J Dermatol*. 1984;110(4):405-410.

109. Yoon T, Kang GY, Han AR, Seo EK, Lee YS. 2,4-Bis(4-hydroxybenzyl)phenol inhibits heat shock transcription factor 1 and sensitizes lung cancer cells to conventional anticancer modalities. *J Nat Prod*. 2014;77(5):1123-1129.

110. Santagata S, Mendillo ML, Tang YC, et al. Tight coordination of protein translation and HSF1 activation supports the anabolic malignant state. *Science*. 2013;341(6143):1238303.

111. Baumann B, Bohnenstengel F, Siegmund D, et al. Rocaglamide Derivatives Are Potent Inhibitors of NF-κB Activation in T-cells. *Journal of Biological Chemistry*. 2002;277(47):44791-44800.

112. Kang KN, Lee YS. RNA aptamers: a review of recent trends and applications. *Adv Biochem Eng Biotechnol*. 2013;131:153-169.

113. Salamanca HH, Antonyak MA, Cerione RA, Shi H, Lis JT. Inhibiting heat shock factor 1 in human cancer cells with a potent RNA aptamer. *PLoS One*. 2014;9(5):e96330.

114. de Billy E, Clarke PA, Workman P. HSF1 in Translation. *Cancer Cell*. 2013;24(2):147-149.

115. Villanueva MT. Microenvironment: HSF1, the troublemaker next door. *Nat Rev Cancer*. 2014;14(9):579.

116. Dai C, Dai S, Cao J. Proteotoxic stress of cancer: implication of the heat-shock response in oncogenesis. *Journal of cellular physiology*. 2012;227(8):2982-2987.

117. Dai C, Whitesell L, Rogers AB, Lindquist S. Heat shock factor 1 is a powerful multifaceted modifier of carcinogenesis. *Cell*. 2007;130(6):1005-1018.

118. Villicana C, Cruz G, Zurita M. The basal transcription machinery as a target for cancer therapy. *Cancer Cell Int*. 2014;14(1):18.

119. Petrocca F, Altschuler G, Tan Shen M, et al. A Genome-wide siRNA Screen Identifies Proteasome Addiction as a Vulnerability of Basal-like Triple-Negative Breast Cancer Cells. *Cancer Cell*. 2013;24(2):182-196.

120. Kumar SK, Dispenzieri A, Lacy MQ, et al. Continued improvement in survival in multiple myeloma: changes in early mortality and outcomes in older patients. *Leukemia*. 2014;28(5):1122-1128.

121. Lü S, Wang J. The resistance mechanisms of proteasome inhibitor bortezomib. *Biomarker Research*. 2013;1:13-13.

122. Stuhmer T, Zollinger A, Siegmund D, et al. Signalling profile and antitumour activity of the novel Hsp90 inhibitor NVP-AUY922 in multiple myeloma. *Leukemia*. 2008;22(8):1604-1612.

123. Davenport EL, Zeisig A, Aronson LI, et al. Targeting heat shock protein 72 enhances Hsp90 inhibitor-induced apoptosis in myeloma. *Leukemia*. 2010;24(10):1804-1807.

124. Chatterjee S, Bhattacharya S, Socinski MA, Burns TF. HSP90 inhibitors in lung cancer: promise still unfulfilled. *Clin Adv Hematol Oncol*. 2016;14(5):346-356.

125. Munje C, Shervington L, Khan Z, Shervington A. Could Upregulated Hsp70 Protein Compensate for the Hsp90-Silence-Induced Cell Death in Glioma Cells? *International Journal of Brain Science*. 2014;2014:9.

126. Shah SP, Lonial S, Boise LH. When Cancer Fights Back: Multiple Myeloma, Proteasome Inhibition, and the Heat-Shock Response. *Molecular Cancer Research*. 2015;13(8):1163-1173.

127. Howlader N, Noone AM, Krapcho M, Miller D, Bishop K, Altekruse SF, et al. (eds.) SEER Cancer Statistics Review 1975-2013, National Cancer Institute. Bethesda, MD, http://seer.cancer.gov/csr/1975_2013/, based on November 2015 SEER data submission, posted to the SEER web site, April 2016.

128. Harousseau JL, Attal M, Avet-Loiseau H, et al. Bortezomib plus dexamethasone is superior to vincristine plus doxorubicin plus dexamethasone as induction treatment

prior to autologous stem-cell transplantation in newly diagnosed multiple myeloma: results of the IFM 2005-01 phase III trial. *J Clin Oncol*. 2010;28(30):4621-4629.

129. Kuhn DJ, Chen Q, Voorhees PM, et al. Potent activity of carfilzomib, a novel, irreversible inhibitor of the ubiquitin-proteasome pathway, against preclinical models of multiple myeloma. *Blood*. 2007;110(9):3281-3290.

130. O'Connor OA, Stewart AK, Vallone M, et al. A phase 1 dose escalation study of the safety and pharmacokinetics of the novel proteasome inhibitor carfilzomib (PR-171) in patients with hematologic malignancies. *Clinical Cancer Research*. 2009;15(22):7085-7091.

131. Richardson P, Hofmeister CC, Rosenbaum CA, et al. Twice-Weekly Oral MLN9708 (Ixazomib Citrate), An Investigational Proteasome Inhibitor, In Combination With Lenalidomide (Len) and Dexamethasone (Dex) In Patients (Pts) With Newly Diagnosed Multiple Myeloma (MM): Final Phase 1 Results and Phase 2 Data. *Blood*. 2013;122(21):535-535.

132. Siegel DS, Martin T, Wang M, et al. A phase 2 study of single-agent carfilzomib (PX-171-003-A1) in patients with relapsed and refractory multiple myeloma. *Blood*. 2012;120(14):2817-2825.

133. Kumar SK, Berdeja JG, Niesvizky R, et al. Safety and tolerability of ixazomib, an oral proteasome inhibitor, in combination with lenalidomide and dexamethasone in patients with previously untreated multiple myeloma: an open-label phase 1/2 study. *The Lancet Oncology*. 2014;15(13):1503-1512.

134. Kumar SK, Bensinger WI, Zimmerman TM, et al. Phase 1 study of weekly dosing with the investigational oral proteasome inhibitor ixazomib in relapsed/refractory multiple myeloma. *Blood*. 2014;124(7):1047-1055.

135. Lindquist S, Craig EA. The heat-shock proteins. *Annu Rev Genet*. 1988;22:631-677.

136. Tatokoro M, Koga F, Yoshida S, Kihara K. Heat shock protein 90 targeting therapy: state of the art and future perspective. *Excli j*. 2015;14:48-58.

137. Seggewiss-Bernhardt R, Bargou RC, Goh YT, et al. Phase 1/1B trial of the heat shock protein 90 inhibitor NVP-AUY922 as monotherapy or in combination with bortezomib in patients with relapsed or refractory multiple myeloma. *Cancer*. 2015;121(13):2185-2192.

138. Zhang Y, Chou SD, Murshid A, et al. The role of heat shock factors in stress-induced transcription. *Methods Mol Biol*. 2011;787:21-32.

139. Yih LH, Hsu NC, Kuo HH, Wu YC. Inhibition of the heat shock response by PI103 enhances the cytotoxicity of arsenic trioxide. *Toxicol Sci*. 2012;128(1):126-136.

140. Shah SP, Lonial S, Boise LH. When Cancer Fights Back: Multiple Myeloma, Proteasome Inhibition, and the Heat-Shock Response. *Mol Cancer Res*. 2015;13(8):1163-1173.

141. Kourtis N, Moubarak RS, Aranda-Orgilles B, et al. FBXW7 modulates cellular stress response and metastatic potential through HSF1 post-translational modification. *Nat Cell Biol*. 2015;17(3):322-332.

142. Xu YM, Huang DY, Chiu JF, Lau AT. Post-translational modification of human heat shock factors and their functions: a recent update by proteomic approach. *J Proteome Res*. 2012;11(5):2625-2634.

143. Niskanen EA, Malinen M, Sutinen P, et al. Global SUMOylation on active chromatin is an acute heat stress response restricting transcription. *Genome Biol*. 2015;16:153.

144. Kinoshita E, Kinoshita-Kikuta E, Takiyama K, Koike T. Phosphate-binding tag, a new tool to visualize phosphorylated proteins. *Mol Cell Proteomics*. 2006;5(4):749-757.

145. Nooka AK, Kastritis E, Dimopoulos MA, Lonial S. Treatment options for relapsed and refractory multiple myeloma. *Blood*. 2015;125(20):3085-3099.

146. Nooka AK, Kaufman JL, Behera M, et al. Bortezomib-containing induction regimens in transplant-eligible myeloma patients: a meta-analysis of phase 3 randomized clinical trials. *Cancer*. 2013;119(23):4119-4128.

147. Neckers L, Workman P. Hsp90 molecular chaperone inhibitors: are we there yet? *Clin Cancer Res*. 2012;18(1):64-76.

148. Nagai N, Nakai A, Nagata K. Quercetin suppresses heat shock response by down regulation of HSF1. *Biochem Biophys Res Commun*. 1995;208(3):1099-1105.

149. Westerheide SD, Kawahara TL, Orton K, Morimoto RI. Triptolide, an inhibitor of the human heat shock response that enhances stress-induced cell death. *J Biol Chem*. 2006;281(14):9616-9622.

150. Bustany S, Cahu J, Descamps G, Pellat-Deceunynck C, Sola B. Heat shock factor 1 is a potent therapeutic target for enhancing the efficacy of treatments for multiple myeloma with adverse prognosis. *Journal of Hematology & Oncology*. 2015;8(1):1-4.

151. Li D, Yallowitz A, Ozog L, Marchenko N. A gain-of-function mutant p53–HSF1 feed forward circuit governs adaptation of cancer cells to proteotoxic stress. *Cell Death & Disease*. 2014;5(4):e1194.

152. Li S, Ma W, Fei T, et al. Upregulation of heat shock factor 1 transcription activity is associated with hepatocellular carcinoma progression. *Mol Med Rep*. 2014;10(5):2313-2321.

153. Chou SD, Murshid A, Eguchi T, Gong J, Calderwood SK. HSF1 regulation of beta-catenin in mammary cancer cells through control of HuR/elavL1 expression. *Oncogene*. 2014.

154. Ocio E, Richardson P, Rajkumar S, et al. New Drugs and Novel Mechanisms of Action in Multiple Myeloma in 2013: A Report from the International Myeloma Working Group (IMWG). *Leukemia*. 2014;28(3):525-542.

155. de la Puente P, Muz B, Azab F, Luderer M, Azab AK. Molecularly Targeted Therapies in Multiple Myeloma. *Leukemia Research and Treatment*. 2014;2014:976567.

156. Keane NA, Reidy M, Natoni A, Raab MS, O'Dwyer M. Targeting the Pim kinases in multiple myeloma. *Blood Cancer J*. 2015;5:e325.

157. Morales AA, Gutman D, Lee KP, Boise LH. BH3-only proteins Noxa, Bmf, and Bim are necessary for arsenic trioxide-induced cell death in myeloma. *Blood*. 2008;111(10):5152-5162.

158. Grad JM, Bahlis NJ, Reis I, Oshiro MM, Dalton WS, Boise LH. Ascorbic acid enhances arsenic trioxide-induced cytotoxicity in multiple myeloma cells. *Blood*. 2001;98(3):805-813.

159. Peng J, Elias JE, Thoreen CC, Licklider LJ, Gygi SP. Evaluation of multidimensional chromatography coupled with tandem mass spectrometry (LC/LC-MS/MS) for large-scale protein analysis: the yeast proteome. *J Proteome Res*. 2003;2(1):43-50.

160. Jaye DL, Iqbal J, Fujita N, et al. The BCL6-associated transcriptional co-repressor, MTA3, is selectively expressed by germinal centre B cells and lymphomas of putative germinal centre derivation. *J Pathol*. 2007;213(1):106-115.

161. Kim EH, Lee YJ, Bae S, Lee JS, Kim J, Lee YS. Heat shock factor 1-mediated aneuploidy requires a defective function of p53. *Cancer Res*. 2009;69(24):9404-9412.

162. Sullivan EK, Weirich CS, Guyon JR, Sif S, Kingston RE. Transcriptional activation domains of human heat shock factor 1 recruit human SWI/SNF. *Mol Cell Biol*. 2001;21(17):5826-5837.

163. Shah SP, Nooka AK, Jaye DL, Bahlis NJ, Lonial S, Boise LH. Bortezomib-Induced Heat Shock Response Protects Multiple Myeloma Cells and is Activated by Heat Shock Factor 1 Serine 326 Phosphorylation. *Oncotarget*. 2016 Jul 26.
doi: 10.18632/oncotarget.10847. [Epub ahead of print.]

164. Howlader N, Noone AM, Krapcho M, Miller D, Bishop K, Altekruse SF, et al. (eds.) SEER Cancer Statistics Review 1975-2013, National Cancer Institute. Bethesda, MD, http://seer.cancer.gov/csr/1975_2013/, based on November 2015 SEER data submission, posted to the SEER web site, April 2016.

165. Hamouda MA, Belhacene N, Puissant A, Colosetti P, Robert G, Jacquel A, et al. The small heat shock protein B8 (HSPB8) confers resistance to bortezomib by promoting

autophagic removal of misfolded proteins in multiple myeloma cells. *Oncotarget*. 2014;5(15):6252-6266.

166. Hornbeck PV, Zhang B, Murray B, Kornhauser JM, Latham V, Skrzypek E. PhosphoSitePlus, 2014: mutations, PTMs and recalibrations. *Nucleic Acids Research*. 2015;43(D1):D512-D520.

167. Goh KC, Novotny-Diermayr V, Hart S, et al. TG02, a novel oral multi-kinase inhibitor of CDKs, JAK2 and FLT3 with potent anti-leukemic properties. *Leukemia*. 2012;26(2):236-243.

168. Ponder KG, Matulis SM, Hitosugi S, et al. Dual inhibition of Mcl-1 by the combination of carfilzomib and TG02 in multiple myeloma. *Cancer Biol Ther*. 2016;17(7):769-777.

169. Hofmeister CC, Berdeja JG, Vesole DH, Suvannasankha A, Parrott T, Abonour R. TG02, an Oral CDK9-Inhibitor, in Combination with Carfilzomib Demonstrated Objective Responses in Carfilzomib Refractory Multiple Myeloma Patients. *Blood*. 2015;126(23):3052-3052.

170. Tragara Pharmaceuticals. Phase 1 Study of TG02 Citrate in Patients With Advanced Hematological Malignancies (TG02-101). Bethesda (MD) National Library of Medicine. 2000- [cited 2016 Nov 13]. Available from: https://clinicaltrials.gov/ct2/show/NCT01204164?term=tragara&rank=3 NLM Identifier: NCT01204164.

171. Tragara Pharmaceuticals. Phase 1 Study of TG02 Citrate in Patients With Chronic Lymphocytic Leukemia and Small Lymphocytic Lymphoma. Bethesda, MD: National Library of Medicine (US). 2000- [cited 2016 Nov 13]. Available from:

https://clinicaltrials.gov/ct2/show/NCT01699152?term=tragara&rank=2 NLM Identifier: NCT01699152.

172. Alvarez-Fernandez S, Ortiz-Ruiz MJ, Parrott T, et al. Potent antimyeloma activity of a novel ERK5/CDK inhibitor. *Clin Cancer Res*. 2013;19(10):2677-2687.

173. Kampinga HH, Hageman J, Vos MJ, et al. Guidelines for the nomenclature of the human heat shock proteins. *Cell Stress & Chaperones*. 2009;14(1):105-111.

174. Maheshwari M, Bhutani S, Das A, et al. Dexamethasone induces heat shock response and slows down disease progression in mouse and fly models of Huntington's disease. *Hum Mol Genet*. 2014;23(10):2737-2751.

175. Ma W, Zhang Y, Mu H, et al. Glucose regulates heat shock factor 1 transcription activity via mTOR pathway in HCC cell lines. *Cell Biol Int*. 2015;39(11):1217-1224.

176. Zhao YH, Zhou M, Liu H, et al. Upregulation of lactate dehydrogenase A by ErbB2 through heat shock factor 1 promotes breast cancer cell glycolysis and growth. *Oncogene*. 2009;28(42):3689-3701.

177. Santagata S, Hu R, Lin NU, et al. High levels of nuclear heat-shock factor 1 (HSF1) are associated with poor prognosis in breast cancer. *Proc Natl Acad Sci U S A*. 2011;108(45):18378-18383.

178. Raynes R, Brunquell J, Westerheide SD. Stress Inducibility of SIRT1 and Its Role in Cytoprotection and Cancer. *Genes Cancer*. 2013;4(3-4):172-182.